Friedrich-Alexander-Universität Erlangen-Nürnberg
Naturwissenschaftliche Fakultät

Approaches to increase abiotic stress tolerance of potato plants *(Solanum tuberosum)*

Ansätze zur Erhöhung der abiotischen Stresstoleranz in Kartoffel *(Solanum tuberosum)*

Der Naturwissenschaftlichen Fakultät

der Friedrich-Alexander-Universität Erlangen-Nürnberg

zur

Erlangung des Doktorgrades Dr. rer. nat.

vorgelegt von

Günter Gerhard Lehretz

Als Dissertation genehmigt von der Naturwissenschaftlichen Fakultät der

Friedrich-Alexander-Universität Erlangen-Nürnberg

Tag der mündlichen Prüfung: 25.05.2020

Vorsitzender des Promotionsorgans:	Prof. Dr. Georg Kreimer
Gutachter:	Prof. Dr. Uwe Sonnewald
	Dr. Mark Taylor

Teile dieser Arbeit sind in folgender Publikation enthalten:

Lehretz, G.G., Sonnewald S., Hornyik, C., Corral, J.M., Sonnewald, U. (2019) Post-transcriptional Regulation of FLOWERING LOCUS T modulates heat dependent source sink development in potato, Current Biology *29*, 1614-1624
https://doi.org/10.1016/j.cub.2019.04.027

Table of contents

Table of contents I
List of abbreviations IV
1 Summary/Zusammenfassung 1
1.1 Summary 1
1.2 Zusammenfassung 3
2 INTRODUCTION 6
2.1 Potato as important food crop 6
2.2 The source sink concept and its relevance for potato 6
2.3 Control of tuberization in potato 9
2.4 Effects of abiotic stress on potato 12
2.4.1 Effects of heat on potato 12
2.4.2 Effects of drought on potato 14
2.5 Aims of this study 17
3 Material and Methods 18
3.1 Material 18
3.1.1 Bacteria 18
3.1.2 Antibiotics 18
3.1.3 Antibodies 18
3.1.4 Oligonucleotides 19
3.1.5 Plasmids and vectors 20
3.1.6 Plants 20
3.1.7 Media and buffer 21
3.2 Methods 24
3.2.1 Plant growth conditions and sample taking 24
3.2.2 Transformation methods 24
3.2.3 DNA-related methods 26

3.2.4 RNA-related methods 29
3.2.5 Protein methods 33
3.2.6 Starch determination 35
3.2.7 Photosynthesis measurements 35
3.2.8 ABA measurements 35
3.2.9 Proline measurements 36
3.2.10 Microscopy methods 36
3.2.11 Floating assays 37
4 RESULTS 38
4.1 small RNA mediated regulation of SP6A modulates heat dependent source sink development in potato 38
4.1.1 Overexpression of codon-optimized SP6A (SP6A^{cop} –HA) in potato 38
4.1.2 Regulation of *SP6A* by a small RNA 45
4.2 Increasing potato drought and heat tolerance by overexpression of Hexokinase and SP6A… 56
4.2.1 Biotechnological characterization of HXK+SP6A transgenic potato 56
4.2.2 Physiological characterization of HXK+SP6A transgenic potato 63
5 DISCUSSION 71
5.1 SP6A as an important regulator of source-sink-balance 71
5.1.1 Overexpression of SP6A strongly increases sink strength 71
5.1.2 Identification and biotechnological utilization of a small RNA regulating *SP6A* under elevated temperatures 73
5.2 Combination of several genes as promising tool for stress tolerant crop plants 78
5.2.1 Overexpression of HXK+SP6A improves water use efficiency 78
5.2.2 Overexpression of HXK+SP6A preserves tuber yield under abiotic stress tolerance 81
6 REFERENCES 88
7 Supplementary data 112
7.1 Supplementary figures 112
7.2 Supplementary tables 115
8 List of figures 116

9 List of publications and conference contributions 118
10 Acknowledgements 119

List of abbreviations

°C ..... degree Celsius
µg ..... microgramm
µl ..... microliter
µm ..... micrometer
AA/BAA ..... acrylamide/bisacrylamide
bHLH ..... basic helix-loop-helix
ß-ME ..... beta-Mercaptoethanol
bp ..... base pairs
CaMV35S ..... Cabbage Mosaic Virus 35S
CDF ..... CYCLING DOF FACTOR
cDNA ..... complementary DNA
CK ..... cytokinin
CO_2 ..... carbon dioxide
cwInv ..... cell wall-bound invertase
E.coli ..... *Escherichia coli*
EDTA ..... ehylendiamintetraacetate
EGTA ..... ethylene glycol-bis (β-aminoethyl ether)-*N*,*N*,*N*′,*N*′-tetraacetate
FT ..... FLOWERING LOCUS T
gDNA ..... genomic DNA
GFP ..... green fluorescent protein
K ..... potassium
kb ..... kilobases
KCl ..... potassium chloride
K_2SO_4 ..... potassium sulfate
LB ..... Luria-Bertani
LD. ..... long day
M ..... molar
$MgCl_2$ ..... magnesiumchloride
ml ..... milliliter
mM ..... millimolar
N.. ..... nitrogen
nt ..... nucleotide
nm ..... nanometer
NaCl ..... sodium chloride

NaOH ..... sodiumhydroxide
P..... phoshphorus
PCR ..... polymerase chain reaction
PEBP.. ..... phosphatidylethanolamine-binding proteins
PTB.. .....polypyrimidine tract-binding
rpm..... rounds per minute
RubisCO.....Ribulose-1,5-bisphosphate carboxylase/oxygenase
SD ..... short day
SDS.....Sodium Dodecyl Sulfat
SOC .....Super-Optimal-Broth-With-Catabolite-Repression
SP3D.....SELF-PRUNING 3D
SP5G .....SELF-PRUNING 5G
SP6A.....SELF-PRUNING 6A
SUSY ..... sucrose synthase
TRIS-HCl..... Tris(hydroxymethyl)-aminomethan-Hydrochlorid
UV-light ..... ultraviolet light
WT .....wild-type
YEB.....Yeast-Extract-Broth

1 Summary/Zusammenfassung

1.1 Summary

The potato plant (*Solanum tuberosum* L.) is, due to its origin from cool mountainous regions, very sensitive to elevated temperatures. As temperatures are increasing due to global warming this has already led to tremendous yield losses. The aim of this work was to gain insights into the regulation of potato tuberization, especially under abiotic stresses. Moreover novel potato plants should be created which could withstand better the challenges of climate change, in particular heat and drought.

In a first approach, transgenic potato plants were generated and characterized. Overexpression of the key tuberization regulator *SP6A* (a *FLOWERING LOCUS T* homologue) should provide insights into the control of source-sink balance. Therefore, under control of a strong promoter a codon-usage optimized version of *SP6A* (*SP6A^{cop}-HA)* was used to achieve strong expression of the transcript.

This resulted in extremely early tuberization but a concurrently impaired shoot growth indicating a strong impact of SP6A on the source-sink balance. These transgenic plants tuberized extremely early, but concurrently exhibited an impaired shoot growth. Additionally, transgenic tubers formed daughter tubers from stored tubers suggesting that the meristem identity of dormant tuber buds was altered. To further unravel the underlying mechanism a transcript profiling experiment was conducted with dormant tuber buds from both wild type and transgenic tubers. Comparative data analysis revealed a differential expression of several transcription factors controlling meristem identity, which supports the findings. Motivated by the severity of the phenotype of *SP6A^{cop}-HA* overexpressing plants, an *in silico* search for putative small regulatory RNAs was performed. This led to the identification of a small RNA, named *SES*, repressing *SP6A* transcript accumulation in a sequence-specific manner, especially under elevated temperatures. The gained knowledge was used to design a construct that abolishes the activity of *SES* by providing an artificial target sequence, referred to as short tandem target mimicry (*STTM*), in excess. This construct was transformed in potato. The resulting plants did not show severe morphologic alterations but tuber formation was maintained even under continuous treatment with elevated temperatures.

In a second approach, it was tested whether the combined expression of two targets will result in improved heat and drought tolerance of potato plants. First *SP6A* was chosen for

overexpression under control of the StLS1 promoter. This was thought to result in a less extreme phenotype but in an improved tuberization under both control and heat. Secondly, transpiration rates should be reduced by a guard-cell specific overexpression of *A. thaliana Hexokinase1* (*AtHXK1*), since high water transpiration is becoming an agricultural problem in the near future due to climate change. Successful regulation of water loss by *AtHXK1* expression was shown previously for other plants like *A. thaliana*, citrus and tomato. The combined expression of these two genes in transgenic potato plants (named HXK+SP6A) resulted in reduced transpiration rates under ambient as well as drought and heat conditions. Measurements of ABA, and proline contents as well as of an ABA responsive proline biosynthesis gene indicated a reduced drought stress in the transgenic lines as compared to the WT. This was not due to impaired ABA signaling as suggested from an ABA floating assay. Most importantly, tuber formation of the transgenic was stable under all stress conditions with no negative impact on starch contents of the tubers, whereas the WT showed less total tuber yields with reduced starch contents.

In the HXK+SP6A potato tubers less induction of cell wall-bound invertase (cwInv) and less repression of sucrose synthase (SUSY) was observed supporting the assumption that more sucrose is available as substrate for starch biosynthesis via SUSY in the amyloplast and less sucrose leaking out of the cell to be hydrolyzed by cwInv. Together this might cause higher starch contents. As a possible explanation an increased supply with assimilates is most likely. To clarify this, physiological and biochemical data were obtained which provide first insights into the molecular mode of action. The transgenic plants were characterized morphologically by thinner but more stems and a repressed axillary bud outgrowth, whereas root growth was enhanced. The stem phenotype suggests less leakage of carbon sources out of the phloem which is supported by esculin loading experiments, explaining a better nourishment of the tuber to the detriment of green biomass production. This might be due to an inhibition of the sucrose exporter SWEET11 by SP6A. Moreover, an accumulation of sugars at the basal stem part might not only promote lateral shoot outgrowth but also root growth. The shift in assimilate partitioning towards root biomass production probably mediated by SP6A-SWEET interaction might, together with overexpression of *AtHXK1*, further contribute to drought stress avoidance.

Together the results gained in this work present a novel strategy for creating new potato plants which are less susceptible to drought and heat and its application can contribute to food security even under the challenges of global climate change.

1.2 Zusammenfassung

Die Kartoffelpflanze (*Solanum tuberosum L*.) ist aufgrund ihrer Herkunft aus kühlen Gebirgsregionen sehr empfindlich gegenüber erhöhten Temperaturen. Da die Temperaturen aufgrund der globalen Erwärmung steigen, hat dies bereits zu enormen Ertragsverlusten geführt. Ziel dieser Arbeit war es, Einblicke in die Regulation der Knollenbildung in Kartoffel, insbesondere unter abiotischem Stress, zu gewinnen. Darüber hinaus sollten neuartige Kartoffelpflanzen geschaffen werden, die den Herausforderungen des Klimawandels, insbesondere Hitze und Dürre, besser standhalten können.

In einem ersten Ansatz wurden transgene Kartoffelpflanzen erzeugt und charakterisiert. Die Überexpression des wichtigsten Regulators der Knollenbildung, *SP6A* (einem *FLOWERING LOCUS T*-Homolog), sollte Einblicke in die Steuerung des *source-sink*-Gleichgewichts geben. Daher wurde unter der Kontrolle eines starken Promotors eine codonoptimierte Version von SP6A verwendet, um eine starke Expression des Transkripts zu erzielen. Dies führte zu einer extrem frühen Knollenbildung, aber gleichzeitig zu einem beeinträchtigten Sprosswachstum, was auf einen starken Einfluss von SP6A auf das *source-sink*-Gleichgewicht hindeutet. Diese transgenen Pflanzen bildeten sehr früh Knollen, zeigten aber gleichzeitig ein gestörtes Sprosswachstum. Zusätzlich bildeten sich Tochterknollen aus gelagerten transgenen Knollen, was darauf hindeutete, dass die Meristemidentität ruhender Knollenaugen verändert war. Um den zugrunde liegenden Mechanismus weiter zu entschlüsseln, wurde ein *transcript-profiling*-Experiment mit ruhenden Knollenaugen sowohl von Wildtyp- als auch von transgenen Knollen durchgeführt. Eine vergleichende Datenanalyse ergab eine unterschiedliche Expression mehrerer Transkriptionsfaktoren, die die Meristemidentität steuern, was die Beobachtungen unterstützt. Aufgrund des besonders stark ausgeprägten Phänotyps dieser transgenen Pflanzen wurde nach kleinen regulatorischen RNAs gesucht. Dies führte zur Entdeckung einer kleinen RNA, genannt *SES*, die die *SP6A* Transkriptakkumulation sequenzspezifisch und insbesondere bei erhöhten Temperaturen reprimiert. Das gewonnene Wissen wurde verwendet, um ein Konstrukt zu entwerfen, das die Aktivität von *SES* aufhebt, indem eine künstliche Zielsequenz, als Short Tandem Target Mimicry (*STTM*) bezeichnet, im Überschuss bereitgestellt wird. Dieses Konstrukt wurde in Kartoffeln transformiert. Die resultierenden Pflanzen zeigten keine schweren morphologischen Veränderungen, aber die Knollenbildung blieb auch bei kontinuierlicher Behandlung mit erhöhten Temperaturen erhalten.

In einem zweiten Ansatz wurde getestet, ob die kombinierte Expression von zwei Zielgenen zu einer verbesserten Hitze- und Trockenheitstoleranz von Kartoffelpflanzen führt. Zuerst wurde *SP6A* für die Überexpression unter Kontrolle des StLS1-Promotors ausgewählt. Es

wurde angenommen, dass dies zu einem weniger extremen Phänotyp führt, jedoch zu einer verbesserten Knollenbildung sowohl unter Kontrolle als auch unter Hitze. Zweitens sollten die Transpirationsraten durch eine schließzellspezifische Überexpression von *A. thaliana* Hexokinase1 (*AtHXK1*) verringert werden, da die hohe Wassertranspiration in naher Zukunft aufgrund des Klimawandels zu einem landwirtschaftlichen Problem werden wird. Eine erfolgreiche Regulierung des Wasserverlusts durch AtHXK1-Expression wurde zuvor für andere Pflanzen wie *A. thaliana*, Zitrone und Tomate gezeigt. Die kombinierte Expression dieser beiden Gene in transgenen Kartoffelpflanzen (genannt HXK+SP6A) führte zu verringerten Transpirationsraten unter ambienten Bedingungen sowie unter Trockenheits- und Hitzebedingungen. Messungen des ABA- und Prolin-Gehalts sowie eines auf ABA ansprechenden Prolin-Biosynthesegens zeigten einen verringerten Trockenstress in den transgenen Linien im Vergleich zum Wildtyp. Dies war nicht auf eine beeinträchtigte ABA-Signalübertragung zurückzuführen, wie aus einem ABA-Floating-Assay hervorging. Am wichtigsten war die Feststellung, dass die Knollenbildung der Transgenen unter allen Stressbedingungen stabil war, ohne den Stärkegehalt der Knollen negativ zu beeinflussen, wohingegen der Wildtyp weniger Gesamtknollenerträge bei verringertem Stärkegehalt aufwies.

In den HXK+SP6A-Kartoffelknollen wurde eine geringere Induktion von zellwandgebundener Invertase (cwInv) und eine geringere Hemmung der Saccharosesynthase (SUSY) beobachtet, was die Annahme stützt, dass mehr Saccharose als Substrat für die Stärkebiosynthese mittels SUSY im Amyloplasten zur Verfügung steht und weniger Saccharose aus der Zelle austritt, um durch cwInv hydrolysiert zu werden. Zusammen kann dies zu höheren Stärkegehalten führen. Als mögliche Erklärung ist eine verbesserte Versorgung mit Assimilaten am wahrscheinlichsten. Um dies zu verdeutlichen, wurden physiologische und biochemische Daten gesammelt, die erste Einblicke in die molekulare Wirkungsweise geben. Die transgenen Pflanzen waren morphologisch durch dünnere, aber mehr Stämme und ein unterdrücktes Auswachsen der Achselknospen gekennzeichnet, während das Wurzelwachstum verstärkt war. Der Stammphänotyp deutet darauf hin, dass weniger Kohlenstoffquellen aus dem Phloem austreten, was durch Esculinbeladungsexperimente unterstützt wird, was eine bessere Ernährung der Knolle, zum Nachteil des Aufbaus grüner Biomasse, erklärt. Dies könnte auf eine Hemmung des Saccharoseexporters SWEET11 durch SP6A zurückzuführen sein. Darüber hinaus könnte eine Anreicherung von Zucker am basalen Stammteil nicht nur das Wachstum von Seitensprossen fördern, sondern auch das Wurzelwachstum. Die Verschiebung der Assimilatverteilung in Richtung Wurzelbiomasseproduktion, die wahrscheinlich durch die SP6A-SWEET11-Interaktion vermittelt wird, könnte, zusammen mit dem AtHXK1-Konstrukt,

dazu beitragen die Ernährung auch unter den Bedingungen des Klimawandels sicherzustellen.

.

2 INTRODUCTION

2.1 Potato as important food crop

The potato plant (*Solanum tuberosum* L.) is a crop plant cultivated for its edible underground storage organs, the potato tubers. Besides other crop plants such as tomato (*Solanum lycopersicum* L.), pepper (*Capsicum annuum* L.), tobacco (*Nicotiana tabacum* L.) and eggplant (*Solanum melongena* L.) it is an important member of the plant family of *Solanaceae* also called nightshades. In 2016, more than 350 million tons of tubers were produced worldwide which makes it besides maize (*Zea mays* L.), rice (*Oryza sativa* L.), wheat (*Triticum aestivum* L.) and cassava (*Manihot esculenta* C.) one of the five most important food crops worldwide (http://faostat3.fao.org/). Compared to cereals or root crops potato tubers are of very high nutritional value as they are rich in starch and low in fat but also contain large amounts of vitamins such as B1, B3, B6 and C as well as important amino acids [1]. Thus, potato tubers cannot only fight undernutrition but also nutritional deficiencies of a large amount of people. Facing an increasing world population potato is therefore considered outstanding in terms of food security [2].

Potato originates from Andean regions and was first cultivated around 10,000 B.C. by native people in Southern Peru [3]. After conquest and colonialization by the Spanish in the 16th century and subsequent transfer of tubers to the “Old World”, potato production strongly increased and became an important source of carbohydrates in human nutrition. It was originally favored for its easy cultivation and meal preparation compared to cereal crops commonly used at that time. Furthermore, potato tubers can serve as animal fodder and as raw material for producing starch for industrial purposes, e.g. in the paper and chemical industry [4], synthesizing biodegradable plastic [5] and distilling alcohol as biofuel [6,7]. Therefore, research on this widely used crop might be rewarding for broad fields in agriculture, industry and food supply.

2.2 The source sink concept and its relevance for potato

Storage organ formation is a quite common phenomenon in plants. The ability to develop storage organs out of leaves, stems and root tissues, for example in succulents like *Aloe,* cactuses and several root crops, has evolved several times independently in earth history. Potato tubers derive from horizontally growing underground lateral shoots called stolons with long internodes and a hook-shaped tip [8,9]. Although stolons have the ability to grow to the surface and form shoots, their predominant function is to spread the habitat of potato

vegetatively as well as to secure a certain number of offsprings in an additional survival strategy besides seeds.

Tubers are in fact the shortened and thickened end part of a stolon. When tuber formation starts, stolons attenuate their longitudinal growth, which is accompanied by a radial cell division in the pith and cortex. Later, this is followed by random cell division and expansion to allow massive growth of the newly formed tuber [10]. This morphological switch is associated with biochemical and structural changes and a switch of phloem unloading in the stolon tip from apoplasmic to symplasmic [11]. Simultaneously, activities of sucrose synthase (SUSY) and fructokinase increase whereas cell-wall bound invertase (cwInv) activity decreases [12–14]. Large amounts of starch and proteins are then deposited which can also be observed by transcriptomic and metabolomic changes [11,15,16].

At the end of the growth season the green tissue of the mother plant dies, SUSY activity in the tuber sharply declines [17], and the tubers then remain dormant in the soil during winter [18]. The length of the dormancy phase is determined by various environmental, physiological and hormonal cues [19–23]. At the beginning of the next growth season the onset of sprouting is characterized by several metabolic and transcriptional changes in the tuber in order to remobilize stored resources and to supply nutrients for the development of new plant tissues [9,20,22,24]. In particular, sucrose is remobilized through breakdown of starch by activation of starch degradation enzymes [25].

This complex process makes potato, besides its agricultural importance, an interesting model organism to study so called source-sink-interactions. In general, plant tissues can be divided into two types. Those which produce an excess of photoassimilates like fully developed mature leaves are called source organs. In contrast, sink tissues, for example young leaves, flowers and roots are not able to produce enough photoassimilates on their own and are therefore dependent on an import of carbon and nutrients.

Carbon which is fixed during photosynthesis is transformed into the non-reducing sugar sucrose serving as the common carbohydrate transport form. The excess of sucrose is unloaded from the mesophyll cells into the apoplast by SUGARS WILL EVENTUALLY BE EXPORTED TRANSPORTER (SWEET) proteins [26] and taken up into the phloem via sucrose proton symporters like SUC2 or SUT1 to be transported further throughout the plant [27–29]. With the surplus of assimilates sink tissues can be supplied, where sucrose is unloaded in large amounts from the phloem. In developing, growing potato tubers this happens symplasmically [11] like in the important tuberous root crop cassava (*Manihot esculenta*) [30]. Sucrose is then either metabolized into starch for storage which occurs via

SUSY or used as energy source for development and growth via cleavage through cwInv [31,32]. Thus, the mode of sucrose cleavage can determine the fate of assimilate utilization [33].

The potato tubers depict an exceptional case since their source-sink property can switch during their life cycle. In order to ensure vigorous outgrowth of shoots in spring, tubers accumulate large amounts of resources like starch and proteins during their formation and thus act as a strong sink [14,34]. Therefore they are referred to as storage sinks contrary to metabolic sinks such as growing leaves [35]. After dormancy, the tuber identity switches towards a source organ, as it is supplying nutrients to the newly developing shoots until enough photoassimilates can be produced by the emerging leaves. This finally results in the degradation of the mother tuber.

In order to improve yield of crop plants understanding the source sink-balance is essential [36,37]. The rate of photosynthesis has been found to be critical for source capacity in many species such as cotton [38], sugarbeet [39], ryegrass [40], sorghum and tomatoes [41]. As improvement of photosynthesis might increase source strength and thus secure food production [42,43], several different approaches have been carried out to achieve this goal. For example, in rice [44] and tobacco [45] the key enzyme of photosynthesis, RuBisCO, was targeted to improve CO_2 fixation. In rice [46] and tobacco [47] the photosynthetic rates were increased through overexpression of a seduheptulose bisphosphatase, especially in combination with fructose 1,6-bisphophate aldolase (FBPA) [48]. These two enzymes act in the Calvin-Benson cycle. Another study has achieved increased source capacity through accelerated recovery from photo protection mechanisms under fluctuating light conditions in tobacco [49]. However, this result seemed to be difficult to transfer in other plant species [50]. Overexpression of a tonoplast monosaccharide transporter (TMT) indirectly promoted sucrose export out of the source leaf through the sequestration of hexoses and thus removing the feedback inhibition on photosynthesis [51]. In the last decade much emphasis was also led on the improvement of photorespiration [52,53], starting with the finding that a photorespiratory bypass through overexpression of an *E. coli* glycolate dehydrogenase increased biomass production in A thaliana [54] and also in potato [55]. Contrary to these findings which suggest a benefit through improvement of source strength other studies report a sink limitation [56–58]. In potato, overexpression of a *Pisum sativum* glucose-6-phosphate/phosphate translocator (GPT) and *Arabidopsis thaliana* adenylate translocator (NTT1) at the amyloplast membrane in the tuber was successful as it increased tuber starch content [59]. Together these two transport proteins provided substrate as well as energy for starch synthesis and thus increased tuber yields by 19 % and starch content around 44 %.

The communication between the source and sink organs in potato is of crucial importance for the plant [36,60,61] and tightly regulated by hormone, nutrient and stress cross signaling [62]. Thus, growth can be adjusted to internal and external stimuli. For mankind, increasing sink strength of crop plants is essential for future food development [60]. Therefore understanding of transport processes is also required [63] but improvement of source capacity together with sink strength is most important [64]. Indeed, in a biotechnological approach a push-pull strategy turned out to be promising and could for example increase starch contents in potato tubers twofold [65].

2.3 Control of tuberization in potato

Since the formation of tubers involves an altered assimilate partitioning and thus a major change in the source-sink balance, it has to be under strict regulation. In fact, source-sink regulation is influenced by various environmental cues. In general, tuberization is favored by short days (SD), low temperatures and low nitrogen supply [9]. In native Andean cultivars like *Solanum tuberosum* group *andigena* it is under strict photoperiodic control, where day length is perceived by the leaves [24].

As indicated by research of the last decade regulation of tuberization in potato is very similar to flowering control in *Arabidopsis thaliana.* The key players in both pathways are homologs of FLOWERING LOCUS T (FT).

In Arabidopsis, FT is activated under long day (LD) by CONSTANS [66,67]. This occurs as follows. Under flowering inducing LD conditions FLAVIN BINDING KELCH REPEAT F BOX (FKF1) is activated by blue light via a light oxygen voltage (LOV) domain to form a complex with GIGANTEA (GI) [68]. This complex binds CYCLING DOF FACTOR 1 (CDF1) and thus marks it for proteolytic degradation[68,69]. CDF1 normally represses CONSTANS (CO) which acts as a transcriptional activator of *FT* [70]. FT was shown to acts as a long distance signal [70,71] which is phloemmobile and also graft transmissible [72–74] but requires interaction with the interacting protein FTIP1 [75] putatively localized at plasmodesmata [76]. In the floral meristem a flower activation complex (FAC) is formed to induce transcription of meristem identitiy genes [77].

In potato, tuberization is also controlled by the photoperiodic pathway [78]. The first hint was given by heterografting experiments of flowering tobacco shoots on potato stocks which induced tuberization and thus suggested that flowering and tuberization are mediated by similar graft transmissible signals [79].

However, in potato several FT homologues have evolved and play a role in tuberization and flowering. They form a small gene family, with the most important being SP6A, SP5G and SP3D. SP6A is the so called tuberigen and especially activated under SD [80]. Overexpression of *SP6A* improved tuberization even under LD, whereas RNAi-based knockdown prevented it also under SD [81]. The CO homologue in potato (COL1) activates *SP5G*, which acts as a repressor of *SP6A* [82]. *SP3D* is also regulated by COL1 and was shown to control flowering [81,83]. Grafting experiments in potato revealed that SP6A is also a phloemmobile graft transmissible signal [81]. Therefore it is assumed to be expressed in phloem companion cells like it was shown for FT in tobacco [84]. In potato, *SP6A* seems to be expressed in leaf veins [85]. According to the current model, SP6A is produced in the leaves and then transported via the phloem to the stolons where it initiates tuberization after an autoregulatory self-amplification loop [80,81,86]. This model is summarized in **Figure 1.**

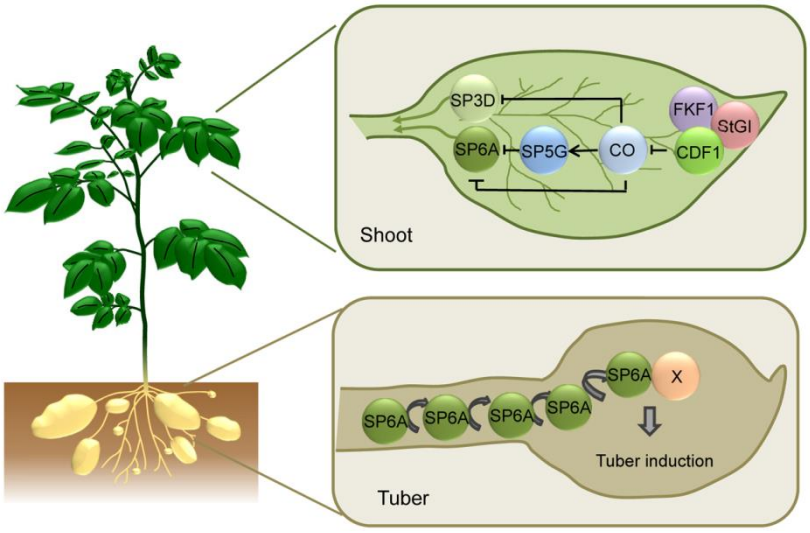

Figure 1. Regulation of tuberization in potato. Under long day lengths GI and FKF1 bind to CDF and mark it for proteolytic degradation. This leads to the activation of CO. Under SD, CDF1 is not degraded by FKF1/GI and inhibits CO which then can no longer activate SP5G, functioning as a repressor of SP6A. SP6A is phloemmobile and moves through the stem to the stolons where it promotes tuberization after an autoregulatory loop (modified after Abelenda *et al*., 2011).

Some interaction partners have been identified recently [87]. Again, similarities to flowering in Arabidopsis and rice have been found. A flowering activation complex (FAC) consists of FT which interacts with FLOWERING LOCUS D (FD), a basic leucine zipper (bZIP) transcription factor [88]. This interaction is mediated by 14-3-3 proteins through an SAP (Arg-X-X-Ser/Thr-Ala-Pro) motif in FD which is essential for floral induction [77,88,89]. To enable the interaction FD is dependent on phosphorylation at the SAP site through a Ca^{2+} dependent protein kinase (CDPK) [90,91]. Finally, FD can activate flowering genes such as APETALA1 to induce floral transition [88,92]. In rice, a similar mechanism has been shown for the rice

homologue of FT called Hd3a [77]. Analogous to the FAC, in potato a tuberization activation complex (TAC) is formed in the stolons, where SP6A interacts with FD-like proteins via 14-3-3 proteins as well [87]. Furthermore, SP6A was shown to inhibit a SWEET protein, namely SWEET11b in stolons, thus preventing sucrose efflux and suggesting a role of SP6A is sucrose partitioning [93]. In Arabidopsis, FT induces the expression of SWEET10 in the leaf veins and thus promotes flowering through the provision of sugars [94].

The function of SP6A and its FT homologues in various species is still under examination. SP6A belongs to a broader protein family called phosphatidylethanolamine-binding proteins (PEBP) [95] consisting of three major groups of proteins exhibiting similarity to FT, TERMINAL FLOWER LIKE (TFL) and MOTHER OF FT AND TFL (MFT). Although the exact molecular activities of SP6A and other FTs in storage organ formation are unknown, this underlies once more the close link between flowering and tuberization.

As mentioned above regulation of flowering is often controlled by day length. Native diploid (2n=24) Andean varieties of potato (*S. tuberosum* group *andigena*) do not tuberize in regions with warmer climate and longer day lengths [1,96]. Unlike those native cultivars modern agronomically used varieties were adapted to European long day conditions most likely by selection for a truncated CDF1 allele. This lacks a binding site for FKF1 and thus escapes LD repression. For cultivation in northern latitudes this was an important breeding step [78].

However, there exist multiple additional signals for tuberization, for example phloem mobile proteins and RNAs [9,97]. For example, *BELLRINGER-like 5* of potato (*BEL5*) functions as a mobile RNA that is transcribed in the leaves, moves through the stem and induces tuber formation through activating CDF1 and SP6A [85]. *BEL5* can be inhibited by COL1 [98]. Additionally, members of the PYRIMIDINE TRACT BINDING (PTB) protein family play important roles in tuberization. These proteins act as RNA-binding splicing regulators and are highly conserved between species which use FT homologues as a regulatory hub for flowering as well as storage organ development [99].

Furthermore, the microRNAs (miRNAs) miR172 and miR156 can stimulate and inhibit tuber formation respectively [100,101]. Moreover, tuberization can be controlled by phytohormones [102].

It has been known for a long time that sucrose acts as a strong tuberization inducer. Similarly sugars promote flowering [103,104]. Sucrose levels are sensed by the content of trehalose 6-phosphate (T6P) which serves as a signaling molecule to regulate developmental and metabolic responses [105,106]. In Arabidopsis, T6P controls flowering in the shoot apical meristem via miR156/157 and also in the leaves via FT [104,106]. In potato, a link between

T6P and SP6A could not be proven yet. However, it is clear that carbon allocation, which is basically sucrose transport, has a strong impact on sink development. This is supported by investigations on sucrose transport proteins such as SUC4, whose suppression promotes tuberization under non inductive LD conditions [107]. Furthermore, as mentioned above, the repression of SWEET11 by SP6A provides a link between photoperiod and sugar transport [93].

In agriculture, it was found that the nutrient composition of the soil also influences shoot and tuber development. An adequate supply with nitrogen (N) is essential for potato plant growth as for many other species [108,109]. Limited nitrogen availability affects potato tuberization in a cultivar dependent manner [110]. Nitrogen fertilization can improve leaf chlorophyll content, tuber swelling and tuber yield [111–113]. However, nitrogen uptake seems to be coupled with carbon allocation through the plant from shoot to root [114]. Recently, more studies underlie a close link between N and sugar partitioning [115], for example by the sugar sensor T6P [106]. Indeed, excessive amounts of N can trigger massive shoot growth and concurrently impair or abolish tuber development [113].

Similar observations were found concerning phosphorus (P). Adequate P supply promotes tuber initiation, starch synthesis, leaf development and also disease resistance [116–118]. High P contents reduce tuber yield and induce zinc or other micronutrient deficiencies [119]. A lack of potassium (K) can reduce sugar levels and affect tuber quality, specific gravity and storability [120,121]. It can further lead to blackspot bruise [122,123]. Although a clear correlation between potassium and tuber yield cannot be found [124,125], fertilization with KCl promotes green biomass development, whereas K_2SO_4 stimulates tuberization [126]. Compared to cereal crops potato plants require a lower amount of fertilizer with a distribution of 40-50%, 10-15% and 50-60% for N, P and K respectively [127].

2.4 Effects of abiotic stress on potato

2.4.1 Effects of heat on potato

Due to global climate change abiotic stresses are a huge threat for crop yields worldwide, especially for potato [15,128–133]. In particular, heat and drought stress periods are predicted to increase. This depicts a special harm for crop plants in the northern hemisphere which are not adapted to such conditions [15,134,135]. As a consequence of global warming potato yields are expected to decrease approximately 30 % by 2050 [15]. Since potato originates from rather cool mountainous regions it is particularly vulnerable to heat and rather prefers growth temperatures between 14 °C and 22 °C [3,96,136]. Therefore cultivation of potato in the warm tropics is impossible [137,138].

For many plants, heat has numerous negative impacts [134,139,140]. For example, heat increases membrane fluidity leading to Ca^{2+} influx from the endoplasmic reticulum (ER) into the cytosol through Ca^{2+} channels. Ca^{2+} is an important second messenger in the cell and leads to specific stress response through interaction with CDPKs or Ca^{2+} binding proteins, which activate signaling cascades. This leads to the phosphorylation of certain transcription factors mediating an altered gene expression. Under heat stress, a conserved response is the increased accumulation of heat shock proteins (HSPs). These HSPs, more precisely the subgroup of HSP70, are formed under heat stress and act as chaperones, which stabilize misfolded proteins and bring them into the correct conformation [141]. Indeed, overexpression of HEAT-SHOCK COGNATE 70 (HSc70) improved potato heat tolerance [142]. Also the expression of eukaryotic elongation factors such as eEF1A were demonstrated to be important for protein translation in potato under heat [143]. Heat induces further molecular changes: the metabolic balance is shifted, which leads to uncoupled flows of adenosine triphosphate (ATP) and reduced nicotinamide adenine dinucleotide (NADH). There is also an accumulation of reactive oxygen species (ROS) which, if not being scavenged by the antioxidative system, have toxic effects on the cell [128].

In potato already mildly elevated temperatures of around 5-10 °C above the optimum, which is around 28 °C, lead to increased shoot elongation, smaller leaves and an upward orientated plant habitus known as shade avoidance phenotype [136]. In addition, elevated temperatures decrease the development of root biomass which further limits water uptake [144,145]. Most importantly yield is strongly reduced [146] by an interplay of many different heat dependent mechanisms [147].

In the shoot, heat has a strong negative impact on photosynthesis [148,149]. Usually plants try to cool the leaves by transpiration since heat inhibits Rubisco [150]. Heat further accelerates senescence, increases photorespiration and dark respiration, but reduces CO_2 assimilation rates [151,152]. In particular, this is due to inactivation of Photosystem II (PSII) and an altered redox state of plastoquinone (PQ) induced by ROS accumulation [150,153,154]. Ribulose-1,5-bisphosphate carboxylase/oxygenase (RubisCO) is a key enzyme for both processes [155]. A feature of this enzyme is the preference for oxygenation instead of carboxylation at higher temperatures since under heat the ratio of solubilized CO_2 over O_2 decreases [156–158]. The educts resulting from O_2 incorporation have to be recycled in and energy expensive way through peroxisomes and mitochondria. This process known as photorespiration reduces CO_2 fixation and thus makes this process especially relevant for crop plants [52].

Together these processes alter assimilate production and allocation, which in principle means a shift in source sink-balance, reflected in an increase of green biomass under heat and a reduced tuber yield [152,159]. This seems to be caused by reduced SP6A expression, thus a lack of the tuberization signal reduces tuber formation [136]. The PHYTOCHROME B (PHYB) photoreceptor was identified as a regulator integrating light and temperature signals [160,161]. The basic helix-loop-helix (bHLH) transcription factor PIF4 interacts with PHYB and can thus mediate adaptation to high temperatures [162]. In Arabidopsis PIF4 can control flowering via directly binding to the FT promoter [163]. In tomato, the FT homologue SP5G is regulated also by PHYB [164].

Moreover, malformation and early sprouting of tubers known as second growth phenotype occur more frequently under heat. Premature breakage of dormancy also affects long time storage [165]. Preservation of starch content even under stress is of agronomic importance. Still not all mechanisms of starch biosynthesis are completely understood [166]. Starch contents of potato tubers decrease under heat [152,167,168]. Mostly this is due to a lower expression as well as activity of a key enzyme in starch biosynthesis, sucrose synthase (SUSY) [17,19,134,169]. SUSY catalyzes the cleavage of sucrose into fructose and UDP-glucose with the latter serving as substrate for starch biosynthesis via UGPase.

Since a dialogue between source and sink organs exists, perception of environmental conditions such as heat affects assimilate partitioning to sink organs due to reduced sink strength [152]. The resulting lack of substrates in the tuber sink contributes further to an impaired starch biosynthesis. A summary of the described processes is shown in **Figure 2**.

Although breeding has adapted the potato plant to many different climate conditions, the best yields are obtained under moderate climates, like in mid Europe [170]. Even in modern cultivars potato tuber formation can further be enhanced by short days and cool temperatures and is hindered by long days and high temperatures [9,80,171]. Global warming has tremendously affected crop yields worldwide. If the increase in temperature cannot be stopped potato yields will decline by 18-32 % in the 2050s [172]. Therefore, in order to meet the nutritional demands of a growing population [173] even under climate change conditions the development of a heat-tolerant potato plant is essential.

2.4.2 Effects of drought on potato

Heat waves are often accompanied by water scarcity, i.e. drought. Elevated temperatures increase water transpiration, which in the end aggravates water shortage for the plant and limits yields [174–176]. Drought or limited water availability are seen phenotypically as wilting of the leaves caused by a decreased turgor pressure of the plant cell. Plant tissue might die if

wilting of the leaves exceeds a critical point known as permanent wilting point, but also limited water availability reduces plant growth. For crop yields climate change depicts a quite harmful scenario as already 70 % of water consumed by mankind is needed for agriculture. Since more than half of the terrestrial region is susceptible to drought this greatly affects plant growth and yield [177,178].

Potato is considered to be rather efficient in water usage. It produces about 40-100 % more calories per unit of water than the commonly used cereal crops maize, wheat and rice (http://www.fao.org/potato-2008/en/potato/water.html). However, it is still susceptible to drought [135], especially during the tuber swelling phase [179,180]. Thus, water stress reduces the photosynthetic rate, decreases plant growth and total biomass production [181,182], shortens the growth cycle [183], negatively affects tuber number [184], tuber size and in the end tuber yield [185].

Various approaches can be pursued to increase the tolerance of potato towards drought stress or to confer drought stress avoidance by increasing the water supply and accessibility [131,186]. Indeed it has been reported that by management of irrigation yields can be maintained whilst saving up to 50 % water compared to conventional watering [187,188].

The search for drought tolerant cultivars is an elaborate task. For Arabidopsis it was possible to identify drought tolerant ecotypes by *in silico* approaches [189]. Also for potato screenings for drought tolerant cultivars were performed [190,191] and some metabolite and transcript markers were identified [192]. Introducing germplasm from native cultivars and landraces can help to improve drought tolerance [135,193] as it was already done successfully for pathogen resistance [194]. Unfortunately these traits are often associated with a low yield potential [195]. Therefore, also transgenic approaches should be envisaged in order to secure optimal plant performance even under this abiotic stress.

In Arabidopsis ß-Amylase turned out to be an interesting target. AtBAM1 was found to be required for maintaining the synthesis of the osmolyte proline through degradation of transitory starch under drought [196]. In potato overexpression of the transcription factor StNF-YB3.1 could promote abscisic acid (ABA)-mediated stomatal closure, unfortunately at the expense of tuber yield [197].

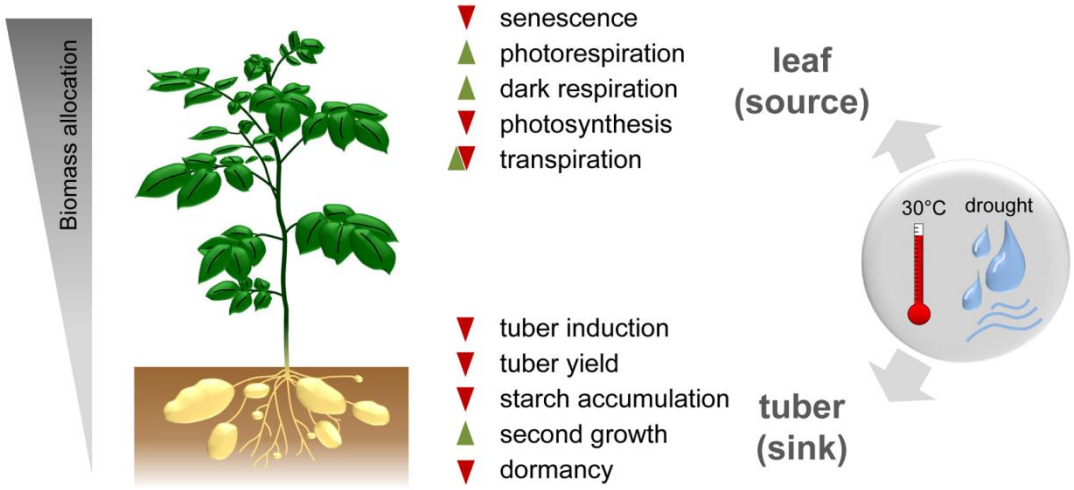

Figure 2. Drought and heat stress responses in potato. Under drought and heat stress both source organs (the leaves) as well as sink organs (the tubers) show molecular and morphological responses leading to a shift in assimilate partitioning in favor of the shoot and to the detriment of tuber yield.

Since water resources are already declining even in mid-europe and water shortages after consecutive dry summers have been reported, a reduced transpiration of crop plants would be a desirable agronomic trait. An important linchpin for achieving this goal would be stomata, formed by guard cells, which control gas exchange. Decreased transpiration could be achieved by reduced stomatal density [198–201]. Drought tolerant cultivars exhibit about five times less stomata and show even an unexpected increased heat tolerance [202].

Additionally, stomatal aperture was shown to increase water use efficiency (WUE) without affecting carbon assimilation or crop yield [203–205]. Overexpression of a blue light activated potassium channel (BLINK1) accelerated stomatal opening and thus increased water use efficiency [204]. A constitutive mild repression of stomatal opening was achieved by overexpression of hexokinase1 (*AtHXK1)* in the guard cells [205–207]. This enzyme is thought to affect sugar signaling pathways and thus trigger stomatal closure [208,209]. In this model an excess of photosynthetic activity can be sensed indirectly via carbohydrate production i.e. glucose. This would then lead to stomatal closure until sugar levels decrease and trigger the signal to open stomata. In this way stomatal conductance is linked to photosynthesis [209]. Therefore it appears to be a promising tool for future design of crop plants.

Drought mediated stomatal closure clearly correlates positively with the contents of the phytohormone abscisic acid (ABA) [210,211]. ABA is broadly used as a biochemical indicator for several stresses, especially drought. The active isomer influencing stomatal movement is

2-cis(S)-ABA [212,213]. When soil drying has been detected in the roots, this was thought to stimulate biosynthesis of ABA in the roots which is then transported to the leaves to trigger stomatal closure [214–217]. Recent studies have shown that is synthesized in phloem companion cells [218,219], guard cells [220] and mesophyll cells [221]. Up to now it is not clear whether also the shoot can control ABA levels in the root, and the influence of hydraulic signals such as leaf turgor pressure also need further investigation.

2.5 Aims of this study

The main goal of this study was to clarify the role of SP6A in the regulation of tuberization in potato and the implementation of the gained knowledge in biotechnological approaches to increase the tolerance of the potato crop towards abiotic stress, in particular drought and heat. The motivation behind this was the vulnerability of potato tuberization to the changing climate conditions in temperate climate zones due to global warming.

At first transgenic potato plants strongly overexpressing the key regulator of tuberization, SP6A, should be characterized. Since tremendous shifts in the source sink balance were observed, this should be investigated deeper in a transcriptional analysis of dormant tuber buds. This might elucidate further the process of tuber initiation. The morphological changes unseen so far in similar overexpression studies were a strong motivation to search for a new *SP6A* regulation mechanism explaining the phenotype. *In silico a* small RNA specific for *SP6A* was identified which should then be characterized in detail. Finally the function of the small RNA should be abolished with overexpression of a target mimicry construct.

In the second approach emphasis was led on a biotechnological utilization of SP6A. This should be combined with overexpression of *AtHXK1* of Arabidopsis as this gene was proven to mediate stomatal closure and thus reduce water consumption. An experimental setup should be designed in order to investigate the behavior of the double transformants under heat, drought and a combination thereof. Since yield turned out to be improved, several morphological, physiological, biochemical and transcriptional data were gathered in order to get first insights into the molecular reasons for stress tolerance.

3 Material and Methods

3.1 Material

If not stated otherwise chemicals, enzymes and consumables were obtained from Carl Roth (Karlsruhe, Germany), Fermentas (St.Leon Rot, Germany), Merck (Darmstadt, Germany), Qiagen (Hilden, Germany), Roche (Mannheim, Germany), Sigma-Aldrich, (St.Louis, USA), ThermoFisher Scientific (Waltham, USA), and VWR (Radnor, USA). Materials for plants cultivation were obtained from Bayerische Gärtnereigenossenschaft (Nürnberg, Germany).

3.1.1 Bacteria

For cloning purposes *Escherichia coli* were used whereas transient and stable transformation of plants was conducted with *Agrobacterium tumefaciens.*

Table 1. Overview of bacteria used

strain	genotype	**reference**
E.coli XL1 blue	*recA1 endA1 gyrA96 thi-1 hsdR17 supE44 relA1 lac*[F`*proAB lacI*^{q}*ZΔ M15* Tn*10* (Tet^{R})]	Bullock *et al.,* 1987 [222]
A. tumefaciens C58C1	RifR; with helperplasmid pGV2260 AmpR (Deblaere *et al.,* 1985) [223]	van Larebeke *et al.*, 1974 [224]

3.1.2 Antibiotics

The following antibiotics were used for selection of competent *E.coli* (strain XL1 blue) or *A. tumefaciens* (strain C58C1)

Table 2. Overview of antibiotics used

antibiotic	**stock concentration**	**dilution used**
Ampicillin (Amp)	200 µg µl^{-1}	1:500
Kanamycin (Kan)	50 µg µl^{-1}	1:1000
Rifampicin (Rif)	50 µg µl^{-1}	1:1000
Spectinomycin (Spec)	50 µg µl^{-1}	1:500
Streptomycin (Strep)	10 µg µl^{-1}	1:250

3.1.3 Antibodies

Table 3. Overview of antibodies used

Antibody	dilution	manufacturer
α-HA	1:1000	Roche, Mannheim
Mouse α-GFP	1:1000	Roche, Mannheim
Rabbit α-Mouse	1:20000	Roche, Mannheim

3.1.4 Oligonucleotides

Oligonucleotides were if applicable designed with the help of Primer 3Plus [225] and obtained from metabion (Planegg, Germany).

Table 4. Overview of oligonucleotides used

number	description	sequence (5`→3`)	Transcript ID	purpose
SS539	UBI-qPCR_fwd	TTCCGACACCATCGACAATGT	PGSC0003DMT400013321	qPCR
SS540	UBI-qPCR_rev	CGACCATCCTCAAGCTGCTT	PGSC0003DMT400013321	qPCR
SS588	SP6A_qPCR_fwd	ACAGTGTATGCCCCAGGTTG	PGSC0003DMT400060057	qPCR
SS589	SP6A_qPCR_rev	AACAGCTGCAACAGGCAATC	PGSC0003DMT400060057	qPCR
SS590	SP6Acop_qPCR_fwd	ACTGTGTACGCTCCAGGATG		qPCR
SS591	SP6Acop_qPCR_rev	CACTGCAGCAACAGGTAATC		qPCR
SS605	SP6A_CDS fwd	ATGCCTAGAGTTGATCCATTGATA	PGSC0003DMT400060057	cloning
SS606	SP6A_CDS rev	TTATGCGCGACGTCCTCCAGTG	PGSC0003DMT400060057	cloning
SS628	Actin_fwd	GACATTTAATGTTCCTGCTATG	PGSC0003DMT400047481	PCR
SS629	Actin_rev	AATGGAGGAACTGCTCCTAGCG	PGSC0003DMT400047481	PCR
SS638	SP6Acop_pRB_GFP_fwd	GGATCCCCAAGGGTTGACCCATTGATTGTTGGA		cloning
SS639	SP6Acop_pRB_GFP_rev	GTCGACTCAAGCTCTCCTACCTCCAGTTCCTGACT		cloning
SS642	M13 fwd	TGTAAAACGACGGCCAGT		sequencing
SS643	M13 rev	CAGGAAACAGCTATGACC		sequencing
SS691	SWEET11_qPCR_fwd	GTGATGCATGTGCATGTTTG	PGSC0003DMT400083992	qPCR
SS692	SWEET11_qPCR_fwd	CCACGGCCAATCTCCTCTAA	PGSC0003DMT400083992	qPCR
SS695	SES_91_fwd BamHI	GGATCCTCTCCAAAAATATTATCGCATCCATG		cloning
SS696	SES_91_rev SalI	GTCGACCTTTTCAAAATTGTTATCGGATGT		cloning
SS728	SES_genomic_fwd_BamHI	GGATCCGGTGAGTTTCTTGATGAAAATTAGAAG		cloning
SS729	SES_genomic_fwd_SalI	GTCGACTGCATACAAACAATAATATGAATAT		cloning
SS790	COI1_qPCR_fwd	GTAGCAACAATTGGGCAAGGG	PGSC003DMT400026065	qPCR
SS791	COI1_qPCR_rev	AGTAAACGGTACATGTTACTGG	PGSC003DMT400026065	qPCR
SS796	STTM_RT_fwd	TGTGTTCTAGAATCCTTCAGTTGT		RT
SS797	STTM_RT_rev	AGGATTCTAGAACACACATATT		qPCR, RT

		CTTCT		
SS815	STTM_qPCR_fwd	TCTAGAATCCTTCAGTTGTTGTTGT		qPCR
SS825	CDF_qPCR_fwd	TGCAGACTCGTCGATTGAAC		qPCR
SS826	CDF_qPCR_rev	GAGTGCCTTTTCCTCACTCG		qPCR
SS873	AtHXK1_qPCR_fwd	CCTCAAGGCCTTCGAAGAGG	AT4G29130	qPCR
SS874	AtHXK1_qPCR_rev	AAGTCCAGCGTGCATCTCAA	AT4G29130	qPCR
SS893	GI_qPCR_fwd	TTGTCTCATTGCTCTGGCACA	Sotub12g025130.1.1	qPCR
SS894	GI_qPCR_rev	AGTGCATCAACCACCTGTCTC	Sotub12g025130.1.1	qPCR
SS1019	P5CS_qPCR_fwd	GCTGCTTATGCTGGCATTCC	PGSC0003DMT400068829, Sotub06g011740	qPCR
SS1020	P5CS_qPCR_rev	GTGCCAACACGTTGTCCATC	PGSC0003DMT400068829, Sotub06g011740	qPCR
SS1025	COL2_qPCR_fwd	TGCAGCCTTTCTTTGCAAGG	PGSC0003DMT400026068	qPCR
SS1026	COL2_qPCR_rev	TTGGCAGAATGGATGTCAGC	PGSC0003DMT400026068	qPCR

3.1.5 Plasmids and vectors

Table 5. Overview of plasmids used

plasmid	description	selection *in planta*	reference
p2228	pBinAR-35S::SP6A^{cop}-HA	Kan	Kirsten Ott
p2962	pBinAR-35S::SP6A^{mod}-HA	Kan	this thesis
p2339	pRB35S-35S::GFP-SP6A^{cop}	Spec, Strep	this thesis
p2354	pGWB6-35S::GFP-SP6A	Kan	Prof. Salomé Prat (Madrid)
p2480	pBinAR-35S::STTM	Kan	this thesis
p2636	HXK+SP6A	Kan	this thesis
p2963	pBinAR-35S::SES$^{pri\text{-}miRNA}$	Kan	this thesis
p2961	pBin19-SES^{genomic}	Kan	this thesis

Table 6. Overview of vectors used

vector	description	reference
pBinAR	Binary vector, KanR	Höfgen and Willmitzer, (1999) [226]
pRB35S-GFP-OCS	Binary vector with GFP, KanR	Max Kraner

3.1.6 Plants

The following transgenic plant were used during this thesis

Table 7. Transgenic plants used

name	lines	Plasmid according to biochemistry dadatbase
SP6A^{cop}-HA	#3, #7, #8, #9	p2228
STTM	#3, # 5, #6, #7, #12	p2480
HXK+SP6A	#3, #17, #27, #28	p2636

3.1.7 Media and buffer

Table 8. Composition of media

Media	component	amount
LB	Bactor Tryptone	10 g/l
	Yeast extract	5 g/l
	NaCl	10 g/l
YEB	Bacto Cattle Extract	5 g/l
	Yeast Extract	1 g/l
	Bacto-Tryptone	5 g/l
	Sucrose	5 g/l
SOC	MgSO4	0.49 g/l
	Yeast Extract	5 g/l
	Tryptone	20g/l
	NaCl	0.584 g/l
	KCl	0.186 g/l
	$MgSO_4$	2.4 g/l
	NaOH	until pH=7.5
	Glucose	after autoclaving 1ml/l

Table 9. Buffers used

Buffer	component	amount
10x TBE	Tris	108 g/l
	Boric acid	55 g/l
	0.5 M EDTA (pH 8.0)	40 ml/l
Z6	Guanidinium chloride	8 M

	MES	20 mM
	EDTA	20 mM
	NAOH	Until pH = 7.0
	ß-ME	70µl per 10 ml
4x Laemmli	Tris pH 6.8	50 mM
	SDS	2 %
	Glycerol	10 %
	ß-ME	5 %
	Bromophenolblue	0.2 %
Transfer buffer	Tris	480mM
	Glycerol	390 mM
	Methanol	20 % (v/v)
	HCl	Until pH = 8.2
10x TBS	Tris-HCl (pH 8.0)	200 mM
	NaCl	5 M (292 g/l)
TBS-T	Tris-HCl (pH 8.0)	20 mM
	Tween 20	0.05 %
TE	Tris-HCl (pH 8.0)	10 mM
	EDTA (pH 8.0)	1 mM
TE-RNAse	TE-buffer	0.1 M
	RNase A	0.01 mg/ml
	mQ	ad 10ml
10x Running Buffer	Tris	250 mM
	Glycin	1.92 M
	HCl	until pH=8.2
	SDS	0.1 %
Solution A (Western Blot)	Tris (0.1 M)	2.4 g
	HCl	until pH = 8.6
	Luminol	50 mg
	mQ	ad 200 ml
Solution B	Para-hydroxy coumarinacid	11 mg
	DMSO	10 ml
ECL	Solution A	1 ml
	Solution B	100 µl
	H_2O_2 (30 %)	30 µl

Solution 1	Tris-HCl (pH 8.0)	25 mM
	EDTA	10 mM
	Glucose	50 mM
Enzyme extraction buffer EEP	Tris HCl pH 6,8	50 mM
	$MgCl_2$	5 mM
	DTT	5 mM
	EDTA	1 mM
	EGTA	1 mM
	glycerol	15% (v/v)
	pefabloc proteinase inhibitor	0.1 M
Incubation buffer	50 mM Na-Acetate	20 µl
	0.5 M sucrose	20 µl
	H_2O	50 µl
Imidazolbuffer	Imidazol	100mM
	$MgCl_2$	5 mM
	HCl (10%)	Until pH = 6.9
Sugar measuring buffer	Imidazolbuffer	237 µl
	ATP (20 mg/ml)	6,6 µl
	NAD (60 mg/ml)	6,6 µl
	G6PDH (350 U/mg)	0,25 µl

3.2 Methods

3.2.1 Plant growth conditions and sample taking

3.2.1.1 Potato (*Solanum tuberosum*)

Potato plants (*Solanum tuberosum* L. ‚Solara') plants were obtained from Bioplant (Ebstorf, Germany. All transgenic plants used were maintained in tissue culture. Potato plants (Solanum tuberosum L. ‚Solara') plants were grown under greenhouse conditions with 16 h supplemental light (250 µE). Plants were maintained and amplified in tissue culture on Murashige and Skoog (MS) medium [227] containing 2% sucrose. Walk-in growth chambers were used for controlled ambient and elevated temperature treatments (20 °C or 27 °C during dark period, 22 °C or 29 °C during light period, respectively) with 350 µE supplemental light. Drought stress was applied by stopping watering for 2-3 days and subsequent adjusting the relative water content (RWC) in the soil to 35 %, while in control condition RWC was 65 %. This was achieved through measurement of soil conductivity using the EM50 soil moisture sensor (Decagon, USA) and calibration of pot weight. Leaf area was measured using a LI-3100 area meter (LI-COR, USA). Plant height was measured from soil surface to apical meristem. Harvest index was calculated as ratio of tuber fresh weight per plant over green fresh weight per plant. Leaf samples were taken from fully developed source leaves (ca. 5^{th} to 8^{th} from top). Tuber samples were taken by punching through the tuber parenchyma and after removing the most outer and inner parts of the tuber slices were cut from the resulting cylinder. Dry weight was measured from a collection of about 25 slices from at least 4 different tubers.

3.2.1.2 Tobacco (*Nicotiana benthamiana*)

For transient assays three-week-old *Nicotiana benthamiana* plants were grown under greenhouse conditions with 16 h supplemental light. Samples were taken from four independent infiltrated leaves.

3.2.2 Transformation methods

3.2.2.1 Plant transformation

3.2.2.1.1 *Solanum tuberosum* transformation

Transformation of potato plants was conducted as described previously [228]. Therefore leaf discs of potato plants grown in tissue culture were incubated in MS medium [227] containing 2 % sucrose. Subsequently 50 µl of agrobacteria were added and mixed for 5 min. After incubation in the dark for 2 days leaf discs were transferred to MS medium supplemented

with 1.6 % glucose, 2 mg/l zeatinribose, 20 µg/ml NAA, 20 g/l GA_3, 0.5 g/l Claforan, 50 mg/l kanamycin and 0.8 % agar to induce callus formation. After 1 week leaf discs were kept on the same medium with reduced Claforan concentration (0.25 g/l). Every 10 days leaf discs or developing calli were put into fresh medium. After shoot formation (after 3-4 transfers), shoots were cut off the leaf disc and transferred to MS-medium containing 2% sucrose and 250 µg/ml Claforan.

3.2.2.1.2 *Nicotiana benthamiana* transformation

Transient transformation of *N. benthamiana* was conducted with *Agrobacterium. tumefaciens*. Therefore 20 ml YEB medium with respective antibiotics was inoculated with the agrobacteria carrying recombinant plasmid and incubated at 28 °C overnight. The cells were harvested by centrifugation at 4500 rpm at 4 °C. the pellet was washed with 10 mM $MgCl_2$ and resuspended in 20 ml 10mM $MgCl_2$ the optical density was adjusted to OD_{600}=0.5. The suspension was infiltrated with a syringe without needle into the abaxial side of a source leaf.

3.2.2.2 Bacteria transformation

3.2.2.2.1 *Escherichia coli* transformation

For transformation of *E. coli* 100 µl of competent *E. coli* strain XL1 blue were thawed on ice and 10 µl of plasmid added. After 30 min incubation on ice a heat shock of 42 °C was applied for 50 seconds. Cells were then cooled on ice for 5 min and regenerated in 1ml SOC medium for 1 h at 37 °C on a shaker. The cells were centrifuged for 2 min at 13000 rpm, the supernatant was discarded and the pellet resuspended in residual medium. Subsequently cells were plated on LB plates containing appropriate antibiotics and incubated overnight at 37°C.

3.2.2.2.2 *Agrobacterium tumefaciens* transformation

For transformation of agrobacteria 100 µl competent cells of strain C58C1 **(Table 1)** were thawed on ice and incubated with 15 µl plasmid DNA on ice for 30 min. Subsequently, the cells were frozen in liquid nitrogen and heat shocked at 37 °C for 5 min. For expression of resistance genes the cells were then incubated in 500 µl YEB medium for 4 h at 28°C. The cells were harvested by centrifugation, the supernatant was discarded and the pellet re-suspended in the residual medium. The suspension was plated on YEB plates with antibiotics and incubated at 28°C for 23-days.

3.2.3 DNA-related methods

3.2.3.1 Isolation of genomic DNA

Two leaf discs (=1 cm²) were homogenized with 600 µl urea buffer (7 M urea, 0.3 M NaCl, 20 mM EDTA, 50 mM Tris-HCl, pH 8.0), mixed and centrifuged (5 min 13000 rpm). Five hundred µl of supernatant were transferred to a new reaction tube. By adding 500 µl of isopropanol and centrifugation (10 min 13000rpm) the DNA was precipitated. After washing with 500 µl 70% EtOH, the pellet was dried for 5 min at 37 ° C, dissolved in 30 µl TE buffer (50 mM Tris HCl, 1 mM EDTA, pH 8.0) at 37 ° C and stored at 4 ° C.

3.2.3.2 Polymerase chain reaction

For amplification of DNA fragments the polymerase chain reaction was used with different primers. Although annealing temperature varied a standard PCR assay was performed as follows:

Table 10. Standard PCR reaction mix per sample

component	amount
Template (gDNA/cDNA)	1 µl
forward Primer (4 µM)	1 µl
reverse Primer (4 µM)	1 µl
dNTPs (25 mM)	0.5 µl
Buffer 10x	2.5 µl
DNA-Polymerase Taq	0.5 µl
H_2O	18.5 µl

Table 11. Standard PCR program

PCR program		
95°C	2 min	
95°C	30 s	33 cycles
59°C	30 s	
72°C	30 s	
72°C	10 min	
12°C	∞	

3.2.3.3 Agarose gel electrophoresis

In order to purify the desired PCR fragment or analyze the PCR reaction an agarose gel electrophoresis was carried out. The PCR products (DNA fragments) were run on an agarose gel 1-2 % following the separation according to size. For a 1 % agarose gel 1 g agarose gel was dissolved in 100 ml TBE buffer and heated in a microwave. Ethidium bromide was added in order to visualize the DNA under UV light for easy excision of the desired fragment.

3.2.3.4 Gel extraction of DNA from agarose gels

DNA fragments for cloning were cut form the gel using a scalpel and processed with the QIAquick Gel Extraction Kit following the manufacturer's instructions.

3.2.3.5 Ligation

DNA fragments were cloned into the respective destination vector using T4-DNA ligase in an appropriate T4 DNA ligation buffer at 16°C overnight to be transformed into *E. coli.*

Table 12. Ligation mixture

component	amount
insert	5 µl
vector	2 µl
T4DNA ligase	3 µl
10x ligation buffer	4 µl
mQ	ad 20 µl

3.2.3.6 Plasmid DNA isolation

For plasmid isolation with alkaline lysis bacteria were grown in 3 ml of LB medium with appropriate antibiotics overnight. Cells were transferred in 1.5 ml reaction tubes and harvested by centrifugation at 13000rpm for 1 min. The pellet was resuspended in 100µl solution 1. Next, 200 µl solution 2 (0.2 M NaOH, 1 % SDS ; mixed fresh before use) were added for cell lysis and mixed gently. Then 150 µl 3 M NaAc pH 4,8 were added and mixed by inverting. The cellular debris was removed by centrifugation for 5 min at 13000 rpm. The supernatant was transferred to a new reaction tube where the DNA was precipitated by adding 900 ml 100 % EtOH and centrifugation for 10 min at 13000rpm. The pellet was washed with 500 µl 80 % EtOH, dried and resuspended in 30 µl TE/RNAse.

3.2.3.7 Restriction analysis

Restriction digestion was performed to prepare fragments or to verify successful cloning (i.e. to prove whether a fragment of the correct size has been inserted into the vector). A typical

restriction assay was performed in 20 ml total volume containing 1x restriction buffer and the plasmid DNA at 37° C for 1 h (or 2 h for preparative DNA digestion) followed by heat inactivation of the enzyme if necessary. The amount of enzyme and DNA was chosen depending on the amount of the DNA and type of restriction enzyme used.

A typical digestion was carried out as follows:

Table 13. Reaction mixture

Preparative digestion mix	**amount**
DNA (Plasmid/ vector)	2 µl
restriction enzyme I	0.5-1.5 µl
restriction enzyme II	0.5-1.5 µl
restriction buffer	2 µl
mQ	ad 20 µl

3.2.3.8 Sequencing

After the insertion of a fragment has been verified by restriction analysis the sequence correctness was confirmed by Sanger sequencing at GATC-Biotech. An aliquot of 2 µl plasmid in 30 µl mQ was sent in to be sequenced via appropriate primers.

3.2.3.9 Gene synthesis

The sequences of *SP6A*^{cop}-HA **(Figure 3)** and STTM **(Figure 20)** were synthesized by GeneArt (Thermo Fisher).They were subsequently cloned into the pBinAR binary vector and transformed into potato (cv. ‚Solara') by *Agrobacterium*-mediated gene transfer to generate *SP6A*^{cop}-HA, STTM and HXK+SP6A overexpressing lines [228].

3.2.3.10 Golden Gate cloning method

The double construct was generated using the GoldenGate cloning system [229–231] by assembling synthetic or PCR amplified gene sequences and modules available from MoClo plant part kits (www.addgene.org) [232] into level 0 and subsequently level 1 vectors to generate the plasmids StLS1::*StSP6A* and KST1::*AtHXK1*. Both plasmids were combined with a Kanamycin-resistance cassette (pICSL70004) into a level 2 vector (pAGM4237, Addgene) which was transformed into potato cv. Solara by *Agrobacterium*-mediated gene transfer to generate the HXK+SP6A lines [228]. An overview of modules used to generate the plasmid is provided in **Table 14.**

Table 14. Golden Gate construct design

Direction	→	←	→	
Position	**1 fwd**	**2 rev**	**3 fwd**	
Name	**HXK**	**SP6A**	**Kanamycin**	Endlink 3
Promotor	KST	StLS1, pICH41551	AtuNOS, pICH87633	pICH41766
5UTR	*AtHXK1* (5'UTR)	*PVX*, pICH44199	TMV, pICH87633	
CDS1	*AtHXK1* (AT4G29130.1)	*StSP6A*, PGSC0003DMT400060057	Kanamycin	
3UTR+ter	*OCS*, pICH41432	*AtAct2*, pICH44300	35S	

3.2.4 RNA-related methods

3.2.4.1 RNA isolation

Samples of source leaves were taken during the first half of the light period, 4 h after dawn. Total RNA was isolated from ca. 100 mg of frozen leaf material by grinding in 1 ml 8 M guanidiumchloride with 0.7 % β-ME [233]. Five hundred µl phenol:chloroform isoamylalcohol (25:24:1) were added to inactivate RNase proteins and vortexed. Phases were separated by 10 min centrifugation at 15000 rpm. From the supernatant 900 µl were transferred to a new reaction tuber where 660 µl EtOH and 40 µl 1 N acidic acid were added to precipitate RNA. After vortexing the RNA was pellet for 10 min at 15000 rpm. The pellet was first washed with 500 µl 3 M NaAc pH 5.2 and then with 500 µl 80 % EtOH. The pellet was dried and resolved in 30 µl DEPC treated water and cooked for 5 min at 65 °C. RNA quantity was measured with ND-1000 Spectrophotometer (NanoDrop Technologies). To verify the integrity of the RNA an aliquot of the sample was loaded on an agarose gel.

3.2.4.2 cDNA synthesis

For cDNA synthesis 1.5 µg RNA was used. To exclude contamination with genomic DNA a DNAse digestion was performed for 45 min at 37 °C. DNase was inactivated by incubation at 65 °C for 10 min.

Table 15. DNAse digestion mix per sample/reaction tube

component	**amount**
RNA	1.5 µg
10x DNAseI $MgCl_2$ buffer	1 µl
DNAse I	1 µl
DEPC-H_2O	ad 10µl

Next, components for cDNA synthesis were added and incubated for 5 min at 65°C followed by 7 min at 37 °C. Subsequently an RNase inhibitor and reverse transcriptase were added.

Table 16. cDNA synthesis reaction mix per well

component	amount
DNAse treated sample	11 µl
5x M-MLV buffer	4 µl
10mM dNTPs	2 µl
50µM oligo-dT 30 primer	1 µl
DEPC-H2O	2 µl
RiboLock™ RNase inhibitor (Thermo)	0.5 µl
RevertAid™ H Minus Reverse Transcriptase (Thermo)	0.5 µl

The reaction was incubated for 2 h at 42 °C and stopped by 70 °C for 10 min. The cDNA was stored at -20 °C. The cDNA synthesis was tested by a PCR using standard protocol **(Table 10)** with primers specific for the housekeeping gene actin.

3.2.4.3 Real Time quantitative PCR (RT-qPCR)

In order to quantify gene expression Real Time quantitative PCR (RT-qPCR) was carried out on an AriaMx device (Agilent Technologies). The housekeeping gene Ubiquitin served as a reference gene (PGSC0003DMT400013321). Usually four biological replicates were analyzed on a 96 well plate in 20 µl reaction assay each.

Table 17. qPCR reaction mix per well

component	amount
cDNA (diluted 1:50)	5 µl
Primer forward (4 µM)	1 µl
Primer revers (4 µM)	1 µl
2x GoTaq qPCR Master Mix	10 µl

Table 18. qPCR standard program

qPCR program	
95 °C	2 min
95 °C	5 s

60 °C	30 s 40 cycles
95 °C	30 s
55 °C	30 s
95 °C	30 s

The Ct value (threshold cycle) were obtained using the Agilent AriaMx program, and fold change in gene expression was determined via the Ct methods as described by Livak and Schmittgen [234].

3.2.4.4 Microarray analysis

Samples for the microarray experiment were taken from tubers 19 days post-harvest. For each replicate eight buds from 4 different tubers were pooled. Sample preparation and labelling were performed by Stephen Reid (AG S. Sonnewald) according to the one-color microarray-based gene expression analysis protocol (v.6.6) including the one-color RNA spike-in kit (Agilent Technologies, Santa Clara, USA). After fragmentation, Cy3-labelled samples were loaded on 8 × 60 K arrays (Agilent Technologies AMADID 033033, [136] and hybridized overnight (17 h, 65 °C). Slides were washed and scanned with a high-resolution scanner (Agilent Technologies,Santa Clara, USA) and aligned with the appropriate template file. The microarray experiment can be found at https://www.ebi.ac.uk/arrayexpress/experiments/E-MTAB-7387.

Data were extracted using feature extraction (v.11.5.1) software by applying the protocol (GE1_1105_Oct12), and generated .txt files were imported into GeneSpring GX (v.12.6) software (Agilent Technologies, Santa Clara, USA) for further analysis. Data were normalized using default settings: intensity values were set to a minimum of one, followed by log2 transformation, per chip normalization to the 75th percentile, and baseline correction to the median of all samples. Entities that passed the quality check (“flags” detected) and showed changes in expression equal or more than twofold were subjected to a one-way analysis of variance against control samples ($P \leq 0.05$) with Benjamini–Hochberg multiple test corrections [235]. A volcano plot was applied to identify statistically significant ($P \leq 0.05$), equal, or more than twofold (FC ≥ 2) differentially expressed entities by pairwise comparison against WT. Functional categorization was taken from Hancock et al. (2014) [136] or was accomplished by homology search against the Arabidopsis genome (www.arabidopsis.org). Hierarchical clustering of genes was performed using Euclidian similarity measure with averaged samples.

3.2.4.5 MiScript qPCR

MiScript qPCR was performed following the manufacturer`s instructions (Qiagen Cat No. ID: 218761, Cat No. ID: 218073).

RNA was diluted to a concentration of 50 ng/µl. In the first step an RNA adaptor is ligated to all small RNAs in the sample. Therefore a master mix of the component was added except for the ligation activator which was added in the end.

Table 19. Adaptor ligation reaction mix per well

component	amount
10x MiScript ligation buffer	2 µl
10x MiScript plant adaptor	2 µl
H_2O	2 µl
Plant RNA ligase	1 µl
RNA	3 µl
2x MiScript ligation activator	10 µl

The mixture is incubated for 1 h at 16 °C then 20 min at 65 °C and cooled at 4 °C. After equilibration at room temperature, to make the ligation activator more fluid, the reaction mix for cDNA synthesis is prepared.

Table 20. MiScript cDNA synthesis reaction mix per well

component	amount
5x RT-Buffer	4 µl
10x RT-nucleics	2 µl
H_2O	9 µl
Reverse transcriptase	1 µl
Ligation product	4 µl

The mixture is incubated for 2 h at 37 °C, then heated for 5 min at 95 °C and cooled at 4 °C. The cDNA is stored at -20 °C, and qPCR can be carried out as follows.

Table 21. MiScript qPCR reaction mix per well

component	amount
Quanitect SYBR Green	10 µl

MiScript Universal Primer	2 µl
MiScript Primer Assay	2 µl
H_2O	1 µl
cDNA (diluted 1:50)	5 µl

Table 22. MiScript qPCR program

qPCR program		
95°C	15 min	
94°C	15 s	45 cycles
55°C	30 s	
70°C	30 s	

3.2.4.6 5`RACE

RNA ligase mediated rapid amplification of 5'-cDNA ends (RLM-5'RACE) was performed with *Solanum tuberosum* group Andigena ADG573 leaf material using the GeneRacer Kit (ThermoFisher) following the manufactures instructions.

3.2.5 Protein methods

3.2.5.1 Protein isolation

Protein extraction was performed as previously described by Laemmli [236]. Leaf discs of source leafs (1 cm^2) were homogenized with 100 µl 2x buffer (50mM Tris-HCl, pH 6.8, 2 % SDS, 10 % glycerol, 0.002 % bromophenolblue, 5 % β-mercaptoethanol). The extracts were boiled at 95 °C for 15 min and centrifuged at 4 °C for 2 min to remove cell debris. In pockets of 12.5 % Polyacrylamide gels 20 µl of the supernatant were loaded. For size estimation 5 µl of PAGE Ruler Prestained Protein ladder (ThermoFisher Scientific) were run alongside the samples.

3.2.5.2 SDS polyacrylamide gel electrophoresis

Sodium dodecylsulfate polyacrylamide gels were used for protein separation according to their size. As described in **Table 23**, 20 µl of the supernatant were loaded onto a 12.5 % SDS polyacrylamide gel,. After polymerization the gel cassette with the separation gel at bottom and the stacking gel with the sample pockets on top was placed in an electrophoresis tank with 1x Running Buffer containing 0.1 % SDS. The gel was run at 120 V for 20 min and subsequently at 150 V for 50 min.

Table 23. SDS-polyacrylamide gel composition

component	amount (Separation gel)	amount (Stacking gel)
3 M Tris-HCl (pH=8.8)	1.12 ml	-
1 M Tris HCl (pH 6.8)	-	625 µl
AA/BAA	3 ml	625 µl
mQ	4.7 ml	1. ml
TEMED	4.5 µl	2.5 µl
ammonium persulfate APS (10% w/v)	67.5 µl	25 µl
SDS (10 %)	90 µl	50 µl

3.2.5.3 Western Blot

Proteins were transferred onto a nitrocellulose membrane (Amersham™ Protran™ 0.45 NC, GE Healthcare) via semidry blot. Therefore three layers of whatman paper soaked with 1x transfer buffer (containing 20 % v/v Methanol) were stacked on the anode followed by a nitrocellulose membrane, the gel and again three layers of whatman paper. Blotting was conducted over 50 min at 150 mA constant electric current. After blotting the membrane was blocked in 5 % skimmed milk powder in TBS-T buffer at room temperature for 60 min. Antibodies were prepared in 1 % milk-TBS-T and incubated overnight at 4 °C. After washing three times for 15 min with TBS-T the membrane was incubated with ECL mix in a darkroom. An X-ray film was exposed until signal could be detected. The film was developed in an Optimax X-ray film processor. Protein blotting was confirmed afterwards by Ponceau staining of the membrane.

3.2.5.4 Bradford assay

Protein contents were determined by measuring absorbance at 595 nm using Bradford reagent (B6916; Bio-Rad Laboratories, USA) [237]. A bovine serum albumin (BSA) calibration curve with defined amounts of protein was used to determine how much protein is in a solution. Three replicates of 0, 1, 2, 3, 4, 5 and 10 µg BSA were combined with 300 µl Bradford reagent (diluted 1: 5 in mQ). Five µl of each sample were added to 300 µl of Bradford reagent and incubated dark at RT for 5-10 min before measuring.

3.2.5.5 Measurements of cell wall-bound invertase and sucrose synthase

Enzymes were extracted from frozen tissue samples (ca. 50 mg) with 500 µl enzyme extraction buffer (EEP) in liquid nitrogen and centrifuged for 10 min at 13000 rpm. All steps were carried out at 4 °C. The pellet was washed twice with 500 µl 5 mM Tris HCl pH 7.0 and

stored at -80 °C. For measurements of cwInv activity the pellet was incubated for 90 min with 90 µl incubation buffer. The reaction was stopped by adding 10 µl 1 M Tris HCl pH 8.0. All samples were spinned down for 2 min at 13000 rpm. Of the supernatant 10-20 µl was incubated with 250 µl sucrose measuring buffer and glucose content was measured by coupled optical test at 340 nm wavelength.

Sucrose synthase (SUSY) activity was extracted as described above for cwInv. Sucrose hydrolytic activity was measured after incubation of the pellet for 90 min with 0.1 M sucrose and coupled optical assay using UDP-glucose as substrate [17].

3.2.6 Starch determination

Starch was extracted using ca. 50 mg of tuber fresh weight grinded in 500 µl 80 % Ethanol and washed with 900 µl 80 EtOH. Pellets were incubated with 1 ml 0.2 M KOH overnight, heated at 95 °C for 90 min and neutralized with ca. 240 µl 1 N acidic acid. An aliquot of 10µl was digested with 90 µl 2 mg/ml Amyloglucosidase diluted in 50 mM sodium acetate buffer pH 5.2. Afterwards glucose contents were determined using a coupled optical assay as described previously [152].

3.2.7 Photosynthesis measurements

Photosynthesis and transpiration rates were measured under greenhouse conditions on fully developed source leaves on the upper middle stem (5^{th} – 8^{th} from top) using a LI-COR 6800 device. All measurements were conducted between three and six hours after dawn (09:00 - 12:00 a.m.) under the respective greenhouse conditions (400-600 µmol m^{-2} s^{-2} light, 400-500 µmol mol^{-1} CO_2, 50 % relative humidity). Temperature was also adjusted according to the treatment in the greenhouse (22 °C and 29 °C, respectively).

3.2.8 ABA measurements

Phytohormones were extracted as described by Pan *et al.,* 2008 [238]. Leaf samples were grinded in liquid nitrogen using acidic buffer (66 % Isopropanol, 0.0002 % HCl). Samples were shaken 30 min at 4 °C followed by adding 2 fold volume chloroform extraction and another incubation at 4 °C while shaking. After centrifugation for 10 min at 4000 rpm at 4 °C the lower phase was transferred to a new reaction tube and vacuum dried at room temperature for 40 min. The pellet was resolubilized in 80 µl methanol. For chromatography 10 µl were injected into a luna C18 RP-column (250x4.6mm, Phenomenex) with precolumn installed in an ICS 3000 HPLC system (Dionex). The flowrate was 0,3 ml/min at 30 ºC with a binary gradient consisting of buffer A (H_2O/ 0.75 % acidic acid, pH 2.55) and buffer B (ACN/ 0.75 % acidic acid) with 0-5min 20 % B, 5-26 min 46 % B, -27 min 90 % B, 27-32 min 90 % B, -34 min 20 % B, 34-45 min 20 % B. The ABA content was measured with a QTrap 3200

mass spectrometer (ABI, Sciex) with ESI-MS/MS and negative ionisation in MRM mode at -4500 volt. Ionsource temperature was 600 ºC. The recorded Q1/Q3 mass transition for ABA was 263/153 Da. Dwelltime was 75 ms, while potentials for DP and Ep were -25 V, CEP and CE -4 V, and CXP was -22 V. Peak areas were quantified by comparison with a standard curve between 0.1 and 500 nM derived from pure ABA purchased from Sigma. Recovery of 3 pmol spiked pure ABA into 100 mg tissue was 98 ± 15.5%.

3.2.9 Proline measurements

Proline contents were measured via HPLC from the same extracts as done for ABA. The samples were re-suspended in purest water and used for HPLC analysis [239]. Prior to the measurement, primary and secondary amino acids were derivatized using 6-aminoquinolyl-N-hydroxysuccinimidylcarbamate (AQC reagent) as a fluorescing substance. Using a reversed phase HPLC (Dionex summit) concentrations of 17 aminoacids were determined. The HPLC consists of a gradient pump, a degasing module, an autosampler and a fluorescence detector RF2000. Chromatograms were recorded using the software chromeleon. The gradient was accomplished with a buffer A (140 mM sodium acetate, pH 5.8 (Suprapur, Merck) and 7 mM triethanolamine (Sigma, Germany)). Acetonitrile (Roti C Solv HPLC, Roth) and HPLC water (Baker) were used as eluents B and C respectivelly. To separate amino acids, a reversed phase C18 column (phenomenex, 4.6 x 250 mm) was used which consists of a modified apolar as matrix. The gradient was produced as follows by 1%, 5 %, 9 %, 18 %, 60 % and 0 % of eluent B at 0.5 min, 27 min, 28.5 min, 44.5 min, and 47.5 min and 50.5 min retention time. The column was equilibrated 10 minute with buffer A at a flow rate of 1 ml per minute and heated at 37 °C during the whole measurement. Sample components were detected and quantified by fluorescence with excitation at 300 and emission at 400 nm [239].

3.2.10 Microscopy methods

3.2.10.1 Light microscopy

In order to measure the length to width ratio of stomata source leaves were coated with transparent nail polish (Ultra quick dry top coat, dm, Germany) by brushing the abaxial side of fully developed source leaves 4 h after dawn. The coatings were immediately removed after drying and photographed with a Leica DMR Microscope. Lengths were measured using the FIJI software.

3.2.10.2 Esculin loading experiments

In order to visualize assimilate transport in the phloem an esculin loading assay was conducted. First, to remove the cuticle from source leaves, the leaf surface was gently

roughened with sandpaper. Per leaf 1 ml Esculin (CAS 66778-17-4, Merck, Germany) was loaded as 10 mg/ml solution. To avoid evaporation the loaded leaves were covered with parafilm. Esculin was excited with a HBO 50 mercury lamp, fluorescence was filtered with a DAPI filter and photographed with a Leica DMR Microscope. Lengths were measured using the FIJI software.

3.2.11 Floating assays

For floating assays, each well of a 12-well plate was filled with 5 ml of 50 µM ABA solution. For one well, i.e. one biological replicate, four leaf discs from four different plants were placed on the liquid surface with the abaxial side down. The plate was incubated under greenhouse conditions for six hours before leaf discs were immediately frozen in liquid nitrogen for subsequent RNA extraction.

4 RESULTS

4.1 small RNA mediated regulation of SP6A modulates heat dependent source sink development in potato

4.1.1 Overexpression of codon-optimized SP6A (SP6A^{cop} –HA) in potato

4.1.1.1 Overexpression of SP6A^{cop}-HA strongly affects source sink balance

To study the tuberization process in potato, *SP6A* was overexpressed in a cultivated potato background. Therefore, codon usage was optimized to improve the expression level of SP6A and avoid transgene silencing. Overall, 24% of the nucleotide sequence in the optimized *SP6A* sequence was altered **(Figure 3)**.

```
Nucleotide alignment of 2 sequences: SP6A, SP6A cop

Score = 1485.0, Identities = 397/549 (72%), Positives = 397/549 (72%), Gaps = 27/549
(4%)

SP6A          1 ATGCCTAGAGTTGATCCATTGATAGTTGGTCGTGTGATAGGTGATGTTTTAGATCCATTC  60
                ATGCC AG GTTGA CCATTGAT GTTGG  G GT AT GG GATGT TT GA CCATT
SP6A cop      1 ATGCCAAGGGTTGACCCATTGATTGTTGGAAGGGTTATTGGAGATGTGTTGGACCCATTT  60
                                    #1                                #2
SP6A         61 ACTAGGTCTGTTGATCTTAGAGTTGTTTATAATAATAAAGATGTGAACAATGCATGTGTG 120
                ACTAGGTC GTTGAT T AG GTTGT TA AATAA AA GATGT AACAATGC TG GTG
SP6A cop     61 ACTAGGTCAGTTGATTTGAGGGTTGTGTACAATAACAAGGATGTTAACAATGCTTGCGTG 120
                  #3                #4
SP6A        121 TTGAAACCTTCACAAGTTGTTATGCAACCTAGGGTTCATATTGGAGGGGACGATCTTCGC 180
                TTGAA CCTTC CAAGTTGT ATGCAACC AG GTTCA ATTGGAGG GA GA  T  G
SP6A cop    121 TTGAAGCCTTCTCAAGTTGTGATGCAACCAAGAGTTCACATTGGAGGTGATGACTTGAGG 180

SP6A        181 AACTTTTACACTCTGATTATGGTGGATCCTGATGCTCCAAGCCCAAGCGACCCTAACTTG 240
                AACTT TACACTCT ATTATGGT GATCCTGA GCTCCA   CCA   GA CCTAACTT
SP6A cop    181 AACTTCTACACTCTTATTATGGTTGATCCTGACGCTCCATCACCATCAGATCCTAACTTA 240

SP6A        241 AGGGAGTATCTACATTGGCTGGTCACAGATATCCCAGCAACTACAAATACAAGCTTTGGA 300
                AG GAGTA  T CA TGG TGGT AC GATAT CCAGC AC AC AA AC    TT GGA
SP6A cop    241 AGAGAGTACTTGCACTGGTTGGTTACTGATATTCCAGCTACAACTAACACTTCATTCGGA 300

SP6A        301 AATGAAGTCGTATGCTACGAGAATCCAACACCTACGATGGGAATTCATCGATTCGTTTTG 360
                AA GA GT GT TGCTA GAGAA CCAAC CCTAC ATGGG ATTCA  G TTCGT TT
SP6A cop    301 AACGAGGTTGTGTGCTATGAGAACCCAACTCCTACTATGGGTATTCACAGGTTCGTGTTA 360

SP6A        361 GTTTTATTTCGACAATCAAGACGTGAAACAGTGTATGCCCCAGGTTGGCGTCAAAATTTC 420
                GT TT TTT G CAATCAAG  G GA AC GTGTA GC CCAGG TGG G CA AA TT
SP6A cop    361 GTGTTGTTTAGGCAATCAAGGAGAGAGACTGTGTACGCTCCAGGATGGAGGCAGAACTTT 420

SP6A        421 AACACAAGAGACTTTGCTGAGCTTTACAATCTTGGATTGCCTGTTGCAGCTGTTTACTTC 480
                AACAC AGAGACTT GC GAG T TACAA  T GGATT CCTGTTGC GC GT TACTTC
SP6A cop    421 AACACTAGAGACTTCGCAGAGTTGTACAACTTGGGATTACCTGTTGCTGCAGTGTACTTC 480

SP6A        481 AATTCCCATAGGGAGAGTGGCACTGGAGGACGTCGCGCATAA------------------ 522
                AA TC CA AGGGAG   GG ACTGGAGG  G  G GC TA
SP6A cop    481 AACTCACACAGGGAGTCAGGAACTGGAGGTAGGAGAGCTTACCCTTATGATGTGCCAGAC 540

SP6A            ---------

SP6A cop    541 TACGCATAA 549
```

Figure 3. Sequence alignment of SP6A and *SP6A^{cop}*-HA construct. Bold letters in *SP6A* and *SP6A^{cop}* sequence indicate small RNA (*SES*) binding site. Arrows indicate the putative post-transcriptional cut sites of the *SP6A* transcript as revealed from 5`RACE. (from Lehretz *et al*., 2019)

This sequence, designated *SP6A^{cop}*, was fused to an HA tag and cloned into a binary vector under the control of the CaMV35S promoter. *Agrobacterium tumefaciens* C58C1 was used to generate the transgenic potato *S. tuberosum* subsp*. tuberosum* L. plants (cv. Solara). Western blot and quantitative real-time PCR (qPCR) confirmed strong SP6A^{cop} expression in four out of ten transgenic lines generated (designated SP6A^{cop}-HA) **(Figure 4a, 4b)**.

During cultivation in tissue culture it could be observed that SP6A^{cop}-HA plantlets grew very weakly and some of them, particularly lines # 3 and # 7, already formed small green tubers.

After the plants had been transferred to the soil, growth was still impaired compared to the wild-type (WT) **(Figure 4c)**. As expected, tuberization was strongly stimulated by *SP6A*^{cop} expression **(Figure 4c)**. After two weeks, SP6A^{cop}-HA plants had already formed tubers whereas WT plants which had up to ten times more green biomass did not even have swollen stolons, and where tuberizing two weeks later **(Figure 4c).**

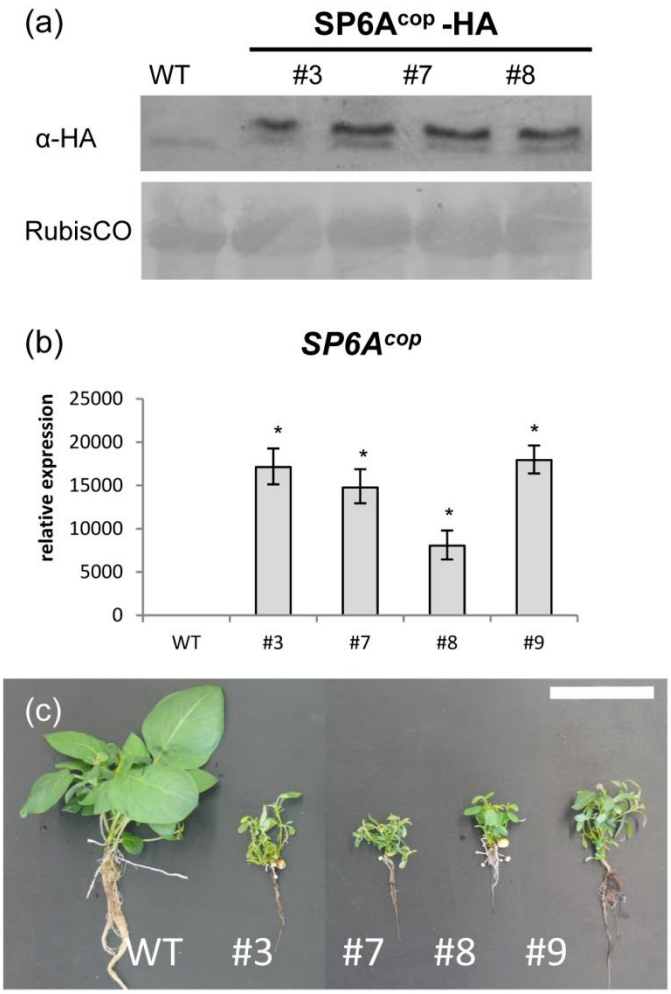

Figure 4. Characterization of transgenic potato plants overexpressing *SP6A*^{cop}-HA. (a) Western Blot analysis of transgenic lines (#3, 7, 8, 9) and wild-type plants (WT) using anti-HA antibody. Ponceau-red stained RubisCO band is shown as loading control. **(b)** Expression of *SP6A*^{cop} was determined by qPCR; bars represent the mean of three independent biological replicates ±SD; Significance compared to wild type was determined by two-tailed t-test (*; p-value < 0.05) **(c)** phenotype of *SP6A*^{cop}-transgenic plants 14d after planting from tissue culture; one representative of 10 plants is shown; the experiment was repeated three times with similar results; scale bar = 5 cm. (from Lehretz *et al*., 2019)

When plants were grown from tubers instead of tissue culture plantlets **(Figure 5a)**, shoot growth was still impaired, since the plants always remained smaller than the WT **(Figure 5b)**, but less pronounced than in tissue culture plants **(Figure 3)**. Strikingly, tuberization of SP6A^{cop}-HA plants started again very early, about two weeks before WT plants **(Figure 5c)**.

Since these plants did not suffer from severe growth defects, but exhibited the early tuberization phenotype, all further experiments were performed with plants grown from tubers. Green biomass accumulation was still less in the transgenic lines (about 20-30 g/plant) than in the WT (about 40 g/plant) **(Figure 5d),** which is consistent with the slower shoot growth. The early initiation of tuberization in SP6A^{cop}-HA lines was associated with a significantly increased total tuber yield **(Figure 5e)**. Total tuber fresh weight was about 1.2-1.9 times more than in the WT. Consequently the harvest index (yield/green biomass) for the transgenics was clearly increased, at least doubled **(Figure 5f)**. Apparently, in the SP6A^{cop}-HA overexpressing plants the translocation of assimilates into the tubers began earlier than in WT plants, suggesting a shift towards sink development.

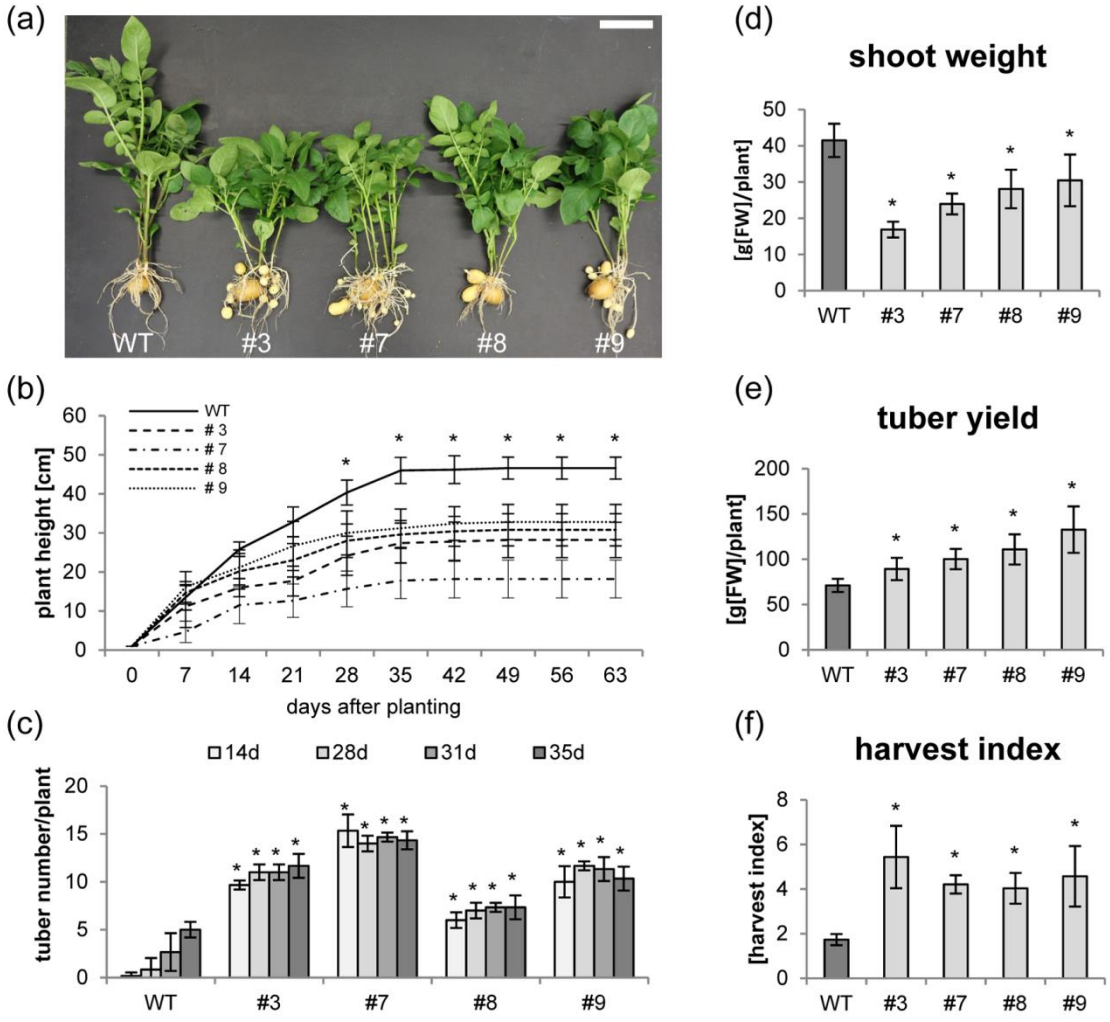

Figure 5. *SP6A^{cop}-HA* overexpression in potato plants induces early tuberization and alters biomass partitioning. (a) Tuber induction occurs earlier in *SP6A^{cop}*-HA lines (#3, 7, 8, 9) than in wild-type plants (WT). Pictures were taken two weeks after planting (scale bar=10 cm) **(b)** Shoot growth of SP6A^{cop}-HA and WT plants was monitored weekly. Values are the mean of 10 plants ± SD **(c)** Number of tubers formed was counted weekly. Values are the mean of 3 plants ± SD **(d)** Shoot weight **(e)** Tuber yield **(f)** Harvest index **(d-f)** FW = fresh weight,

Values are the mean of 10 plants ± SD harvested at the age of 9 weeks; p-values were calculated by two tailed *t*-test by comparing transgenic lines vs. WT (* $p < 0.05$). (from Lehretz *et al*., 2019)

4.1.1.2 Overexpression of SP6A^{cop}-HA forces storage organ development

The length of the dormancy period was not altered in the SP6A^{cop}-HA tubers. In fact, breakage of dormant buds occurred basically at the same time (after about three months) as in WT tubers **(Figure 6a)**. After about six month of storage in the dark, WT tubers formed etiolated shoots from the buds. Contrary to this, almost all SP6A^{cop}-HA tubers produced daughter tubers **(Figure 6b)**.

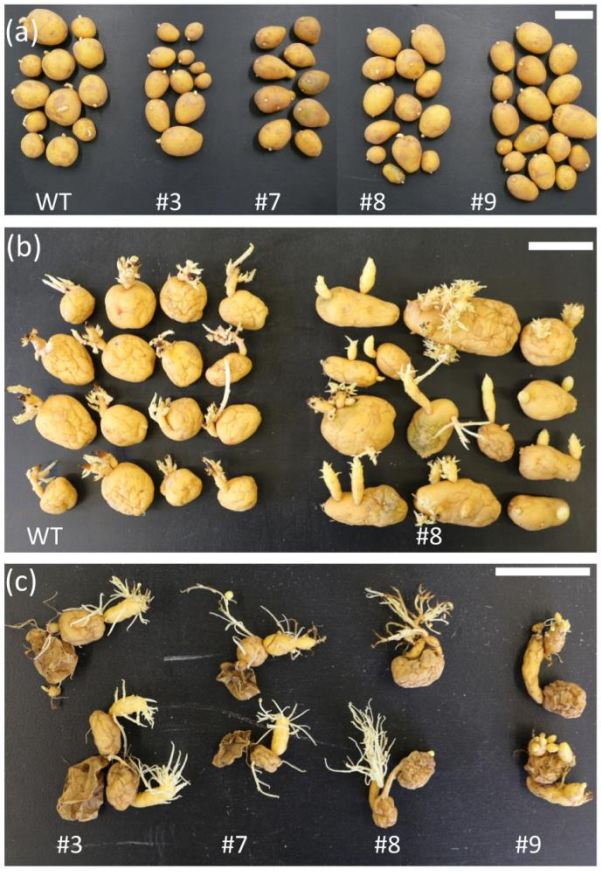

Figure 6. Phenotype of *SP6A^{cop}* overexpressing tubers. (a) Phenotype three months after harvest **(b)** Phenotype six months after harvest **(c)** Phenotype 10 months after harvest; tubers were stored at room temperature; experiment was repeated four times with similar results; scale bar = 5 cm.

From these daughter tubers again granddaughter- and great-granddaughter tubers were formed within ~10-14 months after harvest when the tubers were stored in the dark **(Figure 6c).** This process seems to go on until the resources are exhausted **(Figure 6c).** This suggests that expression of *SP6A* alters meristem identity and promotes tuber growth rather than shoot growth. Surprisingly when tubers were potted into soil shortly after sprouting had begun, most of the SP6A^{cop}-HA tubers where developing rather normal looking shoots **(Figure 7)**.

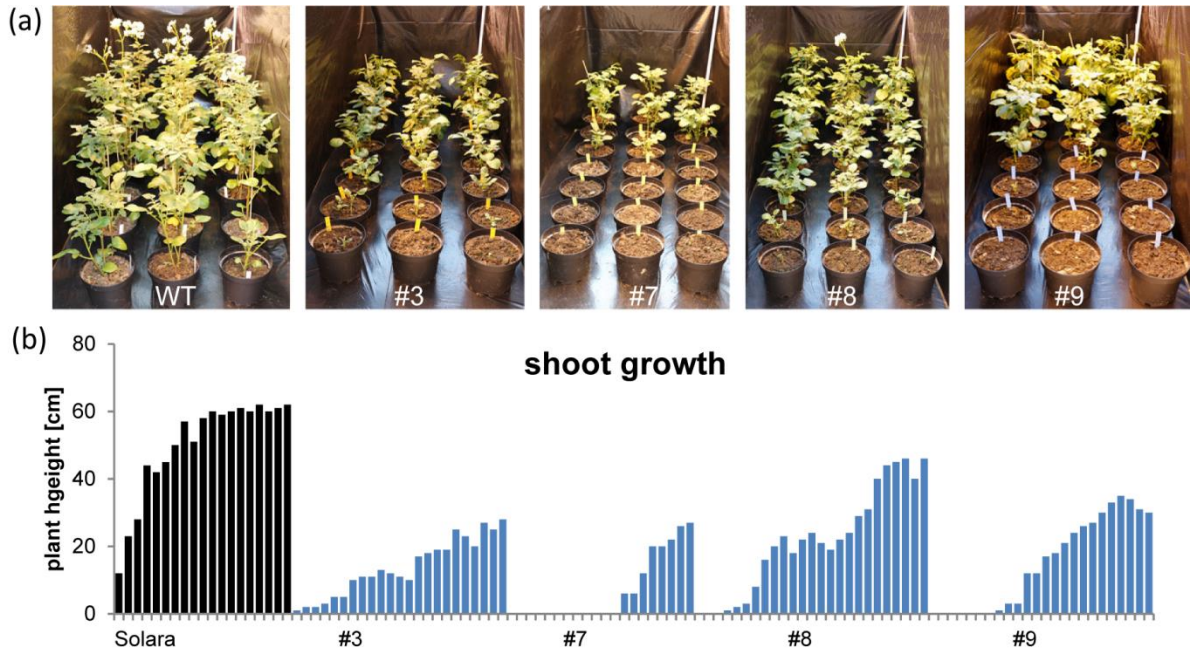

Figure 7. Phenotype of SP6A^{cop}-HA plants grown from tubers. (a) Shoot phenotype of SP6A^{cop}-HA plants eight weeks after potting **(b)** Plant height measured eight weeks after potting; one bar represents one plant of the population.

For upcoming experiments, only plants at the same stage of development were sampled. However, in some individuals, especially in lines # 3 and # 7 (with strong overexpression) development of green biomass was impaired in such a way that either no shoots appeared above the soil or, if at all, extremely late when the WT was already going into senescence **(Figure 7)**.

4.1.1.3 Overexpression of *SP6A^{cop}-HA* alters meristem identity

In order to understand better why SP6A^{cop}-HA tubers preferentially produced new daughter tubers, microarray experiments were performed on dormant tuber buds (sampled 19 days after harvest) consisting of three transgenic lines (# 3, # 7, #9) and WT. Although there were no visible differences at this time, changes in gene expression could determine the fate of meristematic cells at an early stage. A total of 677 transcripts were detected which showed significantly different ($p \leq 0.05$) expression in at least one transgenic line compared to the wild type **(Table S1)**. Among these, 437 transcripts were regulated in the same way in all three transgenic lines. Of these, 245 transcripts with a log2-fold change of ≥ 0.5 or ≤ -0.5 were filtered and analyzed more deeply **(Table S1)**. The functional assignment revealed an accumulation of transcriptional regulators (~ 9 %, 21 transcripts). Eighteen of them were upregulated, while three were slightly down-regulated in the tubers of the transgenic lines **(Figure 8)**.

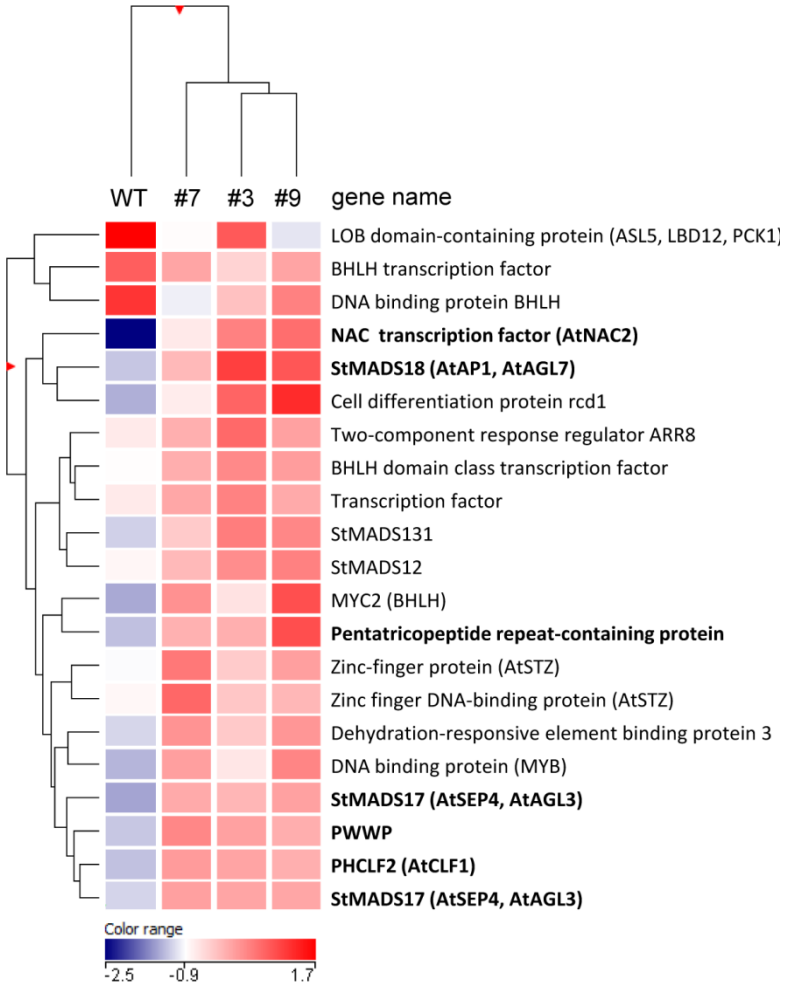

Figure 8. Expression pattern of transcripts within the functional group "RNA regulation of transcription" differentially expressed in dormant buds of SP6A^{cop}-HA tubers. Normalized values were clustered using Euclidean algorithm under standard conditions in GeneSpring 12.6 GX; gene names marked in bold letters changed more than 2-fold as compared to WT. (from Lehretz *et al*., 2019)

Further analysis revealed that three MADS box transcription factors were present among the upregulated transcripts **(Figure 8)**. They code for *StMADS12*, *StMADS17* and *StMADS18*, respectively [240]. *StMADS17* has homology to AGAMOUS-like (AGL) 3 / SEPALLATA (SEP) 4 from Arabidopsis, StMADS18 to AGL7, while the closest homolog of StMADS12 is OsMADS50. In Arabidopsis and rice, these proteins are involved in the regulation of floral meristem development [241–244]. Remarkably, AGL3 / SEP4 plays an important role in the determination of meristem identity [241]. In addition, *PHCLF2*, a gene very similar to *A. thaliana* Curly Leaf (CLF), was also increased in tubers of *SP6A^{cop}-HA* overexpression lines **(Figure 8).** AtCLF is part of the Polycomb repression complex 2, which plays an important role in the control of FT transcription and therefore flowering time [245–247]. In addition, a transcript similar to *AtARR9* (*At3G57040*) was up-regulated in the transgenic tuber buds. *AtARR9* is specifically regulated by the circadian clock and cytokinin, which provides a

functional link between the altered meristematic activity observed in tubers of SP6A^{cop}-HA plants and the cytokinin signaling pathway [248].

In fact, the data suggest few changes in the abundance of transcripts involved in hormone metabolism and signaling, including upregulation of cytokinin oxidase and down-regulation of an ethylene receptor and ethylene sensor protein and a GA2 oxidase **(Table S3).**

Interestingly, the amount of mRNA of the endogenous *SP6A* transcript was reduced in the transgenics about 50-70 %, indicating a feedback response to *SP6A^{cop}* overexpression. The change in transcript amounts of *SP6A* and *SP6A^{cop}* was verified by qPCR **(Figure 9).**

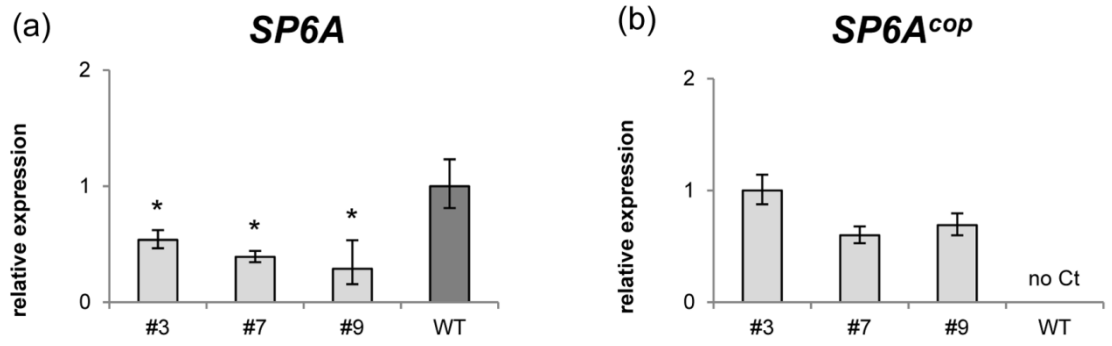

Figure 9. Expression of *SP6A* and *SP6A^{cop}* in dormant buds of tubers of *SP6A^{cop}–HA* overexpressing potato plants. (a) *SP6A* **(b)** *SP6A^{cop}* bars represent mean of 4 biological replicates ± SD; p-values were calculated by two tailed *t*-test by comparing transgenic lines vs. WT (* $p < 0.05$). (from Lehretz *et al*., 2019)

In summary, this microarray analysis supports the idea that overexpression of *SP6A^{cop}* resulted in transcriptional changes that alter the meristem identity, leading to early initiation of tuberization and shifting source-sink equilibrium in favor of sink development. This result can thus be brought in line with the observation of a daughter tuber phenotype in **Figure 6**.

4.1.2 Regulation of *SP6A* by a small RNA

4.1.2.1 Identification of a small RNA as likely reason for the extreme shift in the source sink balance of SP6A^{cop} -HA plants

Overexpression of *SP6A^{cop}* led to a strong phenotype which had not been described for transgenic plants overexpressing an unmodified *SP6A* [81,87]. In those previous studies only comparatively mild changes in plant height, yield and tuber number were observed. Therefore alternative regulatory mechanisms were considered.

One of these could be post-transcriptional regulation, for example miRNA-mediated cleavage of the transcript, which may not happen to the codon-optimized *SP6A^{cop}* mRNA. To further investigate possible regulation of *SP6A* by miRNAs, RNA ligase-mediated rapid amplification

of 5 'cDNA ends (RLM-5'RACE) was performed and free 5' ends of the mRNA were identified in a collaborating laboratory at the James Hutton Institute (Dundee, UK). Sequencing of 10 clones revealed four putative cleavage sites in the SP6A transcript **(Figure 1a)**. Subsequently, in a BLASTn search for complementary regions in the S. phureja DM1-3 genome, a short genomic fragment of *SP6A* comprising 10 bp before and after the cut sites was used [249]. In addition to *SP6A* itself, 96 hits were found **(Table S2)**, all of which were screened for putative stem-loop structures indicative for precursor miRNAs [250]. The criteria were i) a hairpin-like secondary RNA structure of about 80-100 nt length, ii) the relative symmetric appearance of the stem loop structure, i.e. very few asymmetric bulges, and iii) an approximately identical number of nucleotides (less than 3 nt excess on one side), and iv) symmetric loops of normally 1-3 nt in size [250]. In this bioinformatic analysis, a DNA sequence was revealed encoding a putative miRNA corresponding to the 123/124 bp cleavage site # 3 **(Figure 1)**. According to the current gene model of potato [249], this putative small RNA is encoded in an intergenic region upstream of a conserved gene of unknown function (*Sotub03g018760*) on the antisense DNA strand.

This conserved gene of unknown function seems to be extremely low expressed since in silico analysis showed that there are very few reads in RNAseq experiments (http://solanaceae.plantbiology.msu.edu/cgi-bin/gbrowse/potato/?name=Sotub03g018760.1.1) which could also be verified by qPCR. Overall this gene was low expressed. Ct values for *Sotub03g018760* were obtained about 10 cycles later than for ubiquitin (UBI) and no significant changes were detected between control and elevated temperatures (**Figure 10)**.

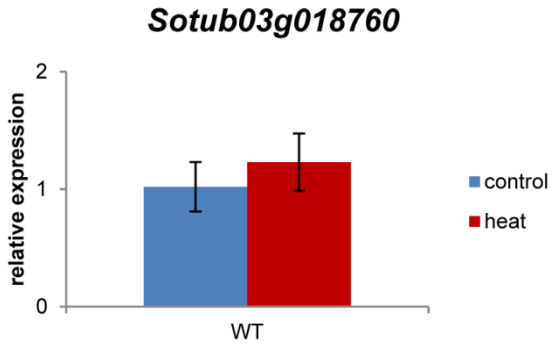

Figure 10. Expression of *Sotub03g018760* in leaves of WT potato plants. bars represent mean of 4 biological replicates ± SD; p-values were calculated by two tailed *t*-test by comparing heats vs. control (* $p < 0.05$).

Next several more characteristics of the small RNA were determined *in silico*. As compared to the query sequence, there is a 1-bp mismatch between the putative small RNA and its target site in Solara **(Figure 11a)**. Folding of the locus around the putative small RNA using MFold [251] revealed a hairpin-like stem-loop structure that is typical of miRNAs **(Figure 11a)**

and gives a free energy of ΔG -16.20. The locus was therefore referred to as "*Suppressor of Expression of SP6A", SES*.

(a)

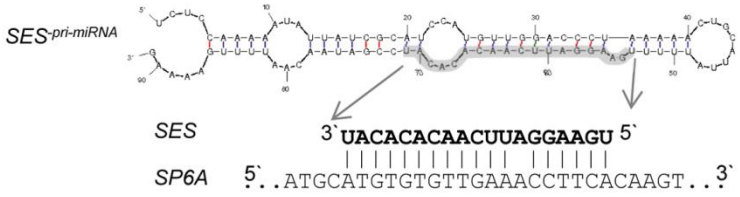

(b)

small RNA sequences	target	expect	UPE	mismatches	mode of action
TTTTGAAGGATTCAACACACAT	*SP6A*	3.0	19.99	2/22	translation
TTTGAAGGATTCAACACACAT	*SP6A*	3.0	20.46	2/21	cleavage
TTGAAGGATTCAACACACAT	*SP6A*	2.5	20.46	2/20	cleavage
TGAAGGATTCAACACACAT	*SP6A*	1.5	20.76	1/19	cleavage
TGAAGGATTCAACACACAT	*SP6A^{cop}*	4.5	21.42	4/19	cleavage

Figure 11. *In silico* identification of a small regulatory RNA suppressing expression of *SP6A* (*SES*). (a) Schematic depiction of the precursor RNA (SES$^{-pri\text{-}miRNA}$), the putative small RNA (SES) and the binding site in the *SP6A* transcript (*PGSC0003DMT400060057*). Folding was performed using Mfold **(b)** Expectation scores and minimum energy for unfolding the target site (UPE) of putative sRNA-sequences for *SP6A* and *SP6A^{cop}* according to psRNA target. (from Lehretz *et al*., 2019)

The online target prediction tool psRNAtarget (Scheme V2) [252] confirmed that the endogenous *SP6A* transcript is most likely a target for the predicted miRNA **(Figure 11b)**. In contrast, *SP6A^{cop}* appears to be a rather poor target, as it has a high expectation value and a higher minimum energy for unfolding the target site **(Figure 11b)**. A comparison between the putative precursor RNA and *SP6A* revealed a 19 nt sequence that most likely targets *SP6A* and leads to cleavage. Therefore, this sequence was used as a probe in all other approaches. Expected values for longer sequences (20-22 nt) were higher (poor target) **(Figure 11b)**.

For further experiments, a 91nt sequence containing the putative pre-miRNA was selected because it matched best the criteria for putative miRNAs described above. It was cloned into an expression vector and designated as *SES$^{-pri\text{-}miRMA}$*. In addition, a genomic region of 2175 bp covering the small RNA together with its putative promoter, termed *SES$^{-genomic}$*, was cloned into the promoter-less vector pBin19. Remarkably, the genomic site of *SES*, and in particular *SES$^{-pri\text{-}miRNA}$* containing the small RNA, could not be found in the genome of the closely related crop plant tomato [253,254] **(Figure 12)**. Furthermore, comparison with other members of *Solanaceae* such as *N. benthamiana* and *S. pennellii* revelaed that *SES* does not appear in these species and could therefore be specific for potato **(Table S3)**.

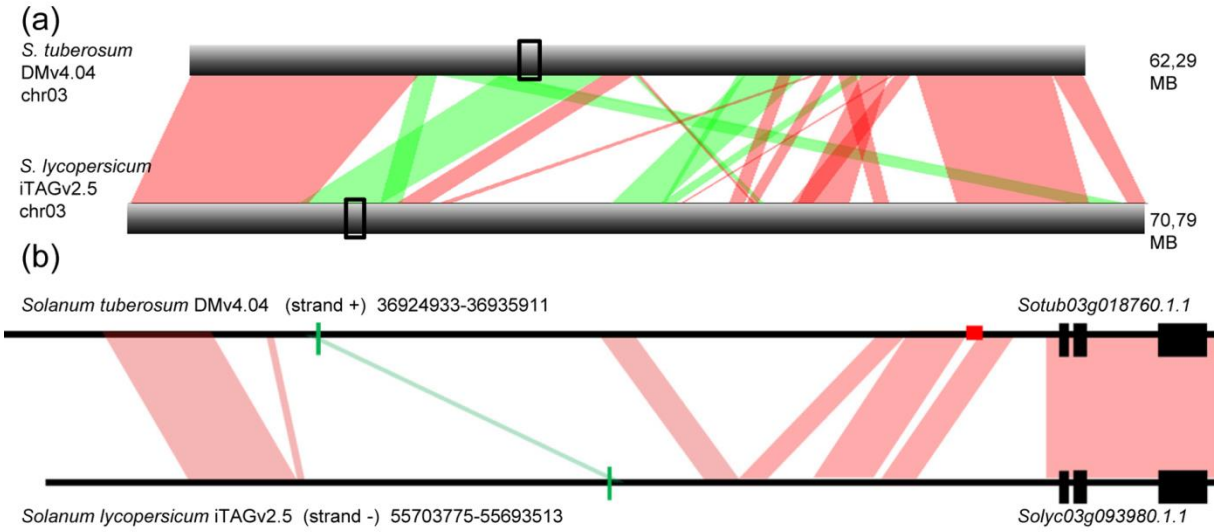

(c)

```
SES locus S.lycopersicum      GACTTAATAG--CTTTAATACAGCAAAATGATGTTCTAACAAAGTAGATCAATTAAAAAC
SES locus S.tuberosum         GCTTTAATAGTAGTTCAATACAGCAAAATGATGTTCTAACAAAGGACATCAATTAAAAAC

SES locus S.lycopersicum      AAAACATTAACCAACTTAAACAAAACGCACACACA-------------------------
SES locus S.tuberosum         AAAACATGGACCAACTTAAACAAAACACACACACACTCGAATTCTCCAAAAATATTATCG

SES locus S.lycopersicum      ------------------------------------------------------------
SES locus S.tuberosum         CATCCATGTTGGACCCTAAAAACTGCATTATTTTTGAAGGATTCAACACACATCCGATAA

SES locus S.lycopersicum      ----------------------TATGTGACATAGCCATTAAATAAAGCGACTCTAGCTAA
SES locus S.tuberosum         CAATTTTGAAAAGCCCAAACAACATA--ACACAACTATT-ATAACAAGACTATTGACAC

SES locus S.lycopersicum      CG----TTCAATCACACCATATTAAAAATATCTTATTAATCGCGGCGAAGTCTGCGGAAA
SES locus S.tuberosum         TGTAAATTCCATCACACCATATTAAGAATATCTTATTAATC---GCGAAGTCTGCGAAAA

SES locus S.lycopersicum      TACTGAGAAGGGTTACTCTCAAATTGATCCCTGTAAATGTGACTGC
SES locus S.tuberosum         TACTCAGAAGGGTTACTCTCAAATTCATCCCTGTAAATGTAACTGT
```

Figure 12. The genomic locus of the small RNA (*SES*) coding region is different between potato and tomato. (a) comparison between potato and tomato chromosome 03 using SyMAP; syntenic genome segments are depicted in colour; red: same orientation; green: inverted orientation **(b)** close-up of boxed sequence regions based on a syntenic block analysis made with Mauve; a short sequence segment comprising the putative pre-miRNA is present in potato (red box) but not in tomato; the region surrounding the small RNA locus is characterized by many small-scale rearrangements; syntenic genome segments are depicted in colour; red: same orientation; green: inverted orientation; black boxes indicate exons of the *Conserved Gene of Unknown Function* Sotub03g018760.1.1 and Solyc03g093980.1.1. *SES*$^{-pri\text{-}miRNA}$ is shown in a red box. **(c)** Alignment of the small RNA locus *SES* in potato comprising the putative pre-miRNA, *SES*$^{-pri\text{-}miRNA}$, (underlined letters) with the mature small RNA *SES* (bold letters) which is not present in the corresponding locus in tomato. (from Lehretz *et al*., 2019)

4.1.2.2 Verification and characterization of the SP6A targeting small RNA in planta

In order to test the biological activity of the predicted miRNA, a fragment encoding *SES*$^{-pri\text{-}miRNA}$ was amplified and cloned under control of the CaMV35S promoter (35S::*SES*$^{-pri\text{-}miRNA}$) into a plant expression vector to perform transient expression assays in *N. benthamiana*. For this purpose, constructs containing either SP6A or SP6A^{cop} alone or together with the *SES*$^{-pri\text{-}}$

miRNA construct were infiltrated and mRNA levels were measured over a time course of 36 hours. There was an increase in expression of *SP6A* over time, but co-infiltration of the *SES-pri-miRNA* construct decreased the level of *SP6A* mRNA **(Figure 13a)**, suggesting that *SP6A* mRNA is degraded in the presence of the predicted miRNA. In contrast, co-expression of 35S: *SP6A^{cop}* with 35S::*SES-pri-miRNA* did not result in lower accumulation of *SP6A^{cop}* mRNA **(13b)**, confirming that *SP6A^{cop}* is a poor target for the predicted miRNA.

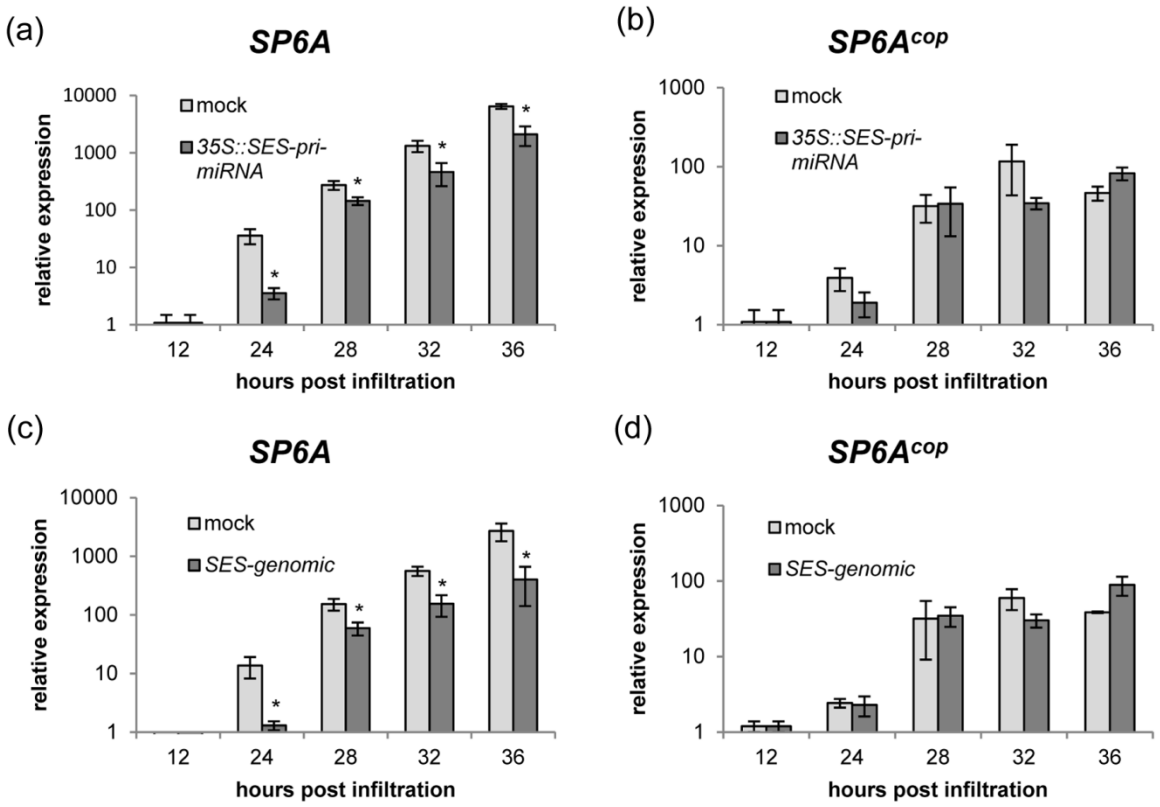

Figure 13. Identification of a small regulatory RNA suppressing expression of SP6A (SES) via *in silico* analysis and transient assays. (a,b) Transient expression of 35S::*SP6A* and 35S::*SP6A^{cop}* in *N. benthamiana* using *A. tumefaciens*; relative expression with or without co-infiltration of 35S::*SES-pri-miRNA* was determined by qPCR **(c,d)** Transient expression of 35S::*SP6A* and *35S::SP6A^{cop}* in *N. benthamiana* using *A. tumefaciens*; relative expression with or without co-infiltration of a construct bearing the genomic sequence of the *SES* locus (*SES-genomic*) was determined by qPCR. Values are the mean of four biological replicates ± SD; statistically significances between samples were determined by two-tailed tests (*, $p < 0.05$). Similar results were obtained in three independent experiments. (from Lehretz *et al*., 2019)

In addition, it was of interest whether the genomic sequence of *SES* (*SES^{genomic}*), which covers the small RNA along with a putative promoter, also exhibits biological activity in this assay when cloned into the promoter-less vector pBin19. Transient expression in N. *benthamiana* along with *SP6A* also caused downregulation of *SP6A* mRNA, similar to the results obtained with 35S::*SES-pri-miRNA* **(Figure 13c)**. As expected, there was no down-

regulation of *SP6A*^{cop} mRNA in the same experimental setup **(Figure 13d)**. Thus, the presence and biological activity of the putative miRNA was verified in silico as well as in transient expression assays in planta. Furthermore, the expression of the small RNA *SES* could be verified by qPCR **(Figure 14a)**.

In order to verify the sequence specificity, the same transient assay was conducted with a new construct, where the *SP6A* transcript sequence was exclusively modified at the putative binding site, *SP6A*^{mod} **(Figure 14b)**. Since the *SP6A*^{mod} transcript could not be affected by coexpression of *SES*, this narrows down the *SES* binding site to the expected locus **(Figure 14b)**.

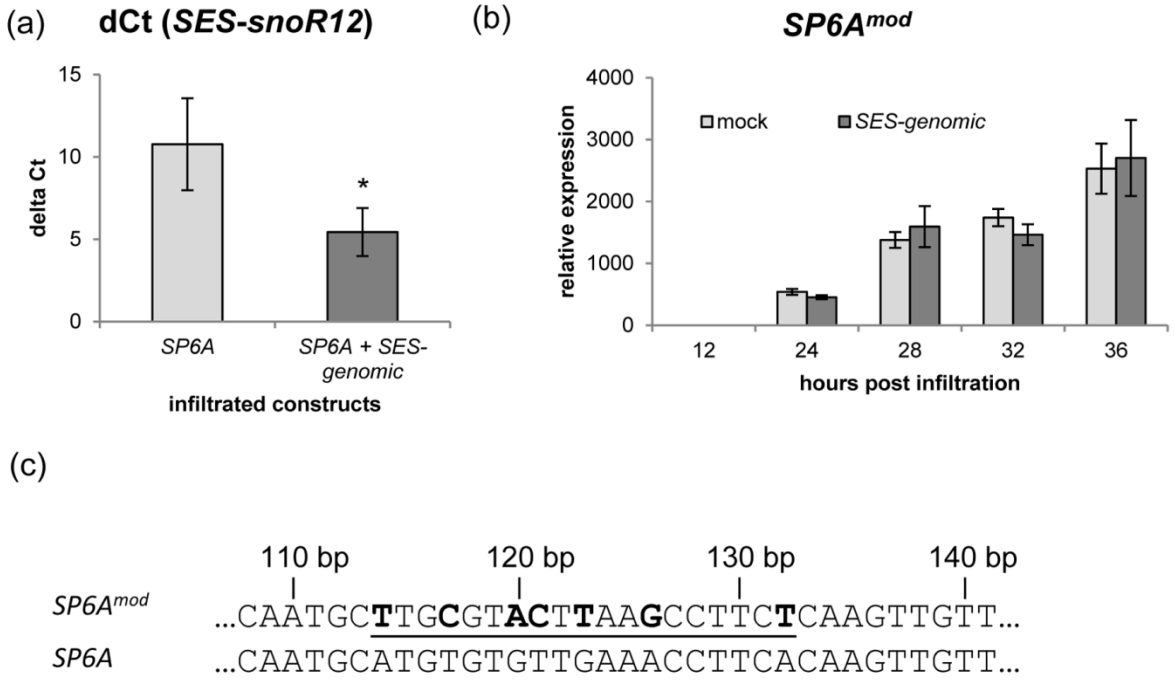

Figure 14. Characterization of *SES*/*SP6A* interaction in transient assays. (a) Verification of smallRNA (*SES)* presence in transient assays via MiScript qPCR. *N. benthamiana* leaves were infiltrated either with SP6A or with *SP6A* and a construct comprising the genomic locus of the small RNA (*SES*$^{-genomic}$). Samples were taken 1 day post infiltration and analysed for the presence of *SES* by miScript qPCR. Values are the mean of 4 biological replicates ± SD; Delta Ct values were significantly (*p<0.05) lower when the genomic locus of *SES* (*SES*$^{-genomic}$) was co-infiltrated, no Ct values could be detected in water control. **(b)** Transient expression of 35S::*SP6A*^{mod} in *N. benthamiana* using *A. tumefaciens*; relative expression with or without co-infiltration of a construct bearing the genomic sequence of the *SES* locus (*SES*$^{-genomic}$) was determined by qPCR. Values are the mean of four biological replicates ± SD; Statistical significances between samples were determined by two-tailed tests (*, p < 0.05). Similar results were obtained in three independent experiments. **(c)** *SP6A*^{mod} sequence differs from endogenous *SP6A* only in the binding site for *SES*, shown in underlined letters. Nucleotide exchanges are marked in bold letters, bases are counted from start codon. (from Lehretz *et al*., 2019)

Moreover, the relevance of this post-transcriptional gene regulation in the commercial potato variety Solara should be analyzed. Thus, the expression patterns of *SP6A* and the small RNA in leaves during the life cycle of a potato plant, e.g. between 14 and 70 days after planting were determined. Under greenhouse conditions, plants began to tuberize between 28d and 35d after planting **(Figure 15).**

Figure 15. Development of WT potato plants. Phenotype of WT potato plants sampled weekly over 9 weeks. Numbers indicate days after planting into soil from tissue culture; tuber induction occurred between 28 and 35 days, experiment was performed twice with similar results. (from Lehretz *et al*., 2019)

At the same time, the expression of *SP6A* was induced 8-fold at 35d shortly after the onset of tuber induction. Its expression increased steadily as the plants aged, suggesting that SP6A also plays a role in the maintenance of tuber growth **(Figure 16a)**. In contrast, the transcript amount of *SES* decreased rapidly after tuber induction (28d) and remained low during further plant development **(Figure 16b)**. This implies that *SES* also suppresses *SP6A* transcript accumulation during early stages of development, e.g. before tuberization.

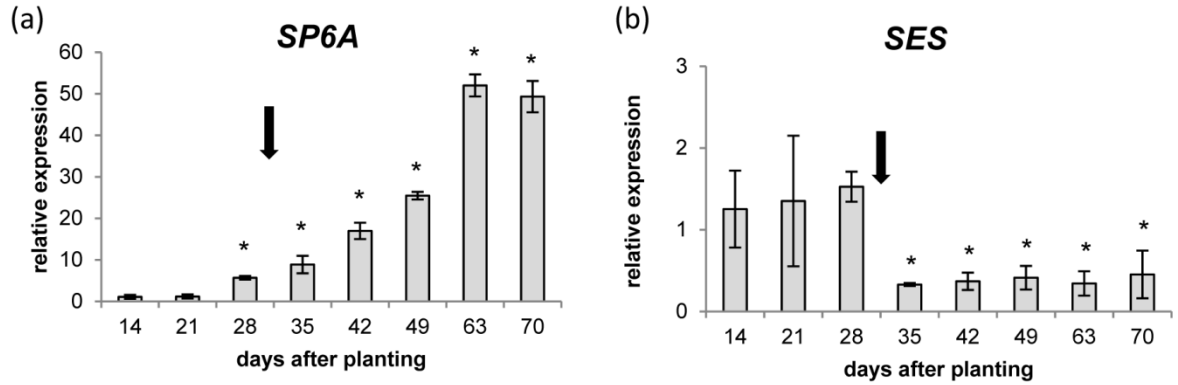

Figure 16. Expression of *SES* and its target *SP6A* during development. (a) Expression of *SP6A* and **(b)** Expression of *SES* during plant development in source leaves. Arrow indicates time point of tuber induction. Bars represent the mean of four biological replicates ± SD; * p-value < 0.05; two tailed *t*-test. Experiment was performed twice with similar results. (from Lehretz *et al*., 2019)

Elevated temperatures are known to have a strong negative impact on tuberization, which can even suppress tuberization completely, depending on when the stress is applied [255].

At the same time, the expression of SP6A decreases [152]. To investigate whether the identified small RNA plays a role in this regulation, the expression of *SES* and *SP6A* in leaves of plants grown under ambient conditions (22°C / 20°C) and at elevated temperatures (27°C / 29°C) were analyzed. While *SP6A* mRNA levels declined, *SES* expression increased at elevated temperatures **(Figure 17a, b)**.

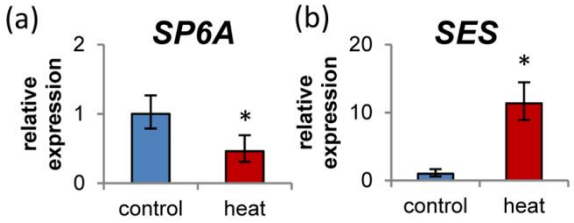

Figure 17. Expression of *SES* and its target *SP6A* under elevated temperatures. Changes in **(A)** *SP6A* and **(B)** *SES* expression in source leaves after heat treatment for three weeks as compared to control. Bars show the mean of three biological replicates; * p-value < 0.05; two tailed *t*-test; heat was applied for three weeks starting from day 28; experiment was repeated three times with similar results. (from Lehretz *et al*., 2019)

In order to understand the putative regulation of *SP6A* by *SES* under heat in more detail, discontinuous heat treatment before and after tuberization was applied, where growth periods of heat altered with control conditions **(Figure 18a)**. It turned out that *SP6A* expression was rising under control conditions which did not occur under altering heat conditions. In fact, *SP6A* levels were at least 70 % lower **(Figure 18b)**. In contrast, expression of *SES* was about four-fold increased. Remarkably, *SES* expression did not fall after one week recovery in between, which is in line with *SP6A* levels **(Figure 18c)**.

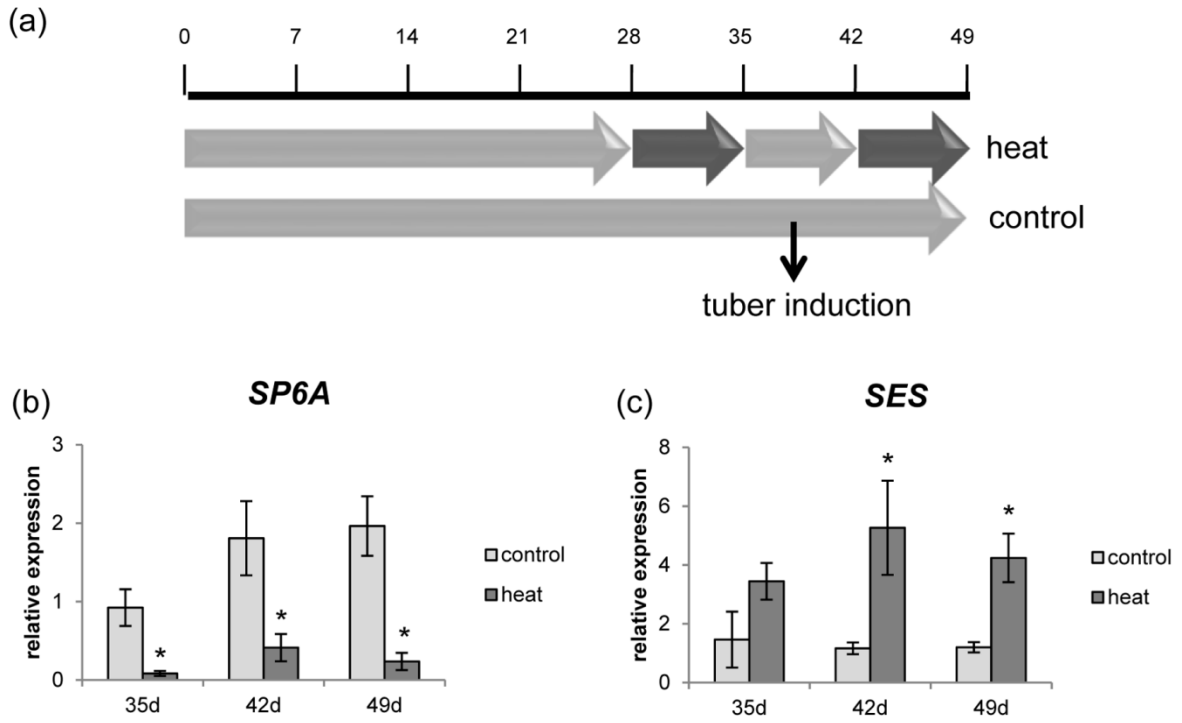

Figure 18. Expression of *SP6A* and *SES* under discontinuous heat treatment. (a) Experimental setup to investigate heat effects at different developmental stages**.** Numbers indicate days after planting into soil from tissue culture; tuber induction occurred between 35 and 42 days. **(b)** *SP6A* and **(c)** *SES* expression; bars represent mean of 4 biological replicates ± SD; p-values were calculated by two tailed *t*-test compared to respective control (* $p < 0.05$). (from Lehretz *et al*., 2019).

As a likely cause of heat induction two putative binding sites for heat shock factor (HSF) were identified [256–258] in an *in silico* approach **(Table S4)**. These are located less than 2 kb upstream of *SES* **(Figure 19)**.

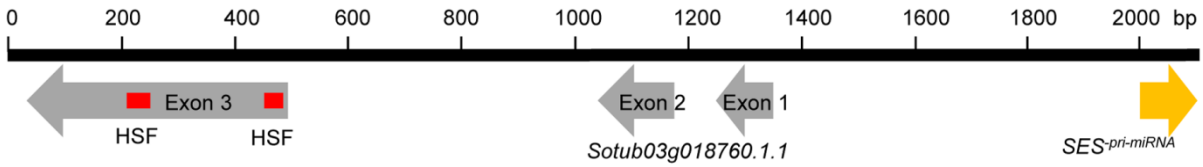

Figure 19. Promoter structure of *SES*. A region 2kb upstream of the putative pre-miRNA, *SES*$^{-pri\text{-}miRNA}$ (yellow arrow), contains a conserved gene of unknown function *Sotub03g018760.1.1* in three exons (grey arrows) on the opposite strand, as well as two putative binding sites for heat shock transcription factors (red boxes). (from Lehretz *et al*., 2019)

In summary, the reciprocal expression pattern of *SP6A* and *SES* suggests that both developmental and environmental changes in *SP6A* transcript levels are modulated by the small RNA in addition to the known regulation via the CDF/CONSTANS module.

4.1.2.3 Heat-resistant tuberization through overexpression of a Short Tandem Target Mimicry Construct

Short tandem target mimicry (STTM) approaches are widely used to sequester endogenous small RNAs and alter their functions [237,259,260]. This allows higher expression of the target gene, especially under conditions where the small RNA is active. Using this strategy, an STTM construct was designed based on a 88 nt spacer, cloned under the control of the CaMV35S promoter **(Figure 20)** and transformed into *S. tuberosum* (cv. Solara).

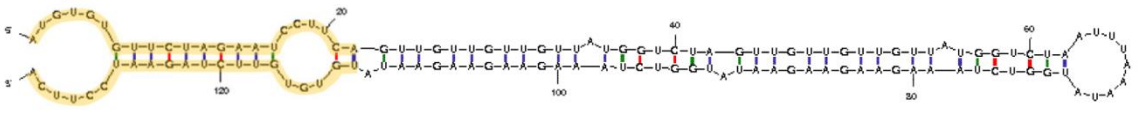

Figure 20. Schematic depiction of the STTM construct. Secondary structure of the construct to sequester endogenous *SES* is shown using Mfold. Binding sites for SES are highlighted. (from Lehretz *et al*., 2019)

Out of 34 transformants five transgenic lines were selected which exhibited high expression of the STTM construct. **(Figure 21a)**. Under control conditions at a young age, STTM plants

appeared to show only slightly earlier tuberization **(Figure 21b)** and a bit more tuber biomass **(Figure 21c)**, but a higher number of tubers **(Figure 21d)** being in line with higher *SP6A* expression **(Figure 21e)**.

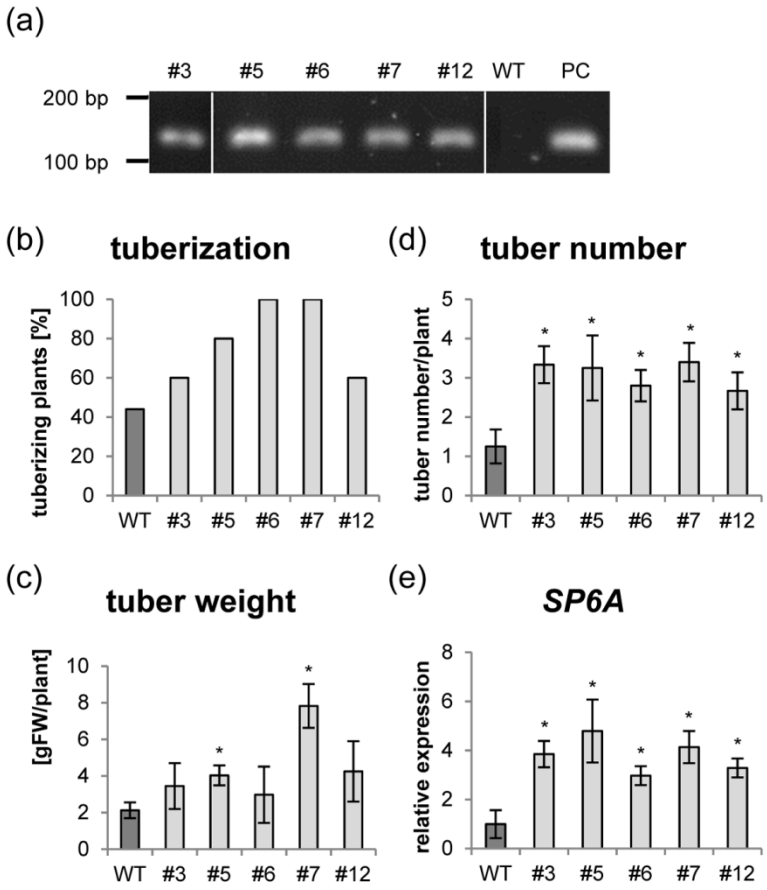

Figure 21. Characterization of *Short Tandem Target Mimicry* (*STTM)* overexpressing potato plants. (a) RT-PCR showing expression of *STTM* construct in five different transgenic lines; PC**=** positive control (pBinAR-35S::STTM). Plants were harvested at the age of 35 days and following data were obtained: **(b)** Tuberization **(c)** Total tuber weight **(d)** Tuber number **(e)** SP6A expression; bars represent mean of 4-9 biological replicates ± SD; p-values were calculated by two tailed *t*-test by comparing transgenic lines vs. WT (* $p < 0.05$). (from Lehretz *et al*., 2019)

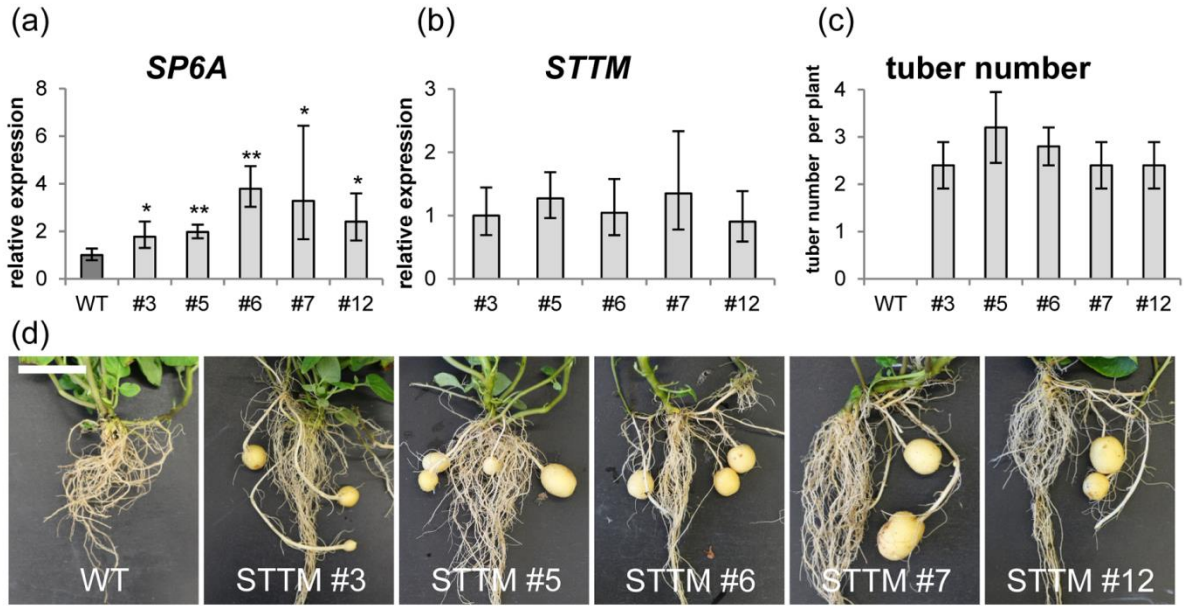

Figure 22. Overexpression of a Short Tandem Target Mimicry (STTM) construct sequestering *SES* can overcome heat-mediated repression of tuberization. (a) *SP6A* expression in leaves of five week old plants grown under elevated temperature for four weeks. Bars show means of four biological replicates ± SD **(b)** Relative expression of *STTM* RNA **(c)** Tuber number in five week old *STTM* overexpressing and WT plants after four weeks of heat treatment. Bars show mean of five plants ± SD. **(a-c)** p-values were calculated by two tailed *t*-test by comparing transgenic lines vs. WT (* $p < 0.05$). **(d)** Belowground phenotype of five week old plants grown under elevated temperature for four weeks; scale bar = 5 cm. One representative of five plants is shown. The experiment was repeated twice with similar results. (from Lehretz *et al*., 2019)

To study the *STTM* effect under heat, five plants per line were exposed to elevated temperatures one week after transfer to the greenhouse. Under these conditions, *SES* is strongly induced while the expression of *SP6A* is downregulated, resulting in the inhibition of tuber formation. The *STTM* construct should therefore be particularly efficient under these circumstances. Thus, leaf samples were taken after four weeks of heat and *SP6A* expression was measured. The *STTM*-expressing lines showed a two- to four-fold increase in SP6A mRNA levels at elevated temperatures compared to WT **(Figure 22a)**. Expression of the *STTM* transcript was similar in all selected transgenic lines **(Figure 22b)**. At elevated temperatures, WT plants did not produce stolons or tubers **(Figure 22c)**. However, all transgenic lines produced tubers under these conditions **(Figure 22d)**. Therefore, expression of the *STTM* construct can overcome the small RNA-mediated down regulation of *SP6A* expression under elevated atmospheric temperatures and thus promote tuberization.

4.2 Increasing potato drought and heat tolerance by overexpression of Hexokinase and SP6A

4.2.1 Biotechnological characterization of HXK+SP6A transgenic potato

4.2.1.1 Reduced transpiration in HXK+SP6A potato plants leads to increased water use efficiency

Previous work has shown that a convincing enhancement of tuberization under comparatively mild but for potato rather harsh heat treatment could be achieved by abolishing the endogenous small RNA *SES* as described above. Although the effect was clearly present it was comparatively mild and could not extensively promote tuberization extending beyond heat stress also under ambient conditions. Thus, the following approach aimed again at a rather classic overexpression of *SP6A*, which might give stronger effects. Anyhow, here the wildtype sequence and not a codon optimized one was used since eventually undesired phenotypes for the latter one, such as daughter tuber formation, could be seen previously as described above. Therefore the leaf and stem specific StLS1 promoter which is active in green plant tissues was used [261].

Moreover, under heat drought is very likely to occur and becomes an agronomic problem. In order to reduce evaporation and thus increase water use efficiency overexpressing hexokinase 1 from *A. thaliana* (*AtHXK1*) under the stomata specific KST1 promoter was shown to be an efficient tool [205–207,262,263] and therefore was included in a transgene construct to improve water use efficiency.

Plasmids bearing the constructs were created using the Golden Gate system [231] and transformed into the commercial potato cultivar Solara using agrobacteria mediated gene transfer. Out of 34 transformants 4 transgenic plants were selected **(Figure 23a)** because they exhibited both expression of *AtHXK1* **(Figure 23b)** as well as a 2-4 fold increased *SP6A* expression at the age of three weeks **(Figure 23c)**.

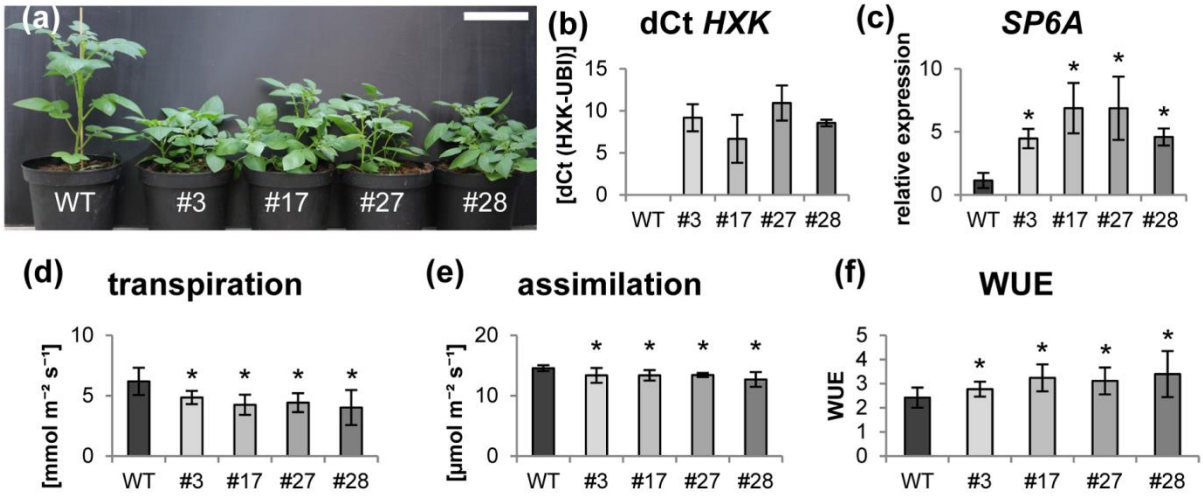

Figure 23. HXK+SP6A potato plants. (a) Phenotype of HXK+SP6A potato plants 21d after planting from tissue culture; scale bar 10cm **(b)** Expression of *AtHXK1* **(c)** Expression of *SP6A* in source leaves **(d)** Transpiration **(e)** Assimilation **(f)** Water use efficiency at 28 days; values are the mean of four biological replicates ± SD, Significance compared to WT was determined by two-tailed t-test (*; p-value < 0.05)

First of all, for a biotechnological characterization, the expected positive effect of AtHXK1 on water consumption was verified. At different plant ages a reduced transpiration rate could be observed for all transgenic plants **(Figure 23d)** which was also confirmed by the stomata width/ length ratio **(Figure 24a)**. To verify this independently, the number of stomata on the abaxial side of the leaves was counted where it turned out that the stomatal density was not significantly altered to the WT **(Figure 24b)**. As expected the reduced stomatal opening also led to a bit less assimilation. However, the effect seems to be neglible as the reduction was rather mild **(Figure 23e)** thus leading to an increased water use efficiency **(Figure 23f)**.

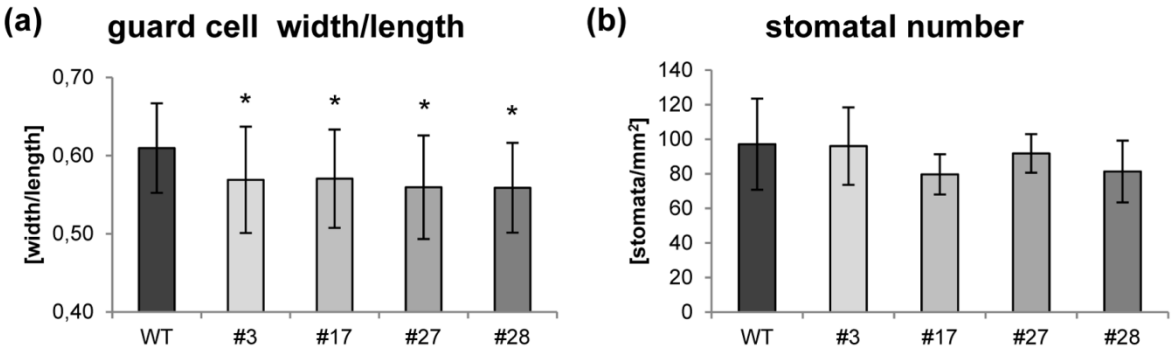

Figure 24. Guard cells of HXK+SP6A potato plants. (a) Guard cell width to length ratio is smaller in the transgenics indicative of closed stomata; bars show mean ± SD, n=40; Significance compared to wild type was determined by two-tailed t-test (*; p-value < 0.05) **(b)** Stomatal number is not significantly altered in the transgenic plants, values are the mean of 10 replicates ± SD, Significance compared to WT was determined by two-tailed t-test (*; p-value < 0.05)

The observation of a reduced shoot length but more bushy growth **(Figure 23a)** was verified by leaf area measurements. Although the plants were smaller **(Figure 25a)** the leaves of the transgenics were smaller **(Figure 24b)** an increased leaf number per plant **(Figure 24c)** resulted in a bit more total leaf area per plant **(Figure 24a)**.

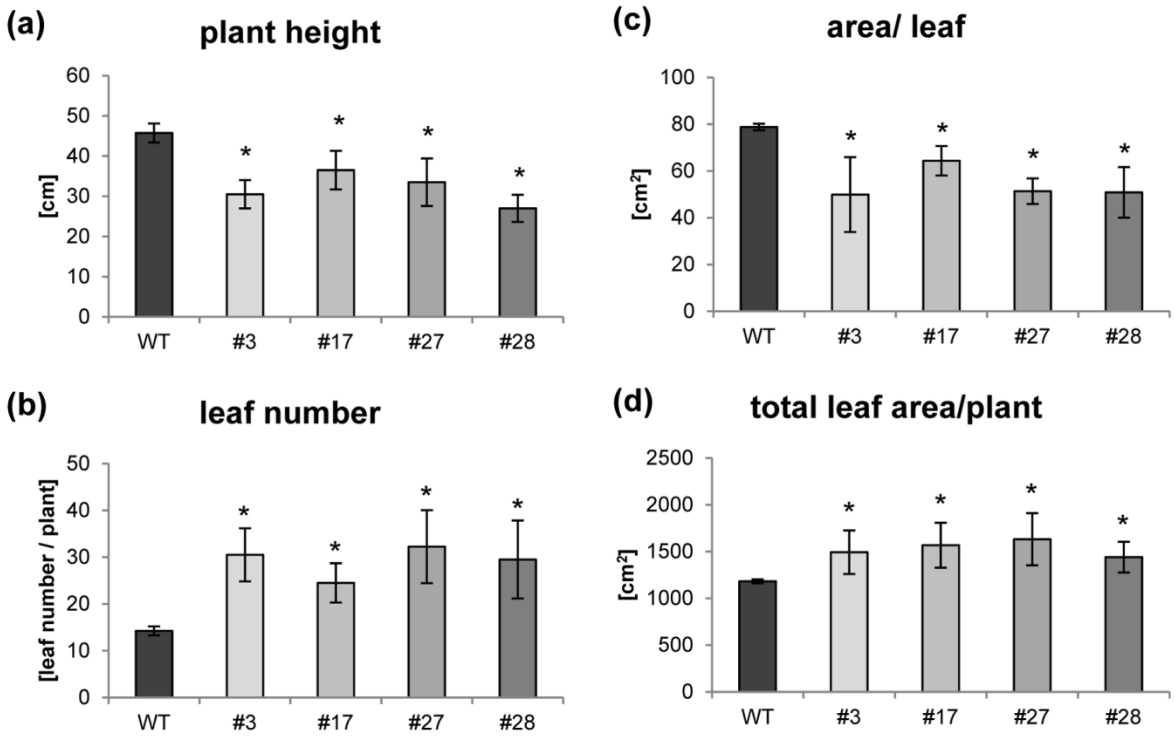

Figure 25. Shoot phenotype of HXK+SP6A potato plants at the age of 5 weeks. (a) Plant height, bars show mean of four plants ± SD, Significance compared to wild type was determined by two-tailed t-test (*; p-value < 0.05) **(b)** Number of leaves per plant, bars show mean of four plants ± SD, Significance compared to wild type was determined by two-tailed t-test (*; p-value < 0.05). **(c)** Mean leaf area, bars show mean of all leaves of one plant of four plants per line, Significance compared to wild type was determined by two-tailed t-test (*; p-value < 0.05) **(d)** Total leaf area per plant; bars show mean of 4 plants ± SD, Significance compared to WT was determined by two-tailed t-test (*; p-value < 0.05)

For further studies physiological and biochemical parameters at single and double stress conditions were determined. All plants were first grown for 4 weeks at well-watered control conditions (approx. 65% RWC) to bring all individuals to a comparable physiological and developmental stage **(Figure 25a)**.

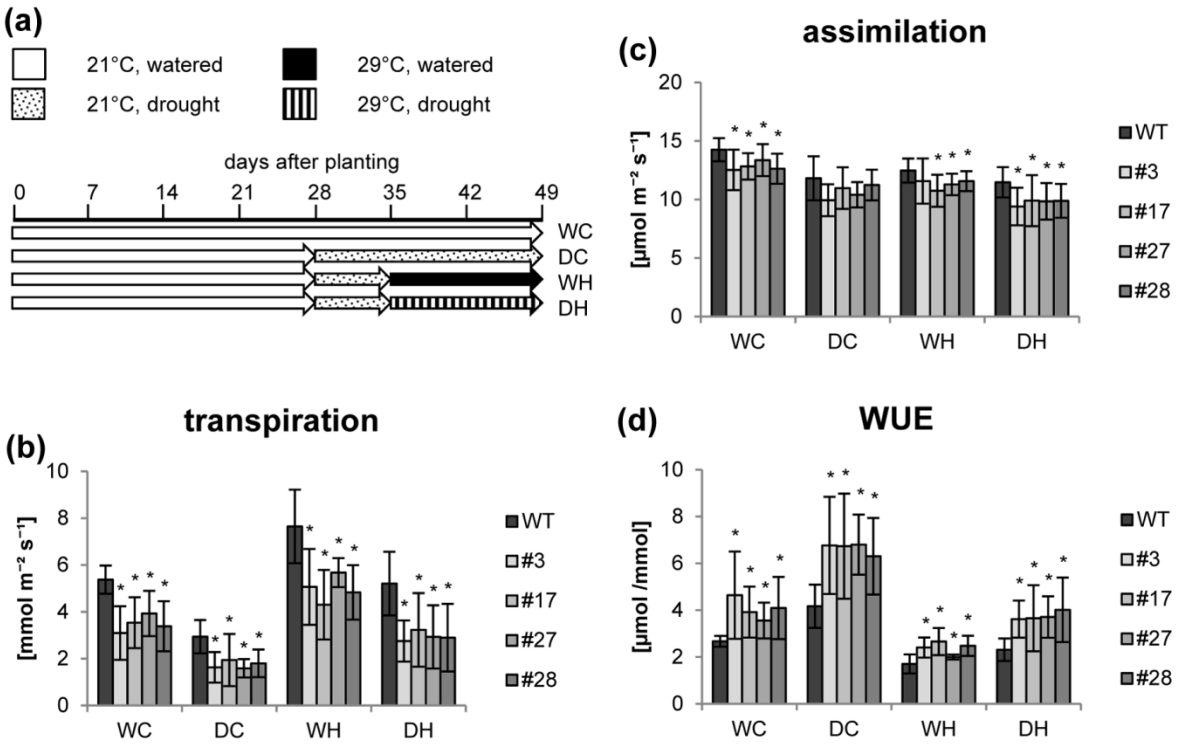

Figure 26. Photosynthesis of HXK+SP6A potato plants under different stress treatments at the age of 5-6 weeks. (a) Experimental setup **(b)** Transpiration **(c)** Assimilation **(d)** WUE, values are the mean of 8-12 replicates ± SD, Significance compared to WT was determined by two-tailed t-test (*; p-value < 0.05)

For one week half of the population was adapted to drought conditions (approx. 40 % RWC) **(Figure 26a)**. Soil humidity was adjusted by daily watering. In order to investigate heat effects, one half of the respectively treated groups was shifted to elevated temperatures and grown for two more weeks until harvest. For each condition water transpiration was determined, which turned out to be reduced in the transgenic lines in control (WC) **(Figure 26b)** and even in drought (DC). Here, also the WT strongly reduces evaporation **(Figure 26b)** but still the transgenics show more reduced values. Under elevated temperatures but well-watered (WH) the WT strongly increases water evaporation, once more to a lower extent in the transgenics **(Figure 26b)**. Under double stress conditions, i.e. drought and heat, (DH) again the transgenics were more effective in keeping the stomata closed. Under all treatments, assimilation turned out to be, if at all, only mildly reduced in comparison to the respective WT **(Figure 26c)**. These results were quite promising as a much lower assimilation could have been expected with the stomata being more closed and thus reducing gas exchange. Consequently the water use efficiency (WUE) was increased under ambient watered conditions (WC), drought (DC), heat (WH) as well as double stress (DH) **(Figure 26d)**.

4.2.1.2 Overexpression of SP6A maintains tuber formation and tuber starch content under drought and heat conditions

The focus of this project was a biotechnological improvement of the tuber crop potato and thus yield parameters were of special interest. As a first phenotypic effect a reduced shoot growth of the transgenics under all conditions was visible as seen before **(Figure 27a, S1)**. Under drought conditions a reduction of plant height as well as green biomass was present in the WT, as expected, but not that strong in the transgenics **(Figure 27a, b)**. However, an increased plant height under well-watered heat conditions (WH), known as shade avoidance phenotype, could be observed in all plants but less pronounced in the transgenics, especially under combined drought and heat (DH) **(Figure 27a)**. A reduction in green biomass was seen in all plants with increasing stress **(Figure 27b)**. Strikingly, in the transgenics this abiotic stress seems to hardly affect tuber yield as values under control were about 30-70 % higher and often not significantly reduced after stress application **(Figure 27c)**. In the WT, double stress (DH) lead to a yield reduction of roughly 70 % whereas the strongest decrease in the transgenics was around 15 % but not significant **(Figure 27c)**. Overall, yield in double stress was 4-5 times higher than the WT **(Figure 27c)**. Although mean tuber weight was lower **(Figure 27d)**, a massively increased tuber number **(Fig 27e)** were probably contributing to higher yield. Finally, the harvest index of the double transgenics was 2-8 times higher **(Figure 27f)**. These data were obtained in two independent experiments as well **(Figures S2, S3)**.

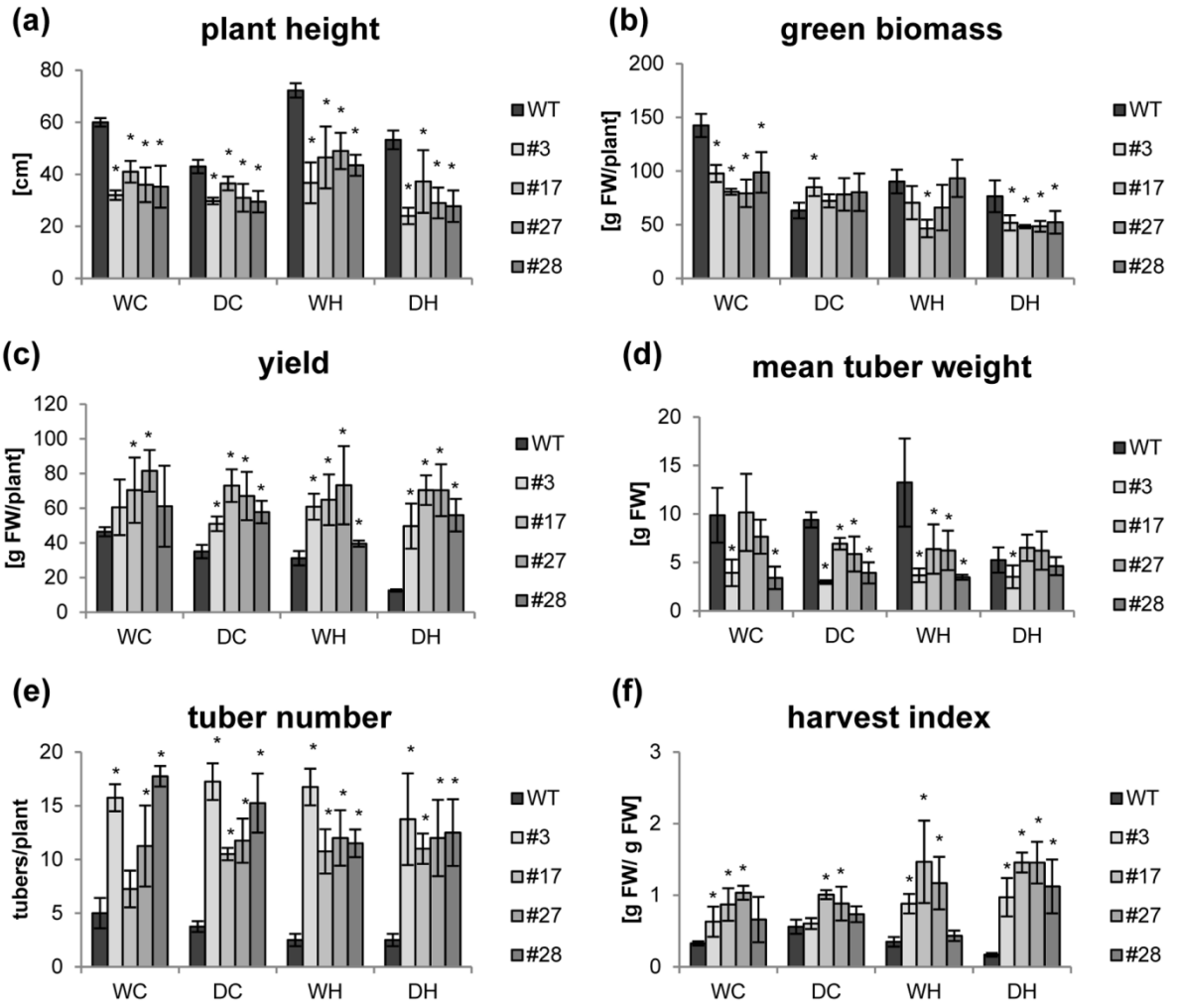

Figure 27. Yield data for HXK+SP6A potato plants. (a) Plant height **(b)** Green biomass **(c)** Yield **(d)** Stolon number **(e)** Tuber number **(f)** Harvest index; plants were harvested at the age of 7 weeks; values are the mean of 4 plants ± SD, Significance compared to WT was determined by two-tailed t-test (*; p-value < 0.05)

The most likely reason for this phenomenon could be enhanced tuber formation driven by the tuber inductor SP6A. Higher *SP6A* levels in the transgenics even under heat could be verified by qPCR **(Figure 28a)**. In contrast in the WT *SP6A* levels decreased upon drought, but even more upon heat **(Figure 28a)**. Double stress conditions led to the strongest reduction. This expression pattern correlates very well with yield reduction (Pearson 0.91)**(Figure 28b),** thus underlying the importance of SP6A for tuber formation **(Figure 27c)**.

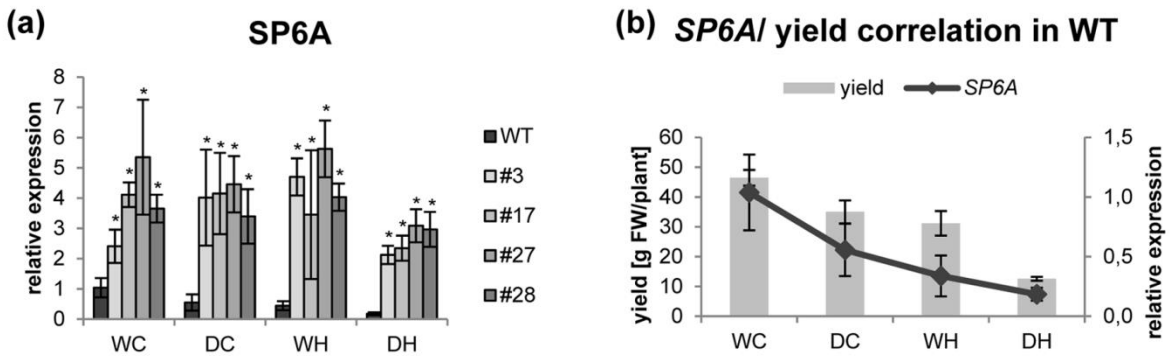

Figure 28. Influence of *SP6A* expression on tuber yield. (a) SP6A expression in leaves of HXK+SP6A potato plants; bars show mean of four replicates ± SD, Significance compared to WT was determined by two-tailed t-test (*; p-value < 0.05) **(b)** Coherence between *SP6A* expression and tuber yield in WT under different stress treatments.

As a possible reason for downregulation of SP6A a small RNA called SES was identified before. In this experiment an upregulation under heat (WH) was visible as expected, but not under drought conditions and double stress **(Figure 29a)**. Therefore alternative regulation mechanisms such as the CDF/CO module were considered. Analysis of the respective genes via qPCR did not reveal any significant changes on transcriptional level between the stress conditions, neither for CDF1, COL1 or COL2 **(Figure 29b-d)**.

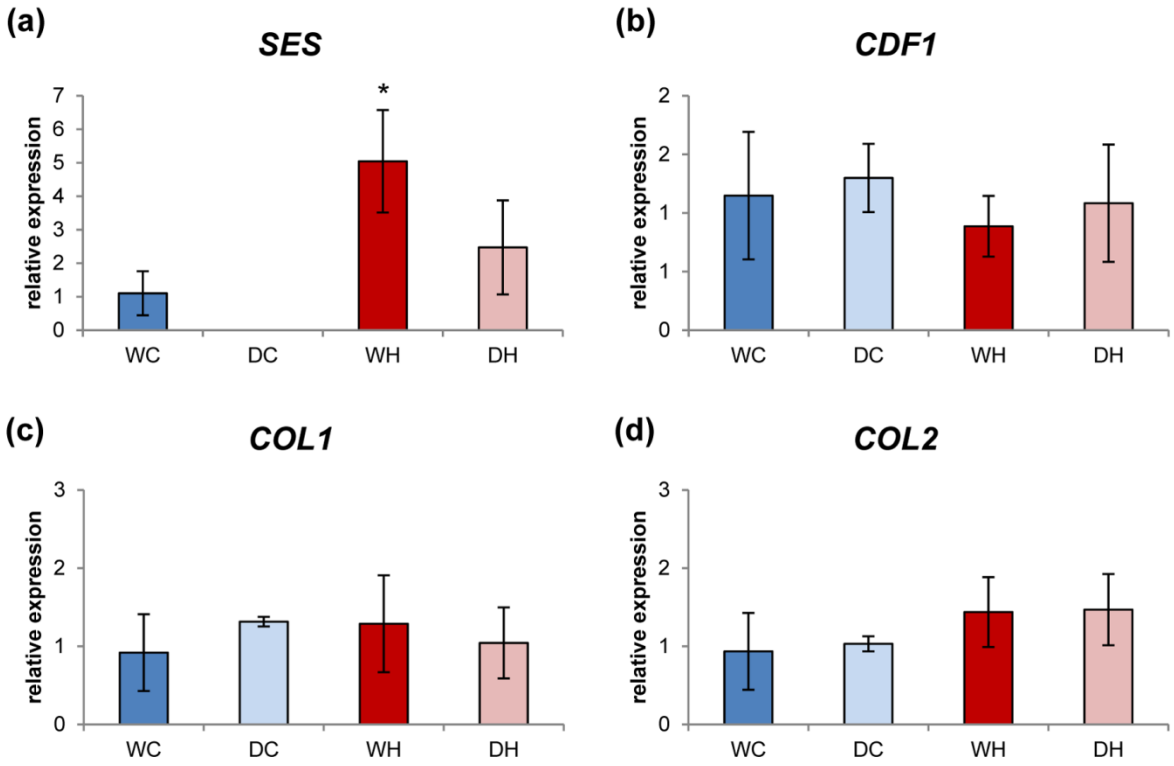

Figure 29. Expression of genes regulating *SP6A* under drought and heat stress. (a) *SES* **(b)** *CDF1* **(c)** *COL1* **(d)** *COL2 ,* bars show mean of four replicates ± SD, Significance compared to WC was determined by two-tailed t-test (*; p-value < 0.05).

The HXK+SP6A plants exhibited a stable tuber fresh weight at a high level under various conditions. However, since more tuber fresh weight in the transgenics would have no agricultural value with reduced dry matter, the dry weight to fresh weight (DW/FW) ratios of harvested tubers were measured to get a first impression.

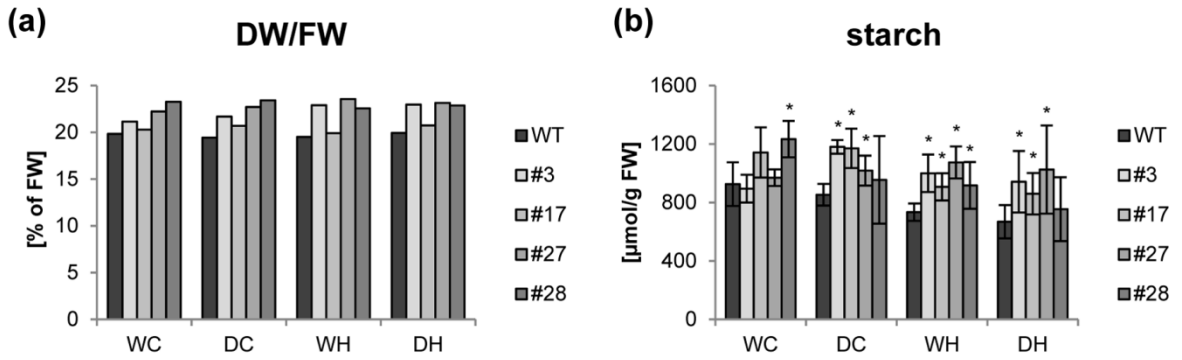

Figure 30. Dry weight/ fresh weight ratio and starch content in HXK+SP6A tubers. (a) dry weight/ fresh weight ratio **(b)** starch content of tubers of HXK+SP6A potato plants under different stress treatments, bars show mean of four replicates ± SD, Significance compared to WT was determined by two-tailed t-test (*; p-value < 0.05).

A slight increase in DW/FW ratio was present in the transgenics **(Figure 30a)**. Concerning starch content, under control conditions no clear changes were observed **(Figure 30b)**. Upon drought in ambient temperature no significant reduction could be spotted in the WT. In contrast, starch levels were clearly reduced upon heat treatment and even further in double stress, as expected **(Figure 30b)**. This is consistent with previous findings [152]. Surprisingly under stress conditions the values of the transgenics were always higher than in the corresponding WT and were not significantly altered to ambient conditions **(Figure 30b)**.

4.2.2 Physiological characterization of HXK+SP6A transgenic potato

4.2.2.1 HXK+SP6A plants confers drought avoidance through reduced water consumption

AtHXK1 was shown to reduce evaporation when expressed in guard cells of *A.thaliana* and citrus [205,206]. Although the molecular mechanism is yet unsolved, this study provides further evidence that the desired effect is also present in the crop plant potato. A reduced

evaporation is assumed to lead to reduced water loss and thus cause less drought stress. To investigate this deeper several parameters were measured.

The content of the phytohormone abscisic acid (ABA) is commonly used as a marker for drought stress. ABA was measured in WT and transgenic lines in source leaves in response to drought, heat and combined stress **(Figure 31a)**. Under well-watered control as well as heat conditions there was no difference between WT and transgenics. The same was true for watered heat conditions. In the WT, ABA levels strongly increased upon drought and combined stress (about 25 and 6 fold respectively), while the increase in the transgenics was only about 2-3 fold in both drought stress conditions **(Figure 31a)**.

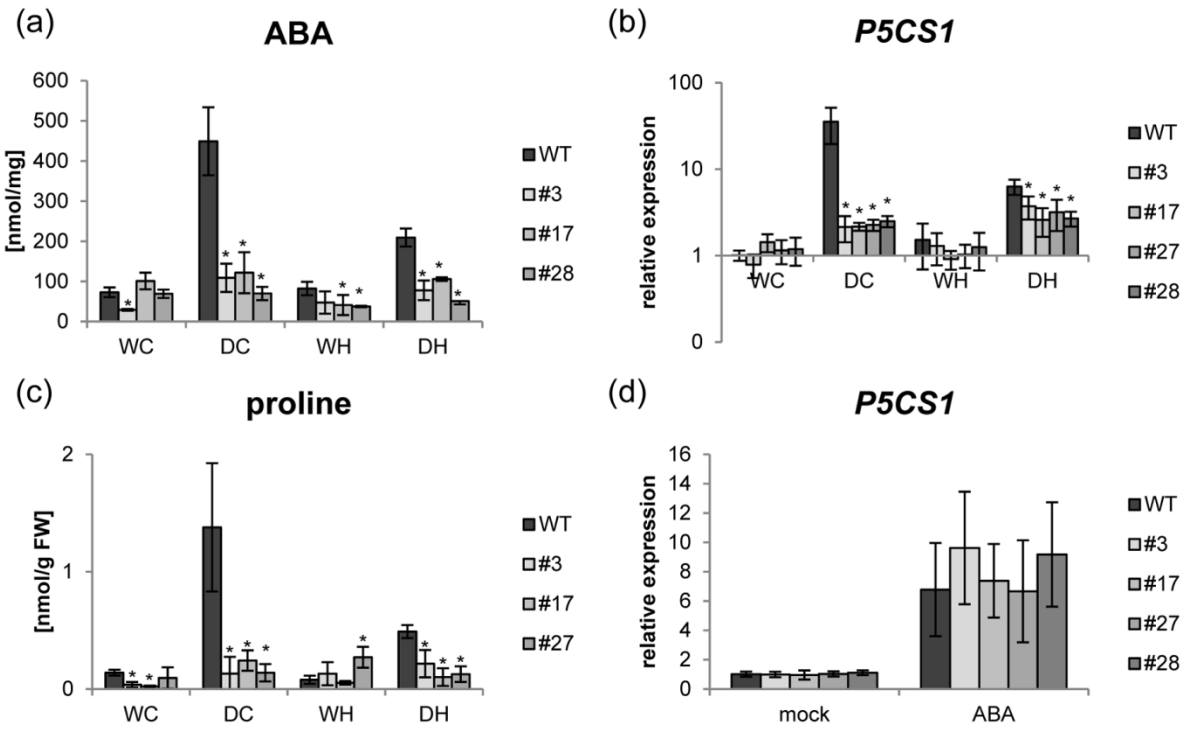

Figure 31. Drought response in leaves of HXK+SP6A potato plants. (a) ABA contents under different stress treatments, values are the mean of three biological replicates ± SD, Significance compared to WT was determined by two-tailed t-test (*; p-value < 0.05) **(b)** *P5CS1* expression in leaves, values are the mean of four biological replicates ± SD, Significance compared to WT was determined by two-tailed t-test (*; p-value < 0.05) **(c)** proline contents, measured from same samples as in (a) Significance compared to WT was determined by two-tailed t-test (*; p-value < 0.05) **(d)** *P5CS1* expression in floated leaf discs; floating assay with 50 µM ABA, values are the mean of four biological replicates ± SD, Significance compared to WT was determined by two-tailed t-test (*; p-value < 0.05)

To further corroborate this finding, the expression of the ABA responsive gene *P5CS1,* an enzyme catalyzing the rate limiting step in proline biosynthesis was examined [264]. The expression pattern reflects quite well the ABA contents **(Figure 31 b).** Similar to the changes in ABA levels there was a strong induction in the WT under drought and double stress,

whereas the increase in the HXK+SP6A plants was rather mild. Additionally, proline measurements are also in line with these results **(Figure 31c)**. Again higher levels were observed in the WT under drought and double stress. Under well-watered conditions heat had no effect on neither ABA, *P5CS1* nor proline contents. Together these results suggest that HXK+SP6A plants did only weakly respond to drought stress.

In order to investigate whether HXK+SP6A expressing plants are impaired in sensing pathways an ABA floating assay was performed. Therefore, leaf discs were incubated on 50 µM ABA solution for six hours and expression of *P5CS1* was determined afterwards. This revealed that all plants were able to sense ABA and react accordingly as implied by *P5CS1* expression **(Fig 29d)**.

4.2.2.2 HXK+SP6A plants show increased sink strength and reduced assimilate leakage

In several studies an enhanced tuberization was achieved by *SP6A* overexpression, as well as during this thesis [81,87]. Since the molecular mechanisms behind it are still poorly understood, the associated physiological and metabolic changes should be investigated deeper in HXK+SP6A plants. Therefore the plants were characterized morphologically. Already at a very young stage these plants showed a dwarf phenotype **(Figure 32a)** but were more branched **(Figure 32b)** which can even be seen in tissue culture. Later during plant growth these changes become more evident with additional shoots emerging from the basal nodes of the shoot contributing to the bushy phenotype **(Figure 32c)**.

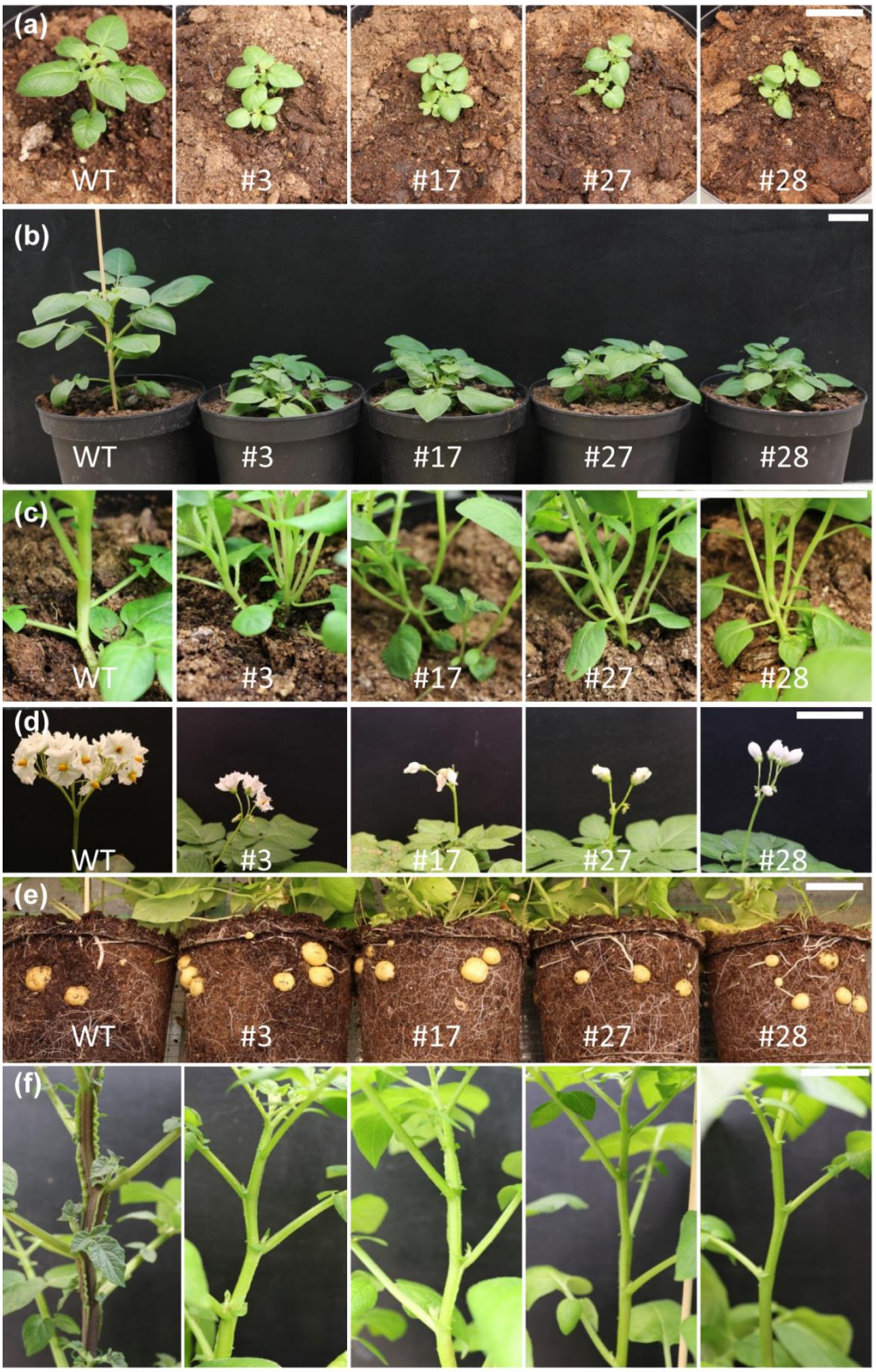

Figure 32. Phenotype of HXK+SP6A potato plants. (a) shoot phenotype at one week after planting (wap) from tissue culture **(b)** shoot phenotype at 2 wap **(c)** stem phenotype at 2 wap **(d)** flower phenotype at 5 wap **(e)** tuber phenotype at five wap **(f)** stem phenotype at six wap **(a-f)** scale bar 5cm, one representative of ten plants is shown each, experiment was repeated three times with similar results.

Mature plants of the WT flower around 5-6 weeks after transfer to the greenhouse **(Figure 32d)** whereas flower buds of the transgenics mostly ceased development, turned yellow and eventually fell off premature. When flowers developed they remained rather closed and were only present in inflorescences of about 1-5 flowers whereas the WT developed 10-15 flowers per inflorescence **(Figure 32d)**. A repression of flowering by overexpression of *SP6A* has been reported previously [265,266].

As stated before tuber formation was strongly increased indicating a shift in source sink balance **(Figure 32e)**. Another very evident phenotype was the purple color of the stem epidermis which was present in the WT but absent in the transgenics **(Figure 32f)**. Moreover, the axillary buds appeared rather dormant in the HXK+SP6A plants **(Figure 32f)**. The measurement of stem diameters conformed that the transgenic lines had about 30% thinner stems **(Figure 33a)**. In contrast they possess about three times more of them **(Figure 33b)**.

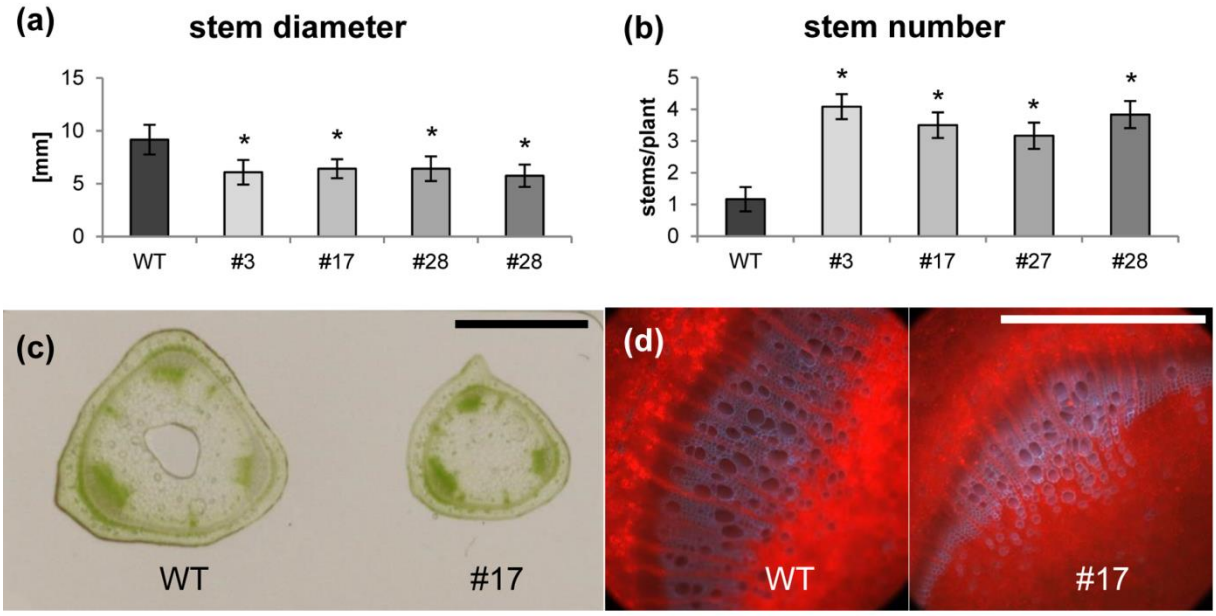

Figure 33. Stem phenotype of HXK+SP6A potato plants. (a) stem diameter, values are the mean of 15 plants ± SD, Significance compared to WT was determined by two-tailed t-test (*; p-value < 0.05) **(b)** stem number, values are the mean of 15 plants ± SD, Significance compared to WT was determined by two-tailed t-test (*; p-value < 0.05) **(c)** stem cross section under bright field; scale bar 5 mm **(d)** stem cross section under UV light; scale bar 1mm.

A microscopic analysis of stem cross sections of WT and line #17 provided further insights into the anatomy. Stems were of triangular shape **(Figure 33c)** and of rather identical morphology. Under UV light which detects chlorophyll and lignin autofluorescence no clear differences was observed besides the reduced overall diameter **(Figure 33d)**.

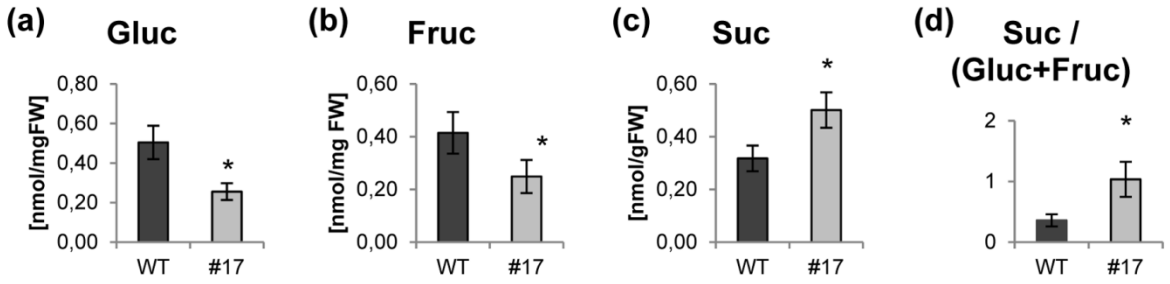

Figure 34. Sugar contents in stem cross sections taken of HXK+SP6A potato plants. (a) Glucose **(b)** Fructose **(c)** Sucrose **(d)** Sucrose/(Glucose+Fructose) ratio**,** samples taken between 6th and 7th leaf from the top values are the mean of five biological replicates ± SD, significance compared to WT was determined by two-tailed t-test (*; p-value < 0.05).

Since these findings suggest that more sucrose is transported through the phloem sugar contents in the stem cross sections taken between source leaves (the 6th and 7th leaf from the top) were measured. Compared to WT in line #17 glucose and fructose contents per mg FW were decreased **(Figure 34a, b)** but sucrose contents **(Figure 34c)** and with it the ratio sucrose/hexoses were increased **(Figure 34d)** indicative of a reduced export into the apoplast and an increased sucrose content in the phloem.

In order to visualize the sugar transport through the stem the fluorescent sucrose analog esculin was loaded into source leaves of the WT and HXK+SP6A #3 and #27 **(Figure 35)**. After 3-4 hours a very faint fluorescence could be observed in WT stem until the first nodium rootwards of the loaded leaf **(Figure 35a)**. Further downwards, in direction of the tuber sink hardly any fluorescence was visible **(Figure 35b, c)**.

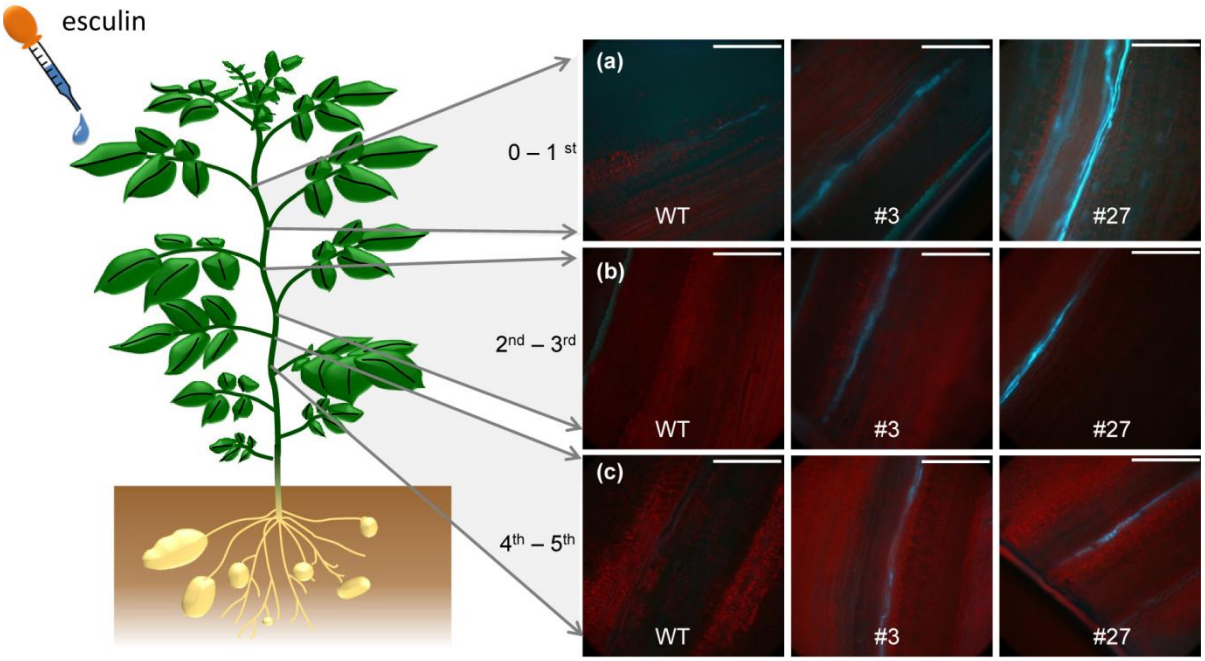

Figure 35. Visualization of esculin transport in longitudinal sections of stems of HXK+SP6A potato plants **(a)** cut between 0 and 1st nodium rootwards of the loaded source leaf **(b)** cut between 1st and 2nd nodium rootwards of the loaded source leaf **(c)** cut between 4th and 5th nodium rootwards of the loaded source leaf; all pictures taken under UV light, blue: esculin; red: chlorophyll autofluorescence, scale bar 0.5 mm.

In contrast in both transgenic lines a brighter fluorescence was observed up to five nodia rootwards. Although a signal was visible it became weaker with increasing distance from the esculin-loaded leaf. This might suggest a lower leakage of sucrose out of the sieve elements in HXK+SP6A plants as compared to WT.

From this one might assume that already at an early developmental stage more assimilates are transported to the bottom end of the stem and might promote root growth. As shown in **Figure 36a** plantlets were grown from tissue culture for two weeks in sand before harvest. Except for line #3 the transgenics showed an about 20- 30% increased root length, whereas growth of green biomass, measured as dry weight, was hardly affected at this time point **(Figure 36 a, b, c).**

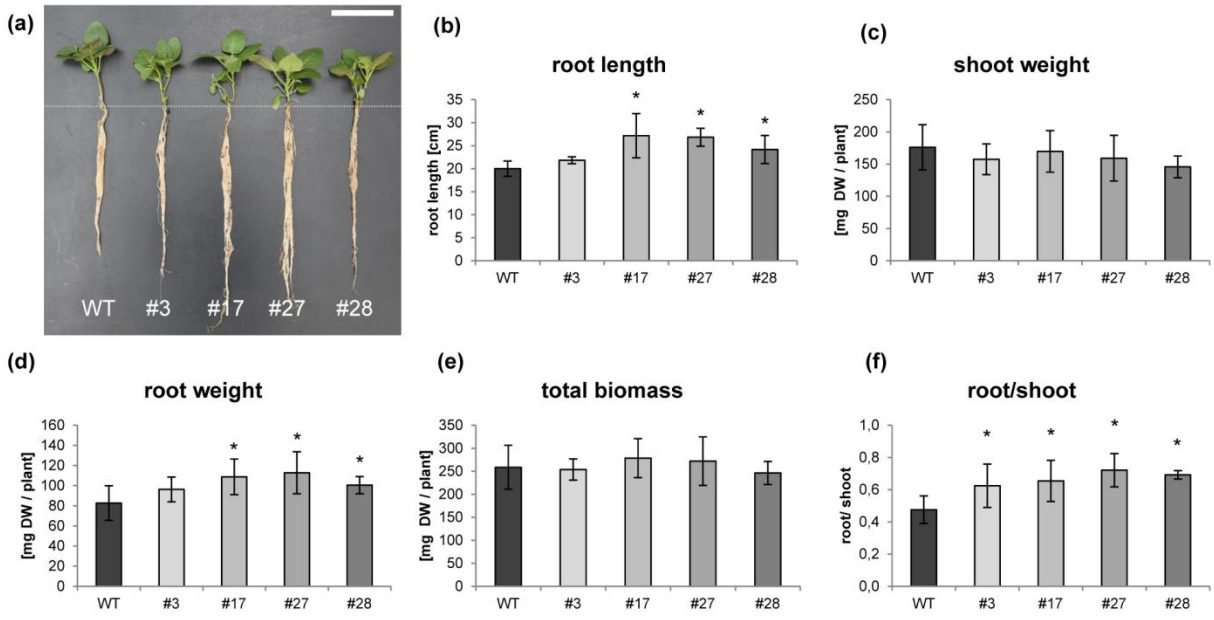

Figure 36. Root phenotype of HXK+SP6A potato plants at the age of 2 weeks (a) overall plant morphology, scale bar = 10cm **(b)** root length **(c)** shoot dry weight **(d)** root dry weight **(e)** total biomass (dry weight) **(f)** root dry weight/shot dry weight ratio; bars show mean of 6 plants ± SD, Significance compared to WT was determined by two-tailed t-test (*; p-value < 0.05).

However, root dry weight was also increased in three out of four lines **(Figure 36d)**, which reflects quite well the higher root length. Since total biomass (dry weight) was not altered in the transgenics **(Figure 36e)**, the ratio of root dry matter to shoot dry matter was shifted towards the root sink in all HXK+SP6A plants **(Figure 36f)**. This is illustrated by the fact that around 32% of total biomass is accumulating in the root system in the WT whereas in the

transgenics the proportion is around 40%. Altogether, this points to a more efficient transport of assimilates to the belowground sink organs in HXK+SP6A plants.

A lower rate of assimilate leakage from the phloem should increase the substrate supply for starch biosynthesis in the tubers. During starch deposition growing tubers are characterized by a high activity of sucrose synthase (SUSY). Since phloem unloading occurs symplasmically at this developmental stage, activities of cell wall-bound invertase (cwInv) are quite low. Heat was shown to reduce SUSY but increase cwInv activity. Since HXK+SP6A plants show enhanced transport through the phloem, these transgenics might have an advantage under elevated temperatures. Therefore activities of SUSY as well as cwInv were measured in growing tubers under heat.

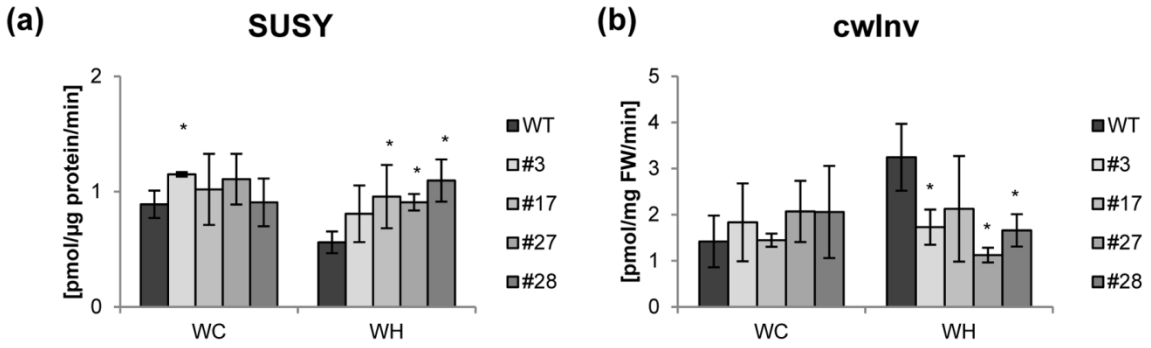

Figure 37. SUSY and cwInv activities in tubers of HXK+SP6A potato plants at the age of 6 weeks (a) SUSY activity **(b)** cw Inv activity; bars show mean of 5 biological replicates ± SD, Significance compared to WT was determined by two-tailed t-test (*; p-value < 0.05).

Under control conditions no clear difference was detected between WT and transgenics **(Figure 37a),** whereas under heat treatment SUSY activity was strongly decreased in the WT. Strikingly, in the transgenics SUSY activity remained unaffected by heat explaining the higher starch contents in the tubers than the WT under those conditions **(Figure 30)**. The activity of cwInv was not significantly changed under control conditions but increased twofold under heat in the WT whereas the HXK+SP6A overexpressing lines did not show significant changes **(Figure 37b)**.

5 DISCUSSION

5.1 SP6A as an important regulator of source-sink-balance

5.1.1 Overexpression of SP6A strongly increases sink strength

In order to secure potato tuber yield even under deteriorating environmental conditions a deeper understanding of developmental and environmental regulation of tuberization is of outstanding interest. Tuberization in potato is a highly complex process involving major changes in morphology, transcriptome, proteome and metabolome [267,268]. It underlies hormonal control for example by gibberellins and cytokinins as well as abiotic stimuli [269].

Even though adaptation to changing climate conditions has taken place over several thousands of years, modern potato cultivars still tuberize most efficiently under SD photoperiods and cool temperatures. In contrast, LD as well as high temperatures (especially during the dark period) are perceived by the leaves and inhibit tuberization [9,13,80]. One key regulator of day length sensitivity is the CDF/CONSTANS module. Due to sequence alterations CDF1 is no longer recognized by its repressor FKF1 which is active under LD. Thus, it can inhibit CONSTANS and mediate tuber formation also under LD [78]. The most pivotal regulator of tuberization might be a close homolog of FLOWERING LOCUS T in Arabidopsis, referred to as SP6A, identified as the tuberigen [81]. SP6A is indirectly activated by CDF1 and repressed by CONSTANS. Overexpression of SP6A enhances tuberization whereas its knock-down prevents tuber formation [81,87]. Under favoring conditions SP6A is produced in the leaves and transported via the phloem to the stolons. There, it interacts with FDL via 14-3-3 proteins to form a tuberization activation complex [87]. Still many more additional players described recently are involved in this process [269–273].

During this thesis the role of SP6A was investigated using transgenic potato plants. Hence *SP6A* was overexpressed in a codon optimized variant (*SP6A*^{cop}*-HA*) driven from the CaMV35S promoter **(Figure 3)**. This could extremely accelerate tuberization underlining the crucial role of this protein in tuber initiation. However, severe shoot growth defects were observed **(Figure 4)**, which have not been described in transgenic plants where an unmodified SP6A was used [81,87]. In those studies plants were of rather normal overall morphology and, if at all, only slightly smaller. Tuber formation occurred earlier, but source-sink-balance was not reported to be as tremendously affected as described in this thesis.

The fact that in *SP6A^{cop}-HA* overexpressors the tuber sink was formed before the source leaves were sufficiently developed indicates that SP6A has the ability to control assimilate allocation and thus shifts the source-sink-balance **(Figures 4 and 5)**.

This hypothesis is further supported by the fact that stored tubers formed daughter tubers instead of shoots implying an altered meristem identity. This was observed for all tubers when stored in the dark at room temperature **(Figure 6)**. When tubers were brought into soil this phenomenon occurred as well, but under this condition most tubers developed shoots **(Figure 7)**. Probably the surrounding soil provides signals which induce shoot rather than tuber development. To elucidate the molecular reasons causing the daughter tuber phenotype transcript profiling experiments were carried out with dormant buds of WT and transgenic tubers sampled shortly after harvest. It was assumed that the meristem identity of dormant buds is already predetermined before the morphology of the sprout can be seen. Indeed, the results suggest a reprogramming of the transcriptome of meristematic cells of *SP6A^{cop}-HA* overexpressing tubers **(Figure 8)**. In particular several transcription factors controlling flower meristem identity in Arabidopsis or rice, for example AGAMOUS likes or MADS box transcription factors, are altered in expression [241–244,274]. Although the function of the potato homologs in tuber development is not clear, this finding implies that the expression of these genes is linked to the different meristem identity, finally leading to daughter tuber formation.

Furthermore, hormone signaling via cytokinin (CK), gibberellin (GA) and ethylene might be affected as well, as indicated from the microarray data **(Figure 8, Table S1).** Hormones are essential for many developmental processes, such as flowering and tuberization. For example, high levels of gibberellins inhibit tuber formation [275] and the amount of GA_1 decreases at the beginning of tuberization [12]. In contrast exogenous application of ABA induces tuber formation [12] probably via a cross talk between GA and ABA [102]. Auxin also plays an important role in regulation of tuber growth [276]. In cross talk with GA [277] it positively influences tuber formation. Auxin is transported form the apical meristem to the stolon, where Auxin levels increase during tuber initiation and remain at a high level [278]. Cytokinin, however, promotes sprouting and regulates dormancy together with GA [279]. CK increases the tuber number but reduces the tuber weight if applied externally [280]. In tomato overexpression of the cytokinin activating enzyme LOG1 in tomato induced aerial minituber formation in the axillary meristems [281].

Moreover, hormones can influence the activity of FTs [282,283]. GA for example was shown to enhance growth in parallel with FT2 in aspen [284].

As flowering and tuberization are closely related processes [87] and homologs of flowering genes enhance tuberization in potato [81] the transcriptional changes might introduce an altered meristem identity in *SP6A*^{cop}*-HA* expressing tubers promoting formation of secondary tubers instead of shoot development. Whilst the exact mode of action remains still elusive, the findings strongly suggest that SP6A fosters sink development. These findings are further in compliance with previous results showing that FT proteins can control storage organ formation across a wide range of species such as swelling of turnip [285], growth of onion bulbs [286], pseudobulbs in orchids [287], and also tuberous root formation in *Callerya speciosa* [288]. In fact, those FT proteins which are thought to be involved in the control of storage organ development are rather conserved amongst many root, tuber or tuberous root crop species including potato (*Solanum tuberosum*), sweet potato (*Ipomoea batatas*), onion (*Allium cepa*), carot (*Daucus carota*), sugar beet (*Beta vulgaris*) and cassava (*Manihot esculenta*) [273]. Moreover, polypyrimidine tract-binding (PTB) proteins share high sequence homology which enables regulatory interactions with FT proteins [99].

From this point of view it becomes more obvious that the function of FT goes beyond flowering time control. Instead it seems that FT proteins play an important role in the regulation of developmental programs. FT homologs might control propagation and, if required, adjust vegetative and generative propagation strategies according to environmental conditions, in order to ensure the maximal growth for the mother plant whilst generating a maximum number of offspring.

In summary, in potato, SP6A is an important player in regulation of the source-sink-balance. Strong overexpression shifted this balance towards the tuber sink. Hence, a tight regulation of these developmental changes is required. For crop breeding purposes a better understanding of these processes is also essential.

5.1.2 Identification and biotechnological utilization of a small RNA regulating *SP6A* under elevated temperatures

SP6A is regulated at the transcriptional level via the CDF/CONSTANS module [78]. In this model, FKF1 and GI bind to CDF1 in leaves thus marking it for proteolytic degradation. Therefore CDF1 no longer inhibits CONSTANS (COL1) which activates SP5G, another FT family member in potato that represses SP6A and thus connects photoperiod to tuberization [78,82,98].

In this study, it was shown that *SP6A* is not only under transcriptional control but does further underlie posttranscriptional regulation by a small RNA, *SES*, which integrates developmental

as well as environmental signals. Many biological processes are regulated by miRNAs [289]. With regard to climate change miRNAs which are responsive to abiotic stress are of special interest and become a putative target for crop improvement [290–292]. In wheat several heat responsive miRNAs have been described [293]. Modulating the expression of miRNAs is thus another way of introducing changes in gene expression of crop plants that will improve yields.

Still, only few miRNAs are well studied in potato. Among them is miR172 promoting tuberization via targeting RAS-RELATED PROTEIN 1 (RAP1) and inducing BEL5 [101]. Tuberization can be repressed by miR156 through downregulation of SQUAMOSA PROMOTER BINDING-LIKE (SPL) transcription factors [294–296]. However, no small RNA was shown so far to be involved in heat mediated repression of tuberization in potato. In *Brachypodium distachyon*, the Pooideae-specific miR5200 targeting FT has been described [297]. This miRNA is induced by short days, preventing FT accumulation and flowering under non-inductive conditions. To extend our knowledge it is of outstanding importance to gain deeper insights into the molecular mechanisms regulating tuberization, in particular SP6A, especially in order to ensure food supply even under challenging environmental conditions.

Here, the discovery of a new small RNA targeting *SP6A* is described. Motivated by the severe phenotypic changes of SP6A^{cop}-HA plants, an *in silico* screening for putative small regulatory RNAs was performed, which led to the identification of a putative 19nt long small RNA called *SES* **(Figure 11 and 12, Table S2)**. Up to now the detailed mechanism of *SES* maturation and processing is not clear and seeks further investigation. Especially the predicted length is unusual for a typical miRNA since 21 and 24 are more common [298]. However sizes can vary from 18 to 25 nt [299] and miRNAs of different length have also been found in potato [300]. These different lengths could be due to non-canonical processing pathways besides DICER [301], although little is known about the pathways in plants [302]. Nevertheless, the data obtained in this study strongly support the inhibition of *SP6A* via *SES* **(Figures 13-18)**. This occurs most likely by transcript cleavage although additional translational repression cannot be ruled out. In transient assays using *N. benthamiana* it was found that *SES* is able to reduce the transcript amount of co-expressed *SP6A* (WT sequence) but not of codon-optimized *SP6A^{cop}* **(Figure 13)**. The assumption that this was due to sequence variation in the predicted *SES* binding site was verified by an experiment using *SP6A^{mod}.* This sequence was only modified in the *SES* binding site and the amount of the corresponding mRNA was not affected by simultaneous expression of *SES* **(Figure 14)**. Together these studies demonstrated the sequence specificity and molecular function of this small regulatory RNA to degrade the *SP6A* mRNA. Further it supports the assumption that

the codon optimized variant is a poor target for *SES*, which might cause the strong phenotype.

An in silico analysis of the genomes of closely related *Solanaceae* species such as *Solanum lycopersicum*, *Solanum pennellii* and *Nicotiana benthamiana* revealed that the genomic locus of *SES* was not present in these species **(Figure 12, Table S3)**. This suggests that *SES* has evolved independently in potato to regulate specifically *SP6A*. Although *SES* targets an *FT* homologue and close homologues of *SP6A* are present in other *Solanaceae*, potato is the only one of these species that tuberizes. The fact that a tuberization specific gene is the target of *SES* could explain why this particular small RNA is not found in other *Solanaceae*. Recently sequences with more or less high similarity to the putative *SES* precursor RNA have been found widely distributed all over the potato genome, thus opening up a possible evolutionary path along which *SES* has evolved (personal communication.José M. Corral).

The expression level of *SES* turned out to be developmentally regulated and repressed in mature plants but induced by elevated temperatures. In contrast, *SP6A* levels are relatively low at the juvenile stage and increase further during tuberization **(Figures 16 and 17)**. Thus, the expression pattern of *SES* implies that *SP6A* is regulated at the post-transcriptional level to adjust the source-to-sink balance depending on developmental and environmental signals Consistent with this observation overexpression of a target mimicry sequence (*STTM*) promoted slightly earlier tuberization and preserved tuberization even under rather high temperatures **(Figures 20-22)**. This allows two assumptions. First, in young plants the expression of *SES* might serve as an additional regulatory layer besides the well-studied CDF/CONSTANS module. When tuber initiation takes place *SES* expression drops drastically releasing this inhibitory signal on *SP6A*. As this alone cannot explain the further increase in *SP6A* levels more regulatory players must be involved. However, these additional regulators must be more important as the effect of *SES* on tuberization earliness is comparatively mild **(Figure 21)**.

Second, elevated temperatures repress tuber induction and tuber growth, which correlates well with a decline in *SP6A* expression and was also observed during this thesis **(Figures 17, 18** and **28)**. Although progress has been made in identifying SP6A interaction partners [87] and also heat adaptation mechanisms [142,303] a rather immediate causal agent for *SP6A* repression under heat has not been found yet. In this study, it could be shown that the small RNA *SES* is strongly induced under heat and contributes to the heat-mediated down-regulation of *SP6A* expression **(Figures 17 and 18)**. A simplified model of the regulation of *SP6A* under ambient and elevated temperatures is shown in **Figure 38**.

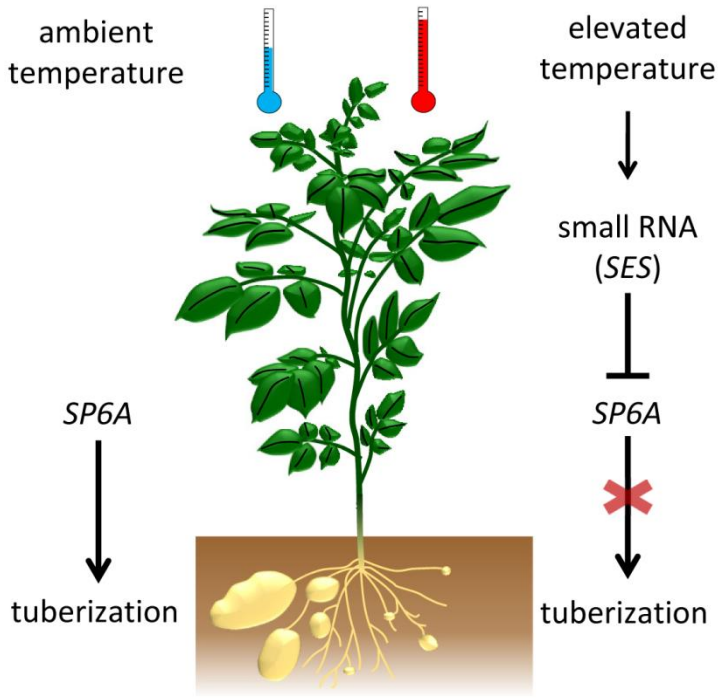

Figure 38. Simplified model of regulation of *SP6A* under ambient and elevated temperatures Under ambient conditions the phloemmobile signal *SP6A* is produced in the leaves and induces tuber formation in the stolons. Under elevated temperatures a small RNA is expressed in the leaves, which inhibits *SP6A*. Therefore tuberization cannot occur. Numerous other regulators not shown here additionally act in concert to adjust tuberization according to photoperiod, development and temperature.

As a likely cause for the heat induction of *SES* two possible heat shock factor (HSF) binding sites [256–258] were identified less than 2 kb upstream of the *SES* transcript **(Figure 19, Table S4)** providing interesting clues for further investigation. The biological function needs to be verified via ß-glucuronidase or luciferase reportergene assays. A co-infiltration with the putatively interacting heat shock proteins would be another strategy to clarify their function. Apart from an activation of *SES* transcription under heat is also possible that expression of *SES* is repressed under cool and ambient temperatures and the repressor is released under higher temperatures.

The role of *SES* in the heat-mediated down-regulation of *SP6A* was confirmed by overexpression of a target mimicry construct (*STTM*), resulting in two- to four-fold higher *SP6A* transcript levels under heat **(Figures 20-22)**. Most importantly, these transgenic plants formed tubers also at elevated temperatures that prevented the formation of stolons and tubers in the commercial variety "Solara" **(Figure 22)**. Thus, expression of the STTM construct can overcome heat-mediated down-regulation of *SP6A* expression. The results

make small RNAs once more an interesting target for abiotic stress tolerance [291,292,304,305]. Various sequencing approaches have been carried out in the past to identify microRNAs in potato, also with respect to stress responses [306–308]. The approach described here provides an additional strategy for the improvement of the potato crop.

Since the origin of the potato lies in the highlands of Southern Peru, one could assume that the modulation of tuberization according to temperature could have been a selective advantage for the first potato plants. The control of SP6A by *SES* is most likely an evolutionary rather old regulatory mechanism that controls the transition from the vegetative to the generative stage and, as a result, influences the balance between source and sink. This might work as follows. If no large differences in photoperiod can be perceived, the regulation of tuberization is likely to depend on temperature changes. As long as the temperature is high, *SES* expression prevents tuberization and promotes shoot growth. This allows a maximum of carbon assimilation and optimal aboveground biomass production. Falling temperatures indicative of an ending vegetation period terminate *SES* expression and induce *SP6A* expression enabling tuberization. At the same time, senescence is induced, mobilizing resources from the shoot to the developing tubers. This allows maximum tuber yield under natural conditions and habitats. During the development of potato plants, the temperature-dependent adaptation of the transition from vegetative to generative growth was advantageous, as it enabled the optimal use of the growing season and the generation of an increasing number of offspring. In the context of global warming, this benefit is becoming a major handicap that limits potato production to temperate and cool climates. Overcoming this ancient mechanism will allow the breeding of heat-tolerant potato varieties, which would be an important contribution to secure future food production.

5.2 Combination of several genes as promising tool for stress tolerant crop plants

5.2.1 Overexpression of HXK+SP6A improves water use efficiency

In the near future global average temperatures are expected to rise further, since unfortunately current efforts to limit global warming to 1.5-2.0 °C above preindustrial times are insufficient. Thus, in order to secure food production designing crop plants which can cope with abiotic stress is of special importance [2,15,131,151,309]. In potato, a preservation of tuberization which is unaffected by heat is essential. Additionally, heat is often accompanied by drought, especially in tepid climate. Therefore, reduction of transpiration is a desirable trait. For this purpose, transgenic potato plants expressing two transgenes, *AtHXK1* of Arabidopsis and *SP6A* of potato, called HXK+SP6A, have been developed and tested for improved stress tolerance towards heat, drought and combined stress conditions.

Up to now only few studies have shown an increased tuber yield under drought or heat conditions. For example repression of TOC1 could preserve tuber yield under elevated temperature presumably via feedback on SP6A [310]. Overexpression of a particular allele of Hsc70 increased heat tolerance by preventing proteins from misfolding [142]. Enhanced drought tolerance was achieved by overexpression of a MYB or a bZIP transcription factor through reduced stomatal aperture or accelerated closure, thus increasing the survival rate after drought stress and preserving tuber yields under drought [311,312]. Overexpression of the potato annexin STANN1 could also promote drought tolerance by interfering with photoprotection and thus overcomes drought mediated reduction in photosynthetic rates [313]. So far an improved yield under combined stress has not been reported yet.

Throughout the history of plant cultivation water consumption of crops has always been an important issue. Although potato plants are relatively efficient in water use efficiency compared to other crops, they are still vulnerable to drought periods. For example, drought leads to a reduction in plant growth, tuber number and tuber size [181–185] and thus depicts an agricultural problem. Decreased transpiration rates via modification of the stomata could improve water usage. A stoma consists of two symplasmically isolated cells referred to as guard cells and neighboring cells. High turgor pressure as a result of high water availability makes the guard cells bend in a C-like shape thus opening a gap in between enabling gas exchange from the atmosphere into the intercellular space in the mesophyll. In case of drought stress the guard cell turgor decreases leading to a collapsed cell shape thus closing

the stoma. Heat leads to stomatal opening whereas combined heat and drought stress close the stomata [314,315].

For many years it was thought that sugars can control stomatal opening via affecting the osmotic potential [209]. This is in line with the findings that a decreased beta-amylase (BAM) activity in stomata confers drought avoidance in *A. thaliana* by stomatal closure which might occur via reduced soluble sugar contents from inhibited starch breakdown in the stomata [196,316].

Recently, AtHXK1 was shown to reduce transpiration when expressed in guard cells (by means of the KST1 promoter) of *A. thaliana,* citrus or tomato without a negative effect on plant growth and CO_2 assimilation [205,206,263]. Although the molecular mechanism is not fully understood yet, it is believed that AtHXK1 controls the stomatal aperture to coordinate transpiration with photosynthesis via sugar signaling pathways [208,209]. AtHXK1 was shown previously to act as a sugar sensor [317]. It is assumed that an excess of sugar, which is not transported by the phloem during high photosynthetic activity, is transported with the transpiration stream in the direction of the guard cells, where it serves as a signal to close the stomata and thereby prevent unnecessary water loss [205,206,209]. Thus it might be also possible that sugars do not acts as osmolytes but rather as signaling molecules [209]

Here, potato plants which express construct provide clear evidence that the desired effect can also be seen in the crop plant potato under control conditions, as they exhibit reduced transpiration rates **(Figure 23)** due to reduced stomatal aperture **(Figure 24)**. This increased water use efficiency significantly. Although CO_2 assimilation per area was slightly affected in the combined approach with SP6A, a bushy growth phenotype with more (smaller) leaves, probably caused by overexpression of SP6A, might compensate for this **(Figure 25)**.

A common drought avoidance strategy of plants is to enlarge the root system in order to exploit water resources in the surrounding soil. The enhanced root growth that was detected in the HXK+SP6A plants **(Figure 36)** could on the one hand be due to a better nourishment of root sink tissue with assimilates, since AtHXK1 is thought to improve the water stream through the plant and thus might improve assimilate partitioning and root growth [263]. It can also be speculated that reduced water transpiration somehow pretends drought stress for the plant which may stimulate increased root growth. The shift in total biomass accumulation from shoot towards root might prepare HXK+SP6A expressing potato better for upcoming dry seasons and thus result in an advantage under field conditions. Hence, one strategy for enhancing the tolerance towards abiotic stress could be the modification of overall plant architecture.

The most common reaction to drought within land plants is closure of the stomata [318]. Therefore, plants that possess a lower stomatal conductivity could have an advantage under limited water availability. Under drought stress the HXK+SP6A expressing lines exhibited a lower transpiration rate compared to WT plants **(Figure 26)**, even though it decreased in both genotypes. The same effect was observed under combined heat and drought stress, whereas treatment with heat alone resulted in an increased transpiration rate as described previously [136,152]. Decreased stomatal conductance therefore increased the tolerance towards drought stress.

The increased drought tolerance in the transgenic lines was verified by measurements of the phytohormone abscisic acid (ABA) **(Figure 31a)**. As expected ABA contents were increased in the WT under drought conditions but to a lesser extent in the transgenics. This implies that the WT plants have consumed more water and therefore feel drought stress whereas reduced water consumption in the HXK+SP6A plants seems to save resources and thus reduces water stress.

Under drought stress plants phytohormones trigger the accumulation of osmolytes [319] . One well-known osmolyte increased under drought is the amino acid proline [320,321], which is like all osmolytes electrically neutral at a physiological pH. Proline can be synthesized from the amino acid glutamate. The enzyme that catalyzes the initial reaction is the Δ1-pyrroline-5-carboxylate synthetase (*P5CS1*), which uses glutamic semialdehyde (GSA) as a substrate [322,323]. After pyrroline-5-carboxylate is formed spontaneously, this is reduced to proline. *P5CS1* was shown to be drought and ABA responsive [323].
Measurements of proline as well as qPCR of the ABA responsive drought marker gene *P5CS1* indicated that drought stress was less severe for the transgenics **(Figure 31 b, c)**. However, the HXK+SP6A plants were still able to react to changing environmental conditions and adapt evaporation under drought and heat. This was confirmed by means of an ABA floating assay, where *P5CS1* reacted similarly in all plants **(Figure 31d)**.

In summary this means that HXK+SP6A plants still need to be adequately supplied with water, but due to lower evaporation rates probably can cope with less water. Under field conditions they probably could endure longer periods of rain absences than WT plants without being severe drought stressed. The reduced transpiration is most likely due to the KST::AtHXK1 construct as it fits very well the observations in Arabidopsis, citrus and tomato. However, the contribution of SP6A overexpression to morphological changes like the improved root growth which putatively mediates drought avoidance is unclear.

Overexpression of *AtHX1* could lead to a significant yield increase and thus have an agricultural relevance, especially for those crops that are not adapted to drought conditions. Some crop plants might consume more water than is required for high CO_2 assimilation rates because drought is unlikely to occur at their place of origin, or breeding for efficient water usage may not be advanced enough or rather difficult.
In fact, in those plants a reduction of stomatal conductance does not necessarily have a negative effect on CO_2 assimilation but will reduce water consumption. In line with this, mild occlusion of the stomata, as achieved by AtHXK1, has a greater impact on water loss than on CO_2 assimilation. A similar situation was observed with WT plants when drought was applied, indicating that potato plants normally consume more water than needed to maintain CO_2 fixation.

In further studies it would be interesting to examine whether and how fast stomata of *AtHXK1* expressors react to other treatments for example biotic stress caused by fungi and bacteria infection. In tobacco NtHXK1 was shown to have dual functions: a catalytic one and a glucose sensing one [324].Since the exact mode of action of AtHXK1 in stomata is still not resolved, one could create transgenic potato plants overexpressing a catalytic inactive form of AtHXK1 which is not impaired in sensing in order to distinguish between catalytic and sugar sensing function. Together with AtHXK1 single transformants this could provide a deeper understanding of functionality and biotechnological relevance of this enzyme.

5.2.2 Overexpression of HXK+SP6A preserves tuber yield under abiotic stress tolerance

5.2.2.1 SP6A might be the main determinant of high tuber yields under abiotic stress

One aim of this thesis was to improve tuber yields. Therefore, the FLOWERING LOCUS T-homologue *SP6A* was chosen for overexpression because it has been identified as a positive key regulator of tuberization [81]. Previous experiments with *SP6A^{cop}-HA* plants described in this thesis have verified its function.

Downregulation of SP6A expression is considered to be the cause of the heat-mediated inhibition of tuber formation [136,152]. This is mediated by both transcriptional and posttranscriptional regulation by a small RNA (*SES*) as shown in this thesis [325]. Expression of a mimicry construct (*STTM*) to sequester *SES* maintained *SP6A* expression and facilitated tuber formation under heat conditions.

For the co-expression with *AtHXK1* a wild-type *SP6A* was overexpressed from the StLS1 promoter [261]. This also resulted in elevated SP6A levels and stimulated tuber formation under control conditions. By using the StLS1 promoter, *SP6A* levels were only moderately increased (5 to 7-fold). Although the HXK+SP6A plants were smaller and accumulated less aboveground biomass , the development of the shoot was not as strongly affected compared to the previous approach using a codon-optimized SP6A version under control of the 35S promoter **(Figures 4 and 23)**. The accessibility for posttranscriptional control might also contribute to a rather controlled overexpression. The number of tubers and the yield increased significantly in HXK+SP6A plants and was stable under drought, heat and combined stress, which is most likely mediated by overexpression of SP6A. In contrast tuber number and tuber yield were clearly decreased in the WT under all three stress conditions.

While heat strongly represses SP6A expression [136], limited data is available on how drought affects SP6A expression. Data of this study suggest that drought also suppresses SP6A expression levels (by approximately 40%), although less pronounced than heat treatment (approximately 65%). Concurrent exposure to both stressors caused the strongest (80%) reduction in SP6A mRNA levels **(Figure 28a)**. Remarkably, the yield reduction correlated well with SP6A expression levels **(Figure 28b)**. This is in compliance with current knowledge and strongly suggests that yield stabilization under stress is controlled to a large extent by SP6A. Therefore, also in commercial cultivars a high level of SP6A expression in both drought and heat might be crucial for maintaining a high potato tuber yield under these circumstances.

However, the causal agent for downregulation of SP6A under drought conditions has not been identified yet. The small RNA inhibiting SP6A under heat can be excluded as it might be even downregulated under drought **(Figure 29a)**. It is likely that other close partners upstream, like small RNAs which have not been identified, target SP6A or interaction partners. The involvement of miRNAs in drought responses in crop plants, including potato, is already known but poorly understood [292,308,326]. As another possibility the members of the CDF/CO pathway were taken into consideration, since they are known to regulate SP6A. Neither for CDF nor for the CONSTANS homologues COL1 or COL2 changes in transcript amount under drought could be detected **(Figure 29b, c, d)**. Therefore, if these regulators play a role at all, it is more likely to occur on protein level via posttranslational inhibition such as phosphorylation or protein degradation, which requires deeper analysis.

Overexpression of SP6A could overcome its transcriptional stress-related repression. Accordingly, tuber fresh weight and tuber number of transgenic HXK+SP6A plants were less affected by stress conditions than in the WT **(Figure 27)**. However, the expression of SP6A

also fell under stress in some lines, which could be due to regulatory mechanisms. Anyhow, the residual SP6A expression was still higher than the WT under well-watered control conditions and therefore apparently sufficient to maintain tuberization and further promote assimilate translocation into growing tubers **(Figure 28a)**. In accordance with this hypothesis, the starch content of the tubers was largely maintained under single and double stress while it decreased with the severity of stress in the WT **(Figure 30)**. As a probable cause for that, the sustained SUSY activity in the tuber parenchyma of HXK+SP6A tubers was identified **(Figure 37a)**. At the same time, the cwInv activity was induced by heat in the WT **(Figure 37b)**, which implies a lower sucrose supply for the tuber under those conditions. Overexpression of SUSY in potato tubers increased starch contents and total tuber yield and in thus in line with the results described here [169]. Overexpression of SP6A like in the HXK+SP6A plants seems to achieve the same effect indirectly.

5.2.2.2 Overexpression of HXK+SP6A promotes branching

Potato plants overexpressing HXK+SP6A overexpressors exhibit a phenotype with massive branching of stolons but also of the shoot especially from basal nodes **(Figure 32)**. Currently, an involvement of branching promoting genes in causing the branched phenotype cannot be excluded yet [327,328]. Overexpression of the TEOSINTE BRANCHED1, CYCLOIDEA, PCF (TCP) transcription factor BRANCHED1 (BRC1) in potato led to a phenotype which is rather similar to the one of HXK+SP6A overexpressors concerning the high tuber number [329]. In fact, BRC1 can regulate axillary bud outgrowth via homeodomain leucine zipper protein (HD-ZIP)-transcription factors [330]. In Arabidopsis BRC1 interacts with FT [331], therefore a link between these genes also in potato is not unlikely and needs to be unravelled.

5.2.2.3 Regulation of sugar partitioning might be controlled by SP6A

Another function of SP6A besides tuber initiation might be to determine plant habitus. SP6A seems to regulate carbon fluxes through the plant and thus further contribute to storage organ development. As the shoot phenotype of HXK+SP6A overexpressing plants indicates, less carbon might be available in these transgenic plants to supply shoot growth, pigment synthesis and axillary bud outgrowth **(Figure 32, 33)**. Sugar measurements indicate that less sucrose is leaking into the stem **(Figure 34)**. Further, esculin loading experiments suggest that the phloem in HXK+SP6A overexpressors is sealed better from the surrounding stem tissue than the WT and thus increases transport efficiency towards the tuber sink **(Figure 35)**. The molecular reason behind it could be the interaction of SP6A with SWEET11 which might prevent sucrose leakage out of the phloem [93]. A simplified schematic model is depicted in **Figure 39**. SWEET proteins were originally identified as sucrose efflux carriers

transporting sucrose out of the mesophyll cells [26]. The finding of this missing transporter has therefore gained general approval amongst plants physiologists as it completed the understanding of the apoplastic phloem loading pathway [332,333]. During tuber development, the type of sucrose unloading changes from the apoplasmic to the symplasmic route [334], thus reducing the sugar export in the stem or tuber apoplast would be desirable.

In order to improve tuber starch contents, a deeper understanding of the obviously improved sucrose partitioning processes in HXK+SP6A potato plants would be beneficial. Two different mechanisms might serve as a possible explanation. On the one hand the interaction of SP6A with SWEET11 might prevent the leakage of sucrose into the apoplast. This would be true if SWEET11 is localized at the phloem companion cells acting as a sucrose exporter. Indeed apoplastic sugar levels of stems are decreased in SWEET11-RNAi plants but increased in 35S::SWEET11 plants. Concurrent transformation of the latter with SUC2::SP6A plants could again lead to decreased sucrose levels [93]. However, if this model would be correct expression of SP6A under the companion cell specific SUC2 promoter or the rolC [335] promoter should give a similar tuberization phenotype as in HXK+SP6A, but this has not been reported [93]. Therefore it might on the other hand be also possible that the export of sucrose is indeed mediated by sucrose exporters for example from the SUC or SUT family. In WT stems sucrose could then be loaded into the apoplast but it is probably immediately taken up by SWEETs in phloem parenchyma cells to be used for tissue makeup or other processes. Due to continuous afterflow this would in the end reduce sucrose transport through the phloem. If SP6A inhibits SWEET in the phloem parenchyma cells, this would first increase sugar levels in the apoplast leading to a feedback inhibition on the unknown sucrose exporter and consequently leave more sucrose in the phloem.

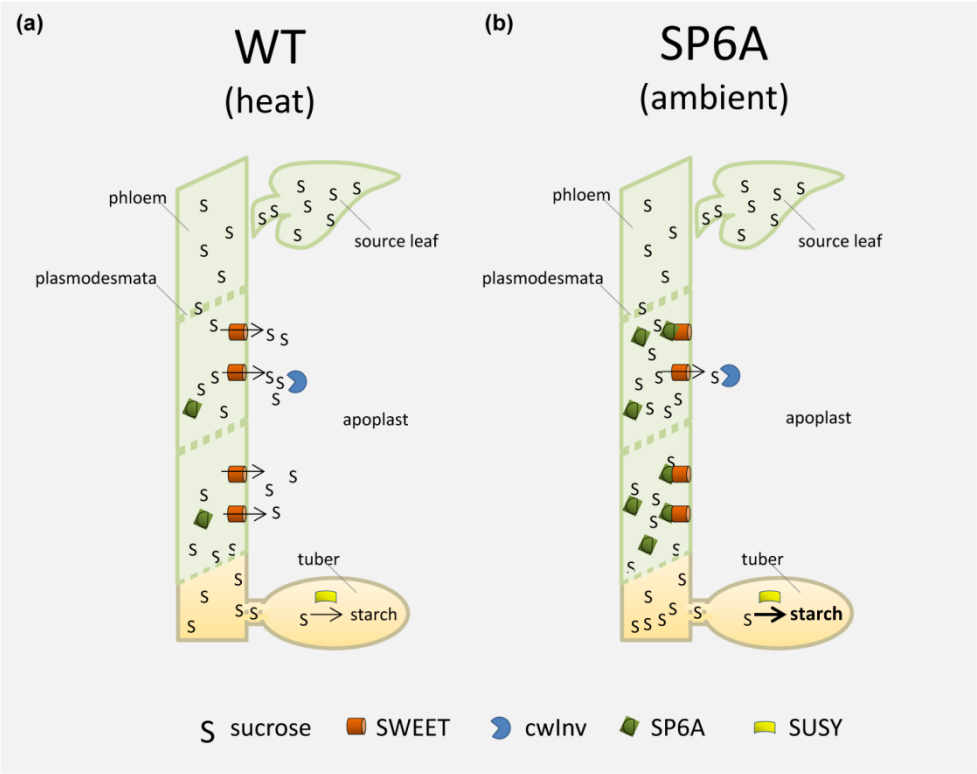

Figure 39. Schematic model of SWEET11-SP6A mediated rerouting of assimilate transport. (a). In the WT, especially under heat conditions, *SP6A* levels are low. Thus SWEET11 proteins are not inhibited and are transporting sucrose coming from the source leaves out of the phloem into the apoplast where it is degraded by cwInv. In the tuber less sucrose is available as a substrate for starch biosynthesis via SUSY **(b) I**n *SP6A* overexpressing potato plants, or under ambient temperatures, *SP6A* levels are high. In this case, many SWEET11 transporters are inhibited by SP6A. This reduces the sucrose leakage and more sucrose is left in the phloem. Finally, more sucrose can be converted into starch, thus increasing the starch content in the tuber.

However, it remains elusive why obviously phloem loading in the leaves is not or not tremendously affected [93] and still functioning to an extent which provides enough assimilates for tuber formation. If it is always the same SWEET protein which is inhibited by SP6A one explanation might be a tissue/cell specific expression or phosphorylation differences influencing the interaction possibilities. A similar occassion has been described for the potassium channel AKT2 of *Arabidopsis.* This transporter changes its properties based on its phosphorylation status [50]. AKT2 is needed to maintain the proton motive force (PMF) required for sucrose reloading into the phloem under low oxygen conditions [336–338].

Either way, the phenotypic data of the HXK+SP6A overexpressors, including shoot morphology and overall plant habitus **(Figure 32)**, together with improved tuber yield **(Figure 27)** and enhanced root growth **(Figure 36)** suggest that more sugars might reach the root and tuber system. This is indicated by root to shoot ratios and harvest indices In fact, from

the shoot morphology it appears that less carbon is fed into the development of aboveground biomass tissues such as stems and the outgrowth of axillary buds. This is further supported by esculin loading experiments **(Figure 35)** revealing that in the transgenics more esculin is visible in the stems even several nodia rootwards of the loaded leaf. In the WT esculin was only hardly detected up to one nodium rootwards. This indicates a diluting effect in the WT stem, due to a loss of carbon in tissues besides the main transport route. Although the experiment was repeated and similar results were obtained in several stems, quantification of the amount of loaded esculin is difficult. Therefore additional experiments should performed for example loading experiments with dyes that cannot be exported by sucrose transporters for example 5-Carboxy-fluoresceindiacetate-acetoxymethylester (CFDA) [339,340].

Consequently, for increased assimilate supply of storage organs the transport path between the most prominent source organs, the leaves, and the sink organs, the tubers, should also be taken into account.
Together, the results obtained further support the assumption that SP6A plays a major role in development of potato tubers through determination of meristem identity and additionally maintenance of tuber sink strength by a targeted direction of assimilate flow. In this study it could be demonstrated how modulation of sugar partitioning might influence source sink balance and thus can be used in a strategy for crop improvement. In previous studies assimilate transport rates were found to be critical for high tuber yield under heat in a comparison of different cultivars [341].

The enhanced root growth observed in HXK+SP6A plants for example could, beyond the reduced transpiration rates, further contribute to improved drought tolerance as water of the soil can be exploited more efficiently. Morphologic alterations of the potato root system under drought have been described before as a mean to cope better with limited water resources [211,342,343]. Moreover, a selection of early tuberizing cultivars might preserve tuber yield, since earliness of tuberization is often correlated with yield stability [344]. Obviously potato plants are most susceptible for stress during this developmental transition stage [345,346]. Since SP6A overexpressing plants tuberize earlier, this might help in addition to avoid yield reductions mediated by late drought in the field.

Taken together, the findings of this study provide a functional link between photoperiodic control and assimilate allocation into developing tubers. Especially under heat the repression of assimilate leakage by high amounts of SP6A protein could be beneficial for tuber yield since potato tends to increase green biomass under these circumstances. Thus the combination of both genes enabled high yield stability in heat, drought, and combined stress. Since both heat and drought affect photosynthetic carbon fixation, one step to further

enhance potato stress resistance could be to combine various approaches to increase CO_2 fixation by simultaneously maintaining the water status of the plants and preserving assimilate allocation to the tubers. It has already been stated that boosting source as well as sink capacity can double the starch yield of potato tubers [65]. In general, a combination of different genes is a promising instrument for the generation of crop plants which are able to secure human nutrition regardless of stress conditions due to climate change.

6 REFERENCES

1. Rodríguez-Falcón, M., Bou, J., and Prat, S. (2006). SEASONAL CONTROL OF TUBERIZATION IN POTATO: Conserved Elements with the Flowering Response. Annu. Rev. Plant Biol. *57*, 151–180.

2. Birch, P.R.J., Bryan, G., Fenton, B., Gilroy, E.M., Hein, I., Jones, J.T., Prashar, A., Taylor, M.A., Torrance, L., and Toth, I.K. (2012). Crops that feed the world 8: Potato: Are the trends of increased global production sustainable? Food Security 4, 477-508

3. Spooner, D.M., McLean, K., Ramsay, G., Waugh, R., and Bryan, G.J. (2005). A single domestication for potato based on multilocus amplified fragment length polymorphism genotyping. Proc. Natl. Acad. Sci. *102*, 14694–14699.

4. Jobling, S. (2004). Improving starch for food and industrial applications. Curr. Opin. Plant Biol. *7*, 210–218.

5. Dufresne, A., Dupeyre, D., and Vigno, M.R. (1999). Cellulose Microfibrils from Potato Tuber Cells : Processing and Characterization of Starch – Cellulose Microfibril Composites. J Appl Polym Sci *76*, 2080–2092.

6. Hashem, M., and Darwish, S.M.I. (2010). Production of bioethanol and associated by-products from potato starch residue stream by Saccharomyces cerevisiae Production of bioethanol and associated by-products from potato starch residue stream by Saccharomyces cerevisiae. Biomass and Bioenergy *34*, 953–959.

7. Tasić, M.B., Konstantinović, B.V., Lazić, M.L., and Veljković, V.B. (2009). The acid hydrolysis of potato tuber mash in bioethanol production. Biochem. Eng. J. *43*, 208–211.

8. Voechting, H. (1887). Ueber die Bildung der Knollen. Naturwiss. Rundsch. *3*, 34–37.

9. Jackson, S.D. (1999). Multiple Signaling Pathways Control Tuber Induction in Potato. Plant Physiol. *119*, 1–8.

10. Xu, X., Vreugdenhil, D., and Lammeren, A.A.V. (1998). Cell division and cell enlargement during potato tuber formation. J. Exp. Bot. *49*, 1998.

11. Viola, R., Roberts, A.G., Haupt, S., Gazzani, S., Hancock, R.D., Marmiroli, N., Machray, G.C., and Oparka, K.J. (2001). Tuberization in Potato Involves a Switch from Apoplastic to Symplastic Phloem Unloading. Plant Cell *13*, 385–398.

12. Xu, X., Lammeren, A.M. Van, Vermeer, E., and Vreugdenhil, D. (1998). The Role of Gibberellin , Abscisic Acid , and Sucrose in the Regulation of Potato Tuber Formation in Vitro 1. Plant Physiol. *117*, 575–584.

13. Kloosterman, B., De Koeyer, D., Griffiths, R., Flinn, B., Steuernagel, B., Scholz, U., Sonnewald, S., Sonnewald, U., Bryan, G.J., Prat, S., *et al.* (2008). Genes driving potato tuber initiation and growth: Identification based on transcriptional changes using the POCI array. Funct. Integr. Genomics *8*, 329–340.

14. Appeldoorn, N.J., de Bruijn, S.M., Koot-Gronsveld, E.A., Visser, R.G., Vreugdenhil, D., and van der Plas, L.H.W. (1997). Developmental changes of enzymes involved in conversion of sucrose to hexose-phosphate during early tuberisation of potato. Planta

202, 1997.

15. George, T.S., Taylor, M.A., Dodd, I.C., and White, P.J. (2017). Climate Change and Consequences for Potato Production : a Review of Tolerance to Emerging Abiotic Stress. Potato Res. *60*, 239–268.

16. Appeldorn, N.J.. (2002). In situ analysis of enzymes involved in sucrose to hexose-phosphate conversion during stolon-to-tuber transition of potato. Physiol. Plant. *115*, 303–310.

17. Zrenner, R., Salanoubat, M., Willmitzer, L., and Sonnewald, U. (1995). Evidence of the crucial role of sucrose synthase for sink strength using transgenic potato plants (Solanum tuberosum L.). Plant J. *7*, 79–107107.

18. Heltoft, P., Wold, A.B., and Molteberg, E.L. (2017). Maturity indicators for prediction of potato (*Solanum tuberosum* L.) quality during storage. Postharvest Biol. Technol. *129*, 97–106.

19. Ferreira, S.J., Senning, M., Sonnewald, S., Keßling, P.-M., Goldstein, R., and Sonnewald, U. (2010). Comparative transcriptome analysis coupled to X-ray CT reveals sucrose supply and growth velocity as major determinants of potato tuber starch biosynthesis. BMC Genomics *11*(93), 1-17.

20. Sonnewald, S., and Sonnewald, U. (2014). Regulation of potato tuber sprouting. Planta *239*, 27–38.

21. Senning, M., Sonnewald, U., and Sonnewald, S. (2010). Deoxyuridine triphosphatase expression defines the transition from dormant to sprouting potato tuber buds. Mol. Breed. *26*, 525–531.

22. Suttle, J. (2007). Dormancy and sprouting. Advances and perspectives. Elsevier BV, Vreugdenhil D (ed). Potato Biol. Biotechnol., 287–309.

23. Muthoni, J., Kabira, J., Shimelis, H., and Melis, R. (2014). Regulation of potato tuber dormancy : A review Review article Regulation of potato tuber dormancy : A review. Am. J. Crop Sci. *8*, 754–759.

24. Chapman, H.W. (1958). Tuberization in the Potato Plant. Physiol. Plant. *11*, 215–225.

25. Biemelt, S., Hajirezaei, M., Hentschel, E., and Sonnewald, U. (2000). Comparative analysis of abscisic acid content and starch degradation during storage of tubers harvested from different potato varieties. Potato Res. *43*, 371–382.

26. Chen, L.-Q., Qu, X.-Q., Hou, B.-H., Sosso, D., Osorio, S., Fernie, a. R., and Frommer, W.B. (2012). Sucrose Efflux Mediated by SWEET Proteins as a Key Step for Phloem Transport. Science *335*, 207–211.

27. Stadler, R., and Sauer, N. (1996). The Arabidopsis thaliana AtSUC2 Gene is Specifically Expressed in Companion Cells. Bot. Acta *109*, 299–306.

28. Kühn, C., Quick, W.P., Schulz, A., Riesmeier, J.W., Sonnewald, U., and Frommer, W.B. (1996). Companion cell-specific inhibition of the potato sucrose transporter SUT1. Plant, Cell Environ. *19*, 1115–1123.

29. Kühn, C., Hajirezaei, M.R., Fernie, A.R., Roessner-Tunali, U., Czechowski, T., Hirner, B., and Frommer, W.B. (2003). The sucrose transporter StSUT1 localizes to sieve elements in potato tuber phloem and influences tuber physiology and development. Plant Physiol. *131*, 102–113.

30. Mehdi, R., Lamm, C.E., Bodampalli, A.R., Müdsam, C., Saeed, M., Klima, J., Kraner, M.E., Ludewig, F., Knoblauch, M., Gruissem, W., *et al.* (2019). Symplasmic phloem unloading and radial post-phloem transport via vascular rays in tuberous roots of *Manihot esculenta*. J. Exp. Bot. *70*, 5559–5573.

31. Fernie, A.R. and Willmitzer, L. 2001 (2001). Molecular and biochemical triggers of potato tuber development. Plant Physiol. *127*, 1459–1465.

32. Ruan, Y.-L. (2014). Sucrose Metabolism: Gateway to Diverse Carbon Use and Sugar Signaling. Annu. Rev. Plant Biol. *65*, 33–67.

33. Ferreira, S.J., and Sonnewald, U. (2012). The mode of sucrose degradation in potato tubers determines the fate of assimilate utilization. Front. Plant Sci. *3*, 1–18.

34. Visser, R.G., Vreugdenhil, D., Hendriks, T., and Jacobsen, E. (1994). Gene expression and carbohydrate content during stolon to tuber transition in potatoes (*Solanum tuberosum*). Physiol. Plant. *90*, 285–292.

35. Frommer, W.B. and Sonnewald, U. (1995). Molecular analysis of carbon partitioning in solanaceous species. J. Exp. Bot. *46*, 587–607.

36. Fernie, A.R., Bachem, C.W.B., Helariutta, Y., Neuhaus, H.E., Prat, S., Ruan, Y., Stitt, M., Sweetlove, L.J., Tegeder, M., Wahl, V., *et al.* (2020). Synchronization of developmental, molecular and metabolic aspects of source–sink interactions. Nat. Plants. 55-66

37. White, A.C., Rogers, A., Rees, M., and Osborne, C.P. (2016). How can we make plants grow faster? A source-sink perspective on growth rate. J. Exp. Bot. *67*, 31–45.

38. Hendrix, D.L., and Huber, S.C. (1986). Diurnal fluctuations in cotton leaf carbon export, carbohydrate content, and sucrose synthesizing enzymes. Plant Physiol. *81*, 584–586.

39. Servaites, J.C., Geiger, D.R., Tucci, M.A., and Fondy, B.R. (1989). Leaf carbon metabolism and metabolite levels during a period of sinusoidal light. Plant Physiol. *89*, 403–408.

40. Wardlaw, I.F. (1990). The control of carbon partitioning in plants. New Phytol. *116*, 341–381.

41. Komor, E. (2000). Source physiology and assimilate transport: the interaction of sucrose metabolism, starch storage and phloem export in source leaves and the effects on sugar status in phloem. Funct. Plant Biol. *27*, 497–505.

42. Simkin, A.J., López-calcagno, P.E., and Raines, C.A. (2019). Feeding the world : improving photosynthetic efficiency for sustainable crop production. J. Exp. Bot. *70*, 1119–1140.

43. Wu, A., Hammer, G.L., Doherty, A., Caemmerer, S. Von, and Farquhar, G.D. (2019). Quantifying impacts of enhancing photosynthesis on crop yield. Nat. Plants *5*, 380–388.

44. Sharwood, R.E., Ghannoum, O., and Whitney, S.M. (2016). Prospects for improving CO_2 fixation in C 3 -crops through understanding C 4 -Rubisco biogenesis and catalytic diversity. Curr. Opin. Plant Biol. *31*, 135–142.

45. Sharwood, R.E., Ghannoum, O., Kapralov, M. V, Gunn, L.H., and Whitney, S.M. (2016). Temperature responses of Rubisco from *Paniceae* grasses provide

opportunities for improving. Nat. Plants *2*, 1–9.

46. Driever, S.M., Simkin, A.J., Alotaibi, S., Fisk, S.J., Madgwick, P.J., Sparks, C.A., Jones, H.D., Lawson, T., Parry, M.A.J., Raines, C.A., *et al.* (2017). Increased SBPase activity improves photosynthesis and grain yield in wheat grown in greenhouse conditions. Phil. Trans. R. Soc. B *372*, 1–10.

47. Lefebvre, S., Lawson, T., Fryer, M., Zakhleniuk, O. V, Lloyd, J.C., and Raines, C.A. (2005). Increased Sedoheptulose-1 , 7-Bisphosphatase Activity in Transgenic Tobacco Plants Stimulates Photosynthesis and Growth from an Early Stage in Development. Plant Physiol. *138*, 451–460.

48. Simkin, A.J., Lopez-calcagno, P.E., Davey, P.A., Headland, L.R., Lawson, T., Timm, S., Bauwe, H., and Raines, C.A. (2017). Simultaneous stimulation of sedoheptulose and the photorespiratory glycine decarboxylase-H protein increases CO_2 assimilation, vegetative biomass and seed yield in Arabidopsis. Plant Biotechnol. J. *15*, 805–816.

49. Kromdijk, J., Głowacka, K., Leonelli, L., Gabilly, S.T., Iwai, M., Niyogi, K.K., and Long, S.P. (2016). Improving photosynthesis and crop productivity by accelerating recovery from photoprotection. Science *354*, 857–862.

50. Gajdanowicz, P., Garcia-Mata, C., Gonzalez, W., Morales-Navarro, S.E., Sharma, T., González-nilo, F.D., Gutowicz, J., Mueller-roeber, B., Blatt, M.R., and Dreyer, I. (2009). Distinct roles of the last transmembrane domain in controlling Arabidopsis K + channel activity. New Phytol. *182*, 380–391.

51. Wingenter, K., Schulz, A., Wormit, A., Wic, S., Trentmann, O., Hoermiller, I.I., Heyer, A.G., Marten, I., Hedrich, R., Neuhaus, H.E., *et al.* (2010). Increased Activity of the Vacuolar Monosaccharide Transporter TMT1 Alters Cellular Sugar Partitioning , Sugar Signaling , and Seed Yield in Arabidopsis. Plant Physiol. *154*, 665–677.

52. South, P.F., Cavanagh, A.P., Lopez-Calcagno, P.E., Raines, C.A., and Ort, D.R. (2018). Optimizing photorespiration for improved crop productivity. J. Integr. Plant Biol. *60*, 1217–1230.

53. Weber, A.P.M., and Bar-Even, A. (2019). Update on Improved Carbon Fixation Update : Improving the Efficiency of Photosynthetic Carbon Reactions. Plant Physiol. *179*, 803–812.

54. Kebeish, R., Niessen, M., Thiruveedhi, K., Bari, R., Hirsch, H.-J., Rosenkranz, R., Stäbler, N., Schönefeld, B., Kreuzaler, F., and Peterhänsel, C. (2007). Chloroplastic photorespiratory bypass increases photosynthesis and biomass production in *Arabidopsis thaliana*. Nat. Biotechnol. *25*, 593–599.

55. Nölke, G., Houdelet, M., Kreuzaler, F., Peterhänsel, C., and Schillberg, S. (2014). The expression of a recombinant glycolate dehydrogenase polyprotein in potato (Solanum tuberosum) plastids strongly enhances photosynthesis and tuber yield. Plant Biotechnol. J. *12*, 734–742.

56. Slewinski, T.L. (2012). In Posidonia oceanica cadmium partitioning induces changes in DNA methylation and Chromatin atterning. J. Exp. Bot. *63*, 4647–4670.

57. Smidansky, E.D., Clancy, M., Meyer, F.D., Lanning, S.P., Blake, N.K., Talbert, L.E., and Giroux, M.J. (2002). Enhanced ADP-glucose pyrophosphorylase activity in wheat endosperm increases seed yield. Proc. Natl. Acad. Sci. *99*, 1724–1729.

58. Fernie, A.R. (2018). Extending the cascade: identification of a mitogen-activated protein kinase phosphatase playing a key role in rice yield. Plant J. *95*, 935–936.

59. Zhang, L., Häusler, R.E., Greitne, C., Haijrazaei, M.-R., Haferkamp, I., Neuhaus, H.E., Flügge, U., and Ludewig, F. (2008). Overriding the co-limiting import of carbon and energy into tuber amyloplasts increases the starch content and yield of transgenic potato plants. Plant Biotechnol. J. *6*, 453–464.

60. Ludewig, F., and Sonnewald, U. (2016). Demand for food as driver for plant sink development. J. Plant Physiol. *203*, 110–115.

61. Sonnewald, U., and Fernie, A.R. (2018). Next-generation strategies for understanding and influencing source-sink relations in crop plants. Curr. Opin. Plant Biol. *43*, 63–70.

62. Yu, S.M., Lo, S.F., and Ho, T.H.D. (2015). Source-Sink Communication: Regulated by Hormone, Nutrient, and Stress Cross-Signaling. Trends Plant Sci. *20*, 844–857.

63. Ludewig, F., and Flügge, U.-I. (2013). Role of metabolite transporters in source-sink carbon allocation. Front. Plant Sci. *4*, 1–16.

64. Sonnewald, U., and Willmitzer, L. (1992). Molecular Approaches to Sink-Source Interactions. Plant Physiol. *99*, 1267–1270.

65. Jonik, C., Sonnewald, U., Hajirezaei, M.R., Flügge, U.I., and Ludewig, F. (2012). Simultaneous boosting of source and sink capacities doubles tuber starch yield of potato plants. Plant Biotechnol. J. *10*, 1088–1098.

66. Suarez-Lopez, P., Wheatley, K., Robson, F., Onouchi, H., Valverde, F., and Coupland, G. (2001). CONSTANS mediates between the circadian clock and the control of flowering in Arabidopsis. Nature *410*, 1116–1120.

67. Valverde, F., Mouradov, A., Soppe, W., Ravenscroft, D., Samach, A., and Coupland, G. (2004). Photoreceptor Regulation of CONSTANS Protein in Photoperiodic Flowering. Science *303*, 1003–1007.

68. Sawa, M., Nusinow, D.A., Kay, S.A., and Imaizumi, T. (2007). FKF1 and GIGANTEA Complex Formation Is Required for Day-Length Measurement in Arabidopsis. Science *318*, 261–266.

69. Imaizumi, T., Schultz, T.F., Harmon, F.G., Ho, L.A., and Kay, S.A. (2005). FKF1 F-Box Protein Mediates Cyclic Degradation of a Repressor of CONSTANS in Arabidopsis. Science *309*, 293–298.

70. Jaeger, K.E., and Wigge, P.A. (2007). FT Protein Acts as a Long-Range Signal in Arabidopsis. Curr. Biol. *17*, 1050–1054.

71. Corbesier, L., Vincent, C., Jang, S., Fornara, F., Fan, Q., Searle, I., Giakountis, A., Farrona, S., Gissot, L., Turnbull, C., *et al.* (2007). Long-Distance Signaling in Floral Induction of Arabidopsis. Science *316*, 1030–1034.

72. Notaguchi, M., Abe, M., Kimura, T., Daimon, Y., Kobayashi, T., Yamaguchi, A., Tomita, Y., Dohi, K., Mori, M., and Araki, T. (2008). Long-distance, graft-transmissible action of Arabidopsis FLOWERING LOCUS T protein to promote flowering. Plant Cell Physiol. *49*, 1645–1658.

73. Notaguchi, M., Daimon, Y., Abe, M., and Araki, T. (2009). Graft-transmissible action of Arabidopsis FLOWERING LOCUS T protein to promote flowering. Plant Signal. Behav. *4*, 123–125.

74. Li, C., Zhang, K., Zeng, X., Jackson, S., Zhou, Y., and Hong, Y. (2009). A cis Element within FLOWERING LOCUS T mRNA Determines Its Mobility and Facilitates Trafficking of Heterologous Viral RNA. J. Virol. *83*, 3540–3548.

75. Liu, L., Liu, C., Hou, X., Xi, W., Shen, L., Tao, Z., Wang, Y., and Yu, H. (2012). FTIP1 is an essential regulator required for florigen transport. PLoS Biol. *10*.

76. Kraner, M.E., Müller, C., and Sonnewald, U. (2017). Comparative proteomic profiling of the choline transporter-like1 (CHER1) mutant provides insights into plasmodesmata composition of fully developed Arabidopsis thaliana leaves. Plant J. *92*, 696–709.

77. Taoka, K., Ohki, I., Tsuji, H., Furuita, K., Hayashi, K., and Yanase, T. (2011). 14-3-3 proteins act as intracellular receptors for rice Hd3a florigen. Nature *476*, 332–335.

78. Kloosterman, B., Abelenda, J.A., Gomez, M.D.M.C., Oortwijn, M., De Boer, J.M., Kowitwanich, K., Horvath, B.M., Van Eck, H.J., Smaczniak, C., Prat, S., *et al.* (2013). Naturally occurring allele diversity allows potato cultivation in northern latitudes. Nature *495*, 246–250.

79. Chailakhyan, M.K., Yanina, L.., Devedzhyan, A.G., and Lotova, G.N. (1981). Photoperiodism and tuberization with grafting of tobacco on potato. Dokl. Akad. Nauk *257*, 1981.

80. Abelenda, J.A., Navarro, C., and Prat, S. (2014). Flowering and tuberization: A tale of two nightshades. Trends Plant Sci. *19*, 115–122.

81. Navarro, C., Abelenda, J.A., Cruz-Oró, E., Cuéllar, C.A., Tamaki, S., Silva, J., Shimamoto, K., and Prat, S. (2011). Control of flowering and storage organ formation in potato by FLOWERING LOCUS T. Nature *478*, 119–122.

82. Abelenda, J.A., Cruz-Oró, E., Franco-Zorrilla, J.M., and Prat, S. (2016). Potato StCONSTANS-like1 Suppresses Storage Organ Formation by Directly Activating the FT-like StSP5G Repressor. Curr. Biol. *26*, 872–881.

83. Seibert, T., Abel, C., and Wahl, V. (2019). Flowering time and the identification of floral marker genes in S. tuberosum spp. andigena. J. Exp. Bot.

84. Chen, Q., Payyavula, R.S., Chen, L., Zhang, J., Zhang, C., and Turgeon, R. (2018). FLOWERING LOCUS T mRNA is synthesized in specialized companion cells in Arabidopsis and Maryland Mammoth tobacco leaf veins. Proc. Natl. Acad. Sci. *115*, 3–8.

85. Sharma, P., Lin, T., and Hannapel, D.J. (2016). Targets of the *StBEL5* Transcription Factor Include the FT Ortholog *StSP6A*. Plant Physiol. *170*, 310–324.

86. Lin, T., Lashbrook, C.C., Cho, S.K., Butler, N.M., Sharma, P., Muppirala, U., Severin, A.J., and Hannapel, D.J. (2015). Transcriptional analysis of phloem- associated cells of potato. BMC Genomics *16*, 1–24.

87. Teo, C.J., Takahashi, K., Shimizu, K., Shimamoto, K., and Taoka, K.I. (2017). Potato tuber induction is regulated by interactions between components of a tuberigen complex. Plant Cell Physiol. *58*, 365–374.

88. Abe, M., Kobayashi, Y., Yamamoto, S., Daimon, Y., Yamaguchi, A., and Ikeda, Y. (2005). FD, a bZIP protein mediating signals from the floral pathway integrator FT at the shoot apex. Science *309*, 1052–1056.

89. Park, S.J., Jiang, K., Tal, L., Yichie, Y., Gar, O., Zamir, D., Eshed, Y., and Lippman,

Z.B. (2014). Optimization of crop productivity in tomato using induced mutations in the florigen pathway. Nat. Genet. *46*, 1337–1342.

90. Kawamoto, N., Sasabe, M., Endo, M., Machida, Y., and Araki, T. (2015). Calcium-dependent protein kinases responsible for the phosphorylation of a bZIP transcription factor FD crucial for the florigen complex formation. Sci. Rep. *5*, 8341.

91. Kawamoto, N., Endo, M., and Araki, T. (2015). Expression of a kinase-dead form of CPK33 involved in florigen complex formation causes delayed flowering. Plant Signal. Behav. *10*, e1086856.

92. Wigge, P., Kim, M., Jaeger, K., Busch, W., Schmid, M., and Lohmann, J. (2005). Integration of spatial and temporal information during floral induction in Arabidopsis. Science *309*, 1056–1057.

93. Abelenda, A., Bergonzi, S., Oortwijn, M., Visser, R.G.F., Sonnewald, U., Bachem, C.W.B., Abelenda, A., Bergonzi, S., Oortwijn, M., Sonnewald, S., *et al.* (2019). Source-Sink Regulation Is Mediated by Interaction of an FT Homolog with a SWEET Protein in Potato. Curr. Biol. *29*, 1178-1186.

94. Andrés, F., Kinoshita, A., Kalluri, N., Fernández, V., Falavigna, V.S., Cruz, T.M.D., Jang, S., Chiba, Y., Seo, M., Mettler-Altmann, T., *et al.* (2020). The sugar transporter SWEET10 acts downstream of FLOWERING LOCUS T during floral transition of Arabidopsis thaliana. BMC Plant Biol. *20*, 1–14.

95. Ahn, J.H., Miller, D., Winter, J., Banfield, M.J., Hwan, J., Yoo, S.Y., Henz, S.R., Brady, R.L., and Weigel, D. (2006). A divergent external loop confers antagonistic activity on floral regulators FT and TFL1. EMBO J. *25*, 605–614.

96. Hardigan, M.A., Laimbeer, F.P.E., Newton, L., Crisovan, E., Hamilton, J.P., Vaillancourt, B., Wiegert-Rininger, K., Wood, J.C., Douches, D.S., Farré, E.M., *et al.* (2017). Genome diversity of tuber-bearing *Solanum* uncovers complex evolutionary history and targets of domestication in the cultivated potato. Proc. Natl. Acad. Sci. *114,* 9999-10008.

97. Suárez-López, P. (2013). A critical appraisal of phloem-mobile signals involved in tuber induction. Front. Plant Sci. *4*, 1–7.

98. González-Schain, N.D., Díaz-Mendoza, M., Zurczak, M., and Suárez-López, P. (2012). Potato CONSTANS is involved in photoperiodic tuberization in a graft-transmissible manner. Plant J. *70*, 678–690.

99. Kondhare, K.R., Kumar, A., Hannapel, D.J., and Banerjee, A.K. (2018). Conservation of polypyrimidine tract binding proteins and their putative target RNAs in several storage root crops. BMC Genomics *19*, 1–13.

100. Bhogale, S., Mahajan, A.S., Natarajan, B., Rajabhoj, M., Thulasiram, H. V., and Banerjee, A.K. (2014). MicroRNA156: A Potential Graft-Transmissible MicroRNA That Modulates Plant Architecture and Tuberization in Solanum tuberosum ssp. andigena. Plant Physiol. *164*, 1011–1027.

101. Martin, A., Adam, H., Diaz-Mendoza, M., Zurczak, M., Gonzalez-Schain, N.D., and Suarez-Lopez, P. (2009). Graft-transmissible induction of potato tuberization by the microRNA miR172. Development *136*, 2873–2881.

102. Wareing, P.F., and Jennings, A.M. V (1980). The Hormonal Control of Tuberisation in Potato. Plant Growth Subst., 293–230.

103. Bernier, G., Havelange, A., Houssa, C., Petitjean, A., and Lejeune, P. (1993). Physiological signals that induce flowering. Plant Cell *5*, 1147–1155.

104. Wahl, V., Ponnu, J., Schlereth, A., Arrivault, S., Langenecker, T., Franke, A., Feil, R., Lunn, J.E., Stitt, M., and Schmid, M. (2013). Regulation of Flowering by Trehalose-6-Phosphate Signaling in Arabidopsis thaliana. Science *339*, 704–708.

105. Lunn, J.E., Feil, R., Hendriks, J.H.M., Gibon, Y., Morcuende, R., and Osuna, D. (2006). Sugar-induced increases in trehalose 6-phosphate are correlated with redox activation of ADPglucose pyrophosphorylase and higher rates of starch synthesis in Arabidopsis thaliana. *148*, 139–148.

106. Figueroa, C.M., Feil, R., Ishihara, H., Watanabe, M., Kölling, K., Krause, U., Höhne, M., Encke, B., Plaxton, W.C., Zeeman, S.C., *et al.* (2016). Trehalose 6 – phosphate coordinates organic and amino acid metabolism with carbon availability. Plant J. *85*, 410–423.

107. Chincinska, I.A., Liesche, J., Krugel, U., Michalska, J., Geigenberger, P., Grimm, B., and Kuhn, C. (2007). Sucrose Transporter StSUT4 from Potato Affects Flowering, Tuberization, and Shade Avoidance Response. Plant Physiol. *146*, 515–528.

108. Ledgard, S.F., Sprosen, M.S., and Steele, K.W. (2008). Nitrogen fixation by nine white clover cultivars in grazed pasture, as affected by nitrogen fertilization. Plant and Soil, *178*, 193–203.

109. Tegeder, M., and Masclaux-Daubresse, C. (2018). Source and sink mechanisms of nitrogen transport and use. New Phytol. *217*, 35–53.

110. Dingenen, J. van, Hanzalova, K., Abd, M., Salem, A., Abel, C., Seibert, T., Giavalisco, P., and Wahl, V. (2019). Limited nitrogen availability has cultivar-dependent effects on potato tuber yield and tuber quality traits. Food Chem. *288*, 170–177.

111. Vos, J., and Biemond, H. (1992). Effects of nitrogen on the development and growth of the potato plant. 1. Leaf appearance, expansion growth, life spans of leaves and stem branching. Ann. Bot. *70*, 27–35.

112. Mauromicale, G., Ierna, A., and Marchese, M. (2008). Chlorophyll fluorescence and chlorophyll content in field-grown potato as affected by nitrogen supply, genotype, and plant age. Photosynthetica *44*, 76.

113. Goffart, J.P., Olivier, M., and Frankinet, M. (2008). Potato crop nitrogen status assessment to improve N fertilization management and efficiency: past–present–future. Potato Res. *51*, 355–383.

114. Wang, L., and Ruan, Y.-L. (2016). Shoot – root carbon allocation, sugar signalling and their coupling with nitrogen uptake and assimilation. Funct. Plant Biol. *43*, 105–113.

115. Nunes-Nesi, A., Fernie, A.R., and Stitt, M. (2010). Metabolic and Signaling Aspects Underpinning the Regulation of Plant Carbon Nitrogen Interactions. Mol. Plant *3*, 973–996.

116. McCollum, R.E. (1978). (1978). Analysis of potato growth under differing P regimes. Agron. J. *70*, 51–57.

117. Grant, C.A., Flaten, D.N., Tomasiewicz, D.J., and Sheppard, S.C. (2001). The importance of early season phosphorus nutrition. Can. J. Plant Sci. *81*, 211–224.

118. Rosen, C.J., Kelling, K.A., Stark, J.C., and Porter, G.A. (2014). Optimizing phosphorus

fertilizer management in potato production. Am. J. Potato Res. *91*, 145–160.

119. Hopkins, B., and Ellsworth, J. (2005). Phosphorus availability with alkaline/calcareous soil. West. Nutr. Manag. Conf. *6*, 88–93.

120. Westermann, D.T., Tindall, T.A., James, D.W., and Hurst, R.L. (1994). Nitrogen and potassium fertilization of potatoes: yield and specific gravity. Am. Potato J. *71*, 417–431.

121. Panique, E., Kelling, K.A., Schulte, E.E., Hero, D.E., Stevenson, W.R., and James, R.V. (1997). Potassium rate and source effects on potato yield, quality, and disease interaction. Am. Potato J. *74*, 379–398.

122. AbdelGadir, A.H., Errebhi, M.A., Al-Sarhan, H.M. and Ibrahim, M. (2003). The effect of different levels of additional potassium on yield and industrial qualities of potato (Solanum tuberosum L.) in an irrigated arid region. Am. J. Potato Res. *80*, 219–222.

123. McNabnay, M., Dean, B.B., Bajem, R.W., and Hyde, G.M. (1999). The Effect of Potassium Deficiency on Chemical , Biochemical and Physical Factors Commonly Associated with Blackspot Development in Potato Tubers. Am. J. Potato Res. *76*, 53–60.

124. Davenport, J.R., and Bentley, E.M. (2001). Does potassium fertilizer form, source, and time of application influence potato yield and quality in the Columbia Basin? Am. J. Potato Res. *78*, 311–318.

125. White, P.J., Bradshaw, J.E., Finlay, M., Dale, B., Ramsay, G., Hammond, J.P., and Broadley, M.. (2009). Relationships between yield and mineral concentrations in potato tubers. HortScience *44*, 6–11.

126. Beringer, H., Koch, K., and Lindhauer, M.G. (1990). Source: sink relationships in potato (*Solanum tuberosum*) as influenced by potassium chloride or potassium sulphate nutrition. Plant Soil *124*, 287–290.

127. Trehan, S.P., Upadhayay, N.C., Sud, K.C., Kumar, M., Jatav, M.K., and Lal, S.S. (2008). Nutrient Management in Potato. Cent. Potato Res. Inst. *Technical*, 90.

128. Mittler, R., Finka, A., and Goloubinoff, P. (2012). How do plants feel the heat? Trends Biochem. Sci. *37*, 118–125.

129. Fahad, S., Bajwa, A.A., Nazir, U., Anjum, S.A., Farooq, A., Zohaib, A., Sadia, S., Nasim, W., Adkins, S., Saud, S., *et al.* (2017). Crop Production under Drought and Heat Stress: Plant Responses and Management Options. Front. Plant Sci. *8*, 1–16.

130. Dahal, K., Li, X., Tai, H., Creelman, A., and Bizimungu, B. (2019). Improving Potato Stress Tolerance and Tuber Yield Under a Climate Change Scenario – A Current Overview. Front. Plant Sci. *10*, 1–16.

131. Lamaoui, M., Jemo, M., Datla, R., and Bekkaoui, F. (2018). Heat and Drought Stresses in Crops and Approaches for Their Mitigation. Front. Plant Sci. *6*, 1–14.

132. Craufurd, P., and TR, W. (2009). Climate change and the flowering time of annual crops. J. Exp. Bot. *60*, 2529–2539.

133. Mittler, R. (2006). Abiotic stress, the field environment and stress combination. Trends Plant Sci. *11*, 15–19.

134. Lafta, A.M., and Lorenzen, Ja.H. (1995). Effect of Temperature on Carbohydrate

Metabolism in Potato Plants. J. Plant Physiol. *109*, 637–643.

135. Monneveux, Philippe, Ramírez, David A, Pinob, M.-T. (2013). Drought tolerance in potato (S. tuberosum L.): Can we learn from drought tolerance research in cereals? Plant Sci. *205*, 76–86.

136. Hancock, R.D., Morris, W.L., Ducreux, L.J.M., Morris, J.A., Usman, M., Verrall, S.R., Fuller, J., Simpson, C.G., Zhang, R., Hedley, P.E., *et al.* (2014). Physiological, biochemical and molecular responses of the potato (Solanum tuberosumL.) plant to moderately elevated temperature. Plant, Cell Environ. *37*, 439–450.

137. Borah, M.N., and Milthorpe, F.L. (1962). Growth of the potato as influenced by temperature. Indian J. Plant Physiol. *5*, 53–72.

138. Awan, A.B. (1964). Influence of mulch on soil moisture, soil temperature and yield of potatoes. Am. Potato J. *41*, 337–339.

139. Went, F.W. (1953). The effect of temperature on plant growth. Annu. Rev. Plant Physiol. *4*, 347–362.

140. Hatfield, J.L., and Prueger, J.H. (2015). Temperature extremes : Effect on plant growth and development. Weather Clim. Extrem. *10*, 4–10.

141. Sung, D., Kaplan, F., and Guy, C.L. (2001). Plant Hsp70 molecular chaperones : Protein structure , gene family , expression and function. Physiol. Plant. *113*, 443–451.

142. Trapero-Mozos, A., Morris, W.L., Ducreux, L.J.M., McLean, K., Stephens, J., Torrance, L., Bryan, G.J., Hancock, R.D., and Taylor, M.A. (2018). Engineering heat tolerance in potato by temperature-dependent expression of a specific allele of HEAT-SHOCK COGNATE 70. Plant Biotechnol. J. *16*, 197–207.

143. Momčilović, I., Pantelić, D., Zdravković-Korać, S., Oljača, J., Rudić, J., and Fu, J. (2016). Heat-induced accumulation of protein synthesis elongation factor 1A implies an important role in heat tolerance in potato. Planta *244*, 671–679.

144. Huang, B., Rachmilevitch, S., and Xu, J. (2012). Root carbon and protein metabolism associated with heat tolerance. J. Exp. Bot. *63*, 3455–3465.

145. Wahid, A., Gelani, S., Ashraf, M., and Foolad, M.R. (2007). Heat tolerance in plants : An overview. Environ. Exp. Bot. *61*, 199–223.

146. Kim, Y.U., Seo, B.S., Choi, D.H., Ban, H.Y., and Lee, B.W. (2017). Impact of hightemperatures on the marketable tuber yield and related traits of potato. Eur. J. Agron. *89*, 46–52.

147. Kim, Y., Lee, B., and Lee, B. (2019). Differential Mechanisms of Potato Yield Loss Induced by High Day and Night Temperatures During Tuber Initiation and Bulking : Photosynthesis and Tuber Growth. Front. Plant Sci. *10*, 1–9.

148. Hammes, P.S., and De Jager, J.. (1990). Net photosynthetic rate of potato at high temperatures. Potato Res. *33*, 515–520.

149. Prange, R.K., McRae, K.B., Midmore, D.J., and Deng, R. (1990). Reduction in potato growth at high temperature: role of photosynthesis and dark respiration. Am. Potato J. *67*, 357.

150. Mathur, S., Agrawal, D., and Jajoo, A. (2014). Photosynthesis: response to high temperature stress. J. Photochem. Photobiol. B Biol. *137*, 116–126.

151. Singh, B., Kukreja, S., and Goutam, U. (2019). Impact of heat stress on potato (Solanum tuberosum L .): present scenario and future opportunities. J. Hortic. Sci. Biotechnol. *0*, 1–18.

152. Hastilestari, B.R., Lorenz, J., Reid, S., and Sonnewald, S. (2018). Deciphering source and sink responses of potato plants (*Solanum tuberosum* L .) to elevated temperatures. Plant Cell Environ. *41*, 2600-2616.

153. Asada, K. (2006). Production and scavenging of reactive oxygen species in chloroplasts and their functions. Plant Physiol. *141*, 391–396.

154. Yamamoto, Y. (2016). Quality control of photosystem II: the mechanisms for avoidance and tolerance of light and heat stresses are closely linked to membrane fluidity of the thylakoids. Front. Plant Sci. *7*, 1136.

155. Salvucci, M.E., and Crafts-Brandner, S.. (2004). Inhibition of photosynthesis by heat stress: the activation state of Rubisco as a limiting factor in photosynthesis. Physiol. Plant. *120*, 179–186.

156. Berry, J., and Bjorkman, O. (1980). Photosynthetic response and adaptation to temperature in higher plants. Annu. Rev. Plant Physiol. *31*, 491–543.

157. Jordan, D.B., and Ogren, W.L. (1984). The CO2/O2 specificity of ribulose 1, 5-bisphosphate carboxylase/oxygenase. Planta *161*, 308–313.

158. Kobza, J. and Edwards, G.E. 1987 (1987). Influences of leaf temperature on photosynthetic carbon metabolism in wheat. Plant Physiol. *83*, 69–74.

159. van Dam, J., Kooman, P.L., and Struik, P.C. (1996). Effects of temperature and photoperiod on early growth and final number of tubers in potato (*Solanum tuberosum* L .). Potato Res. *39*, 51–62.

160. Legris, M., Klose, C., Burgie, E., Rojas, C., Neme, M., Hiltbrunner, A., Wigge, P., Schäfer, E., Vierstra, R., and Casal, J. (2016). Phytochrome B integrates light and temperature signals in Arabidopsis. Science *354*, 897–900.

161. Jung, J.H., Domijan, M., Klose, C., Biswas, S., Ezer, D., Gao, M., Khattak, A.K., Box, M.S., Charoensawan, V., Cortijo, S., *et al.* (2016). Phytochromes function as thermosensors in Arabidopsis. Science *354*, 886–889.

162. Proveniers, M.C.G., and Van Zanten, M. (2013). High temperature acclimation through PIF4 signaling. Trends Plant Sci. *18*, 59–64.

163. Kumar, S.V., Lucyshyn, D., Jaeger, K.E., Alós, E., Alvey, E., Harberd, N.P., and Wigge, P.A. (2012). Transcription factor PIF4 controls the thermosensory activation of flowering. Nature *484*, 242–245.

164. Cao, K., Yan, F., Xu, D., Ai, K., Yu, J., Bao, E., and Zou, Z. (2018). Phytochrome B1-dependent control of SP5G transcription is the basis of the night break and red to far-red light ratio effects in tomato flowering. BMC Plant Biol. *18*, 1–12.

165. Bodlaender, K.B.A., Lugt, C., and Marinus, J. (1964). The induction of second-growth in potato tubers. Eur. Potao J. *7*, 1964.

166. Van Harsselaar, J.K., Lorenz, J., Senning, M., Sonnewald, U., and Sonnewald, S. (2017). Genome-wide analysis of starch metabolism genes in potato (*Solanum tuberosum* L.). BMC Genomics *18*, 1–18.

167. Krauss, A., and Marschner, H. (1984). Growth rate and carbohydrate metabolism of tubers exposed to high temperatures. Potato Res. *27*, 297–303.

168. Mohabir, G., and John, P. (1988). Effect of temperature on starch synthesis in potato tuber tissue and in amyloplasts. Plant Physiol. *88*, 1222–1228.

169. Baroja-Fernández, E., Muñoz, F.J., Montero, M., Etxeberria, E., Sesma, M.T., Ovecka, M., Bahaji, A., Ezquer, I., Li, J., and Prat, S. (2009). Enhancing Sucrose Synthase Activity in Transgenic Potato (Solanum tuberosum L .) Tubers Results in Increased Levels of Starch , ADPglucose and UDPglucose and Total Yield. Plant Cell Physiol. *50*, 1651–1662.

170. Haverkort, A.J. (1990). Ecology of potato cropping systems in relation to latitude and altitude. Agric. Syst. *2*, 251–272.

171. Fernie, A.R., and Willmitzer, L. (2019). Molecular and Biochemical Triggers of Potato Tuber Development. Plant Physiol. *127*, 1459–1465.

172. Hijmans, R.J. (2003). The effect of climate change on global potato production. Am. J. Potato Res. *80*, 271–279.

173. Zaheer, K., and Akhtar, M. (2016). Potato production, usage, and nutrition—a review. Crit. Rev. Food Sci. Nutr. *56*, 711–721.

174. Gregory, L.E. (1965). Physiology of tuberization in plants. Encycl. Plant Physiol *15*, 1328–1354.

175. Slater, J.W. (1968). The effect of night temperature on tuber initiation of the potato. Eur Potato J 11:14 – 22. Eur Potato J *11*, 14–22.

176. Ahn, Y.J., Claussen, K., and Zimmerman, J.L. (2004). Genotypic differences in the heat-shock response and thermotolerance in four potato cultivars. Plant Sci. *166*, 901–911.

177. Kogan, F.N. (1997). Global drought watch from space. Bull. Am. Meteorol. Soc. *78*, 621–636.

178. Tripathi, D.K., Singh, S., Singh, S., Chauhan, D.K., Dubey, N.K., and Prasad, R. (2016). Silicon as a beneficial element to combat the adverse effect of drought in agricultural crops," Water Stress and Crop Plants: ASustainable Approach. ed. P. Ahmad (Hoboken, NJ John Wiley Sons, Ltd.), 682–694.

179. Van Loon, C.D. (1981). The effect of water stress on potato growth, development, and yield. Am. Potato J. *58*, 51–69.

180. Levy, D. (1985). The response of potatoes to a single transient heat or drought stress imposed at different stages of tuber growth. Potato Res. *28*, 415–424.

181. Deblonde, P.M.K., and Ledent, J.F. (2001). Effects of moderate drought conditions on green leaf number, stem height, leaf length and tuber yield of potato cultivars. Eur. J. Agron. *14*, 31–41.

182. Dalla Costa, L., Delle Vedove, G., Gianquinto, G., Giovanardi, R., and Peressotti, A. (1997). Yield, water use efficiency and nitrogen uptake in potato: influence of drought stress. Potato Res. *40*, 19–34.

183. Kumar, S.N., Govindakrishnan, P.M., and Swarooparani, D.N. (2015). Assessment of impact of climate change on potato and potential adaptation gains in the Indo-

Gangetic Plains of India. Int. J. Plant Prod. *9*, 151–170.

184. Eiasu, B.K., Soundy, P., and Hammes, P.S. (2007). Response of potato (Solanum tuberosum) tuber yield components to gel-polymer soil amendments and irrigation regimes. N Z J Crop Hort Sci *35*, 25–31.

185. Schafleitner, R., Oscar, R., Rosales, G., Gaudin, A., Aliaga, A.A., Martinez, G.N., Rosalina, L., Marca, T., Bolivar, L.A., Delgado, F.M., *et al.* (2007). Capturing candidate drought tolerance traits in two native Andean potato clones by transcription profiling of field grown plants under water stress. Plant Physiol. Biochem. *45*, 673–690.

186. Schafleitner, R. (2009). Growing More Potatoes with Less Water. Trop. Plant Biol. *2*, 111–121.

187. Lipiec, J., Doussan, C., Nosalewicz, A., and Kondracka, K. (2013). Effects of drought and heat stress on plant growth and yield: a review. Inter Agrophys *27*, 463–477.

188. Levy, D., Coleman, W.K., and Veilleux, R.E. (2013). Adaptation of Potato to Water Shortage : Irrigation Management and Enhancement of Tolerance to Drought and Salinity. Am. J. Potato Res. *90*, 186–206.

189. Prasch, C.M., Sonnewald, U., Prasch, C.M., and Sonnewald, U. (2013). In silico selection of Arabidopsis thaliana ecotypes with enhanced stress tolerance. Plant Signal. Behav. *162,* 1849-1866.

190. Sprenger, H., Kurowsky, C., Horn, R., Erban, A., Seddig, S., Rudack, K., Fischer, A., Walther, D., Zuther, E., Köhl, K., *et al.* (2016). The drought response of potato reference cultivars with contrasting tolerance. Plant Cell Environ. *39*, 2370–2389.

191. Aliche, E.B., Oortwijn, M., Theeuwen, T.P.J.M., Bachem, C.W.B., Visser, R.G.F., and Linden, C.G. Van Der (2018). Drought response in fi eld grown potatoes and the interactions between canopy growth and yield. Agric. Water Manag. *206*, 20–30.

192. Sprenger, H., Erban, A., Seddig, S., Rudack, K., Thalhammer, A., Le, M.Q., Kopka, J., Hincha, D.K., Walther, D., Zuther, E., *et al.* (2018). Metabolite and transcript markers for the prediction of potato drought tolerance. Plant Biotechnol. J. *16*, 939–950.

193. Redden, R. (2013). New approaches for crop genetic adaptation to the abiotic stresses predicted with climate change. Agronomy *3*, 419–432.

194. Haverkort, A., Boonekamp, P., Hutten, R., Jacobsen, E., Lotz, L., Kessel, G., Vossen, J., and Visser, R. (2016). Durable late blight resistance in potato through dynamic varieties obtained by cisgenesis: scientific and societal advances in the DuRPh project. Potato Res. *59*, 35–66.

195. Cabello, R., Chujoy, E., Mendiburu, F., Bonierbale, M., and Monneveux, P. (2012). Large-scale evaluation of potatoes improved varieties, pre-breeding material and landraces for drought tolerance. Am. J. Potato Res. *89*, 400–410.

196. Zanella, M., Borghi, G.L., Pirone, C., Thalmann, M., Pazmino, D., Costa, A., Santelia, D., Trost, P., and Sparla, F. (2016). β -amylase 1 (BAM1) degrades transitory starch to sustain proline biosynthesis during drought stress. J. Exp. Bot. *67*, 1819–1826.

197. Xuanyuan, G., Lu, C., Zhang, R., and Jiang, J. (2017). Overexpression of StNF-YB3 . 1 reduces photosynthetic capacity and tuber production , and promotes ABA-mediated stomatal closure in potato (Solanum tuberosum L .). Plant Sci. *261*, 50–59.

198. Yan, F., Sun, Y., Song, F., and Liu, F. (2012). Differential responses of stomatal

morphology to partial root-zone drying and deficit irrigation in potato leaves under varied nitrogen rates. Sci Hort *145*, 76–83.

199. Sun, Y., Yan, F., Cui, X., and Liu, F. (2014). Plasticity in stomatal size and density of potato leaves under different irrigation and phosphorus regimes Plasticity in stomatal size and density of potato leaves under different irrigation and phosphorus regimes. J. Plant Physiol. *171*, 1248–1255.

200. Caine, R.S., Yin, X., Sloan, J., Harrison, E.L., Mohammed, U., Biswal, A.K., Dionora, J., Chater, C.C., Coe, R.A., Bandyopadhyay, A., *et al.* (2019). Rice with reduced stomatal density conserves water and has improved drought tolerance under future climate conditions. New Phytol. *221*, 371–384.

201. Hughes, J., Hepworth, C., Dutton, C., Dunn, J.A., Hunt, L., Stephens, J., Waugh, R., Cameron, D.D., and Gray, J.E. (2017). Reducing Stomatal Density in Barley Improves Drought Tolerance without Impacting on Yield. Plant Physiol. *174*, 776–787.

202. Boguszewska-Mankowska, D., Nykiel, M., and Zarzyńska, K. (2017). Physiological and biochemical parameters of potato cultivars evaluation to drought and heat stress. Proc. 20th Trienn. EAPR Conf. 9th-14th July 2017, Versaille, Fr.

203. Glowacka, K., Kromdijk, J., Kucera, K., Xie, J., Cavanagh, A.P., Leonelli, L., Leakey, A.D.B., Ort, D.R., Niyogi, K.K., and Long, S.P. (2018). Photosystem II Subunit S overexpression increases. Nat. Commun. *9*, 1–9.

204. Papanatsiou, M., Petersen, J., Henderson, L., Wang, Y., Christie, J.M., and Blatt, M.R. (2019). Optogenetic manipulation of stomatal kinetics improves carbon assimilation, water use, and growth. Science *363*, 1456–1459.

205. Kelly, G., Moshelion, M., David-schwartz, R., Halperin, O., Wallach, R., Attia, Z., and Belausov, E. (2013). Hexokinase mediates stomatal closure. Plant J. *75*, 977–988.

206. Lugassi, N., Kelly, G., Fidel, L., Yaniv Y.i, Attia, Z., Levi, A., Alchanatis, V., Moshelion, M., Raveh, E., Carmi, N., Granot, D. (2015). Expression of Arabidopsis Hexokinase in Citrus Guard Cells Controls Stomatal Aperture and Reduces Transpiration. Front. Plant Sci. *6*, 1–11.

207. Kelly, G., Lugassi, N., Belausov, E., Wolf, D., Khamaisi, B., Brandsma, D., Fidel, L., Ben-zvi, B., Egbaria, A., Acheampong, A.K., *et al.* (2017). The Solanum tuberosum KST1 partial promoter as a tool for guard cell expression in multiple plant species. J. Exp. Bot. *68*, 2885–2897.

208. Kottapalli, J., David-schwartz, R., Khamaisi, B., Brandsma, D., Lugassi, N., Egbaria, A., Kelly, G., and Id, D.G. (2018). Sucrose-induced stomatal closure is conserved across evolution. PLoS One, 1–17.

209. Granot, D., and Kelly, G. (2019). Evolution of Guard-Cell Theories : The Story of Sugars. Trends Plant Sci. *24*, 507–518.

210. Steuer, B., Stuhlfauth, T., and Heinrich, P. (1988). The efficiency of water use in water stressed plants is increased due to ABA induced stomatal closure. Photosynth. Res. *18*, 327–336.

211. Puértolas, J., Ballester, C., Elphinstone, E.D., and Dodd, I.C. (2014). Two potato (Solanum tuberosum) varieties differ in drought tolerance due to differences in root growth at depth. Funct. Plant Biol. *41*, 1107–1118.

212. Dörffling, K. (1982). Das Hormonsystem der Pflanzen. Thieme, Stuttgart New York.

213. Milborrow, B. (1978). Abscisic acid. In: Phytohormones and related compounds - A comprehensive treatise. Letham, Goodwin, Higgins, Elsevier/North- Holl. Biomed. Press. Amsterdam *1*, 295–347.

214. Cornish, K., and Zeevaart, J. (1984). Abscisic acid metabolism in relation to water stress and leaf age in Xanthium strumarium. Plant Physiol. *76*, 1029–1035.

215. Zeevaart, J., and Boyer, G. (1984). Accumulation and transport of abscisic acid and its metabolites in Ricinus and Xanthium. Plant Physiol. *74*, 934–939.

216. Zhang J, S.U.& D.W. (1987). Control of stomatal behaviour by abscisic acid which apparently originates in the roots. J. Exp. Bot. *38*, 1174–1181.

217. Dodd, I.C. (2005). Control of stomatal behaviour by abscisic acid which apparently originates in the roots. Plant Soil *274*, 251–270.

218. Endo, A., Sawada, Y., Takahashi, H., Okamoto, M., Ikegami, K., Koiwai, H., Seo, M., Toyomasu, T., Wataru, M., Nakazono, M., *et al.* (2008). Drought Induction of Arabidopsis 9-cis-Epoxycarotenoid Dioxygenase Occurs in Vascular Parenchyma Cells. Plant Physiol. *147*, 1984–1993.

219. Kuromori, T., Sugimoto, E., and Shinozaki, K. (2014). Intertissue Signal Transfer of Abscisic Acid from VascularCells to Guard Cells. Plant Physiol. *164*, 1587–1592.

220. Bauer, H., Ache, P., Lautner, S., Fromm, J., Hartung, W., Al-rasheid, K.A.S., Sonnewald, S., Sonnewald, U., Kneitz, S., Lachmann, N., *et al.* (2013). The Stomatal Response to Reduced Relative Humidity Requires Guard Cell-Autonomous ABA Synthesis. Curr. Biol. *23*, 53–57.

221. McAdam, S.A.M., and Brodribb, T.J. (2018). Mesophyll Cells Are the Main Site of Abscisic Acid Biosysnthesis in Water-Stressed Leaves. Plant Physiol. *177*, 911–917.

222. Bullock, W.O., Fernandez, J.M., and Short, J.M. (1987). XL1-blue - a high efficiency plasmid transforming recA Escherichia coli strian with ß-Galactosidase selection. Biotechniques *5*, 376–379.

223. Deblaere, R., Bytebier, B., Greve, H. De, Brussel, V.U., Deboeck, F., Brussel, V.U., and Montagu, M. Van (1985). Efficient octopine Ti plasmid-derived vectors for Agrobacterium-mediated gene transfer to plants. Nucleic Acids Res.

224. Van Larebeke, N., Engler, G., Holsters, H., van den Elsacker, S., Zaenen, I., Schilperport, R.A., and Schell, J. (1974). Large plasmid in Agrobacterium tumefaciens essential for crown gall-inducing ability Multiple divergent copies of endogenous C-type virogenes in mammalian cells. Nature *252*, 169–170.

225. Untergasser, A., Nijveen, H., Rao, X., and Bisseling, T. (2007). Primer3Plus , an enhanced web interface to Primer3. Nucleic Acids Res. *35*, 71–74.

226. Höfgen, R., and Willmitzer, L. (1988). Storage of competent cells for Agrobacterium transfonnation. Nucleic Acids Res. *16*, 9877.

227. Murashige, T., and Skoog, F. (1962). A revised medium for rapid growth and bio assays with tobacco tissue cultures. Physiologia Plantarum , 15 , pp.473 – 497. Physiol. Plant. *15*, 473–497.

228. Rocha-Sosa, M., Sonnewald, U., Frommer, W., Stratmann, M., Schell, J., and

Willmitzer, L. (1989). Both developmental and metabolic signals activate the promoter of a class I patatin gene. EMBO J. *8*, 23–29.

229. Engler, C., Kandzia, R., and Marillonnet, S. (2008). A One Pot , One Step , Precision Cloning Method with High Throughput Capability. PLoS One *3*.

230. Engler, C., Gruetzner, R., Kandzia, R., and Marillonnet, S. (2009). Golden Gate Shuffling : A One-Pot DNA Shuffling Method Based on Type IIs Restriction Enzymes. PLoS One *4*.

231. Weber, E., Engler, C., Gruetzner, R., Werner, S., and Marillonnet, S. (2011). A Modular Cloning System for Standardized Assembly of Multigene Constructs. PLoS One *6*, 1–11.

232. Werner, S., Engler, C., Weber, E., Gruetzner, R., Werner, S., Engler, C., Weber, E., Gruetzner, R., Werner, S., Engler, C., *et al.* (2012). Fast track assembly of multigene constructs using Golden Gate cloning and the MoClo system and the MoClo system. Bioeng. Bugs *3*, 38–43.

233. Logemann, J., Schell, J., and Willmitzer, L. (1987). Improved Method for the Isolation of RNA from Plant Tissues Improved Method for the Isolation of RNA from Plant Tissues Improved Method for the Isolation of RNA from Plant Tissues. Anal. Biochem. *163*, 16–20.

234. Livak, K.J., and Schmittgen, T.D. (2001). Analysis of relative gene expression data using real-time quantitative PCR and the 2-ΔΔCT method. Methods *25*, 402–408.

235. Benjamini, Y., and Hochberg, Y. (1995). Controlling the false discovery rate: A practical and powerful approach to multiple testing. J. R. Stat. Soc. *57*, 1995.

236. Laemmli, U.K. (1970). Cleavage of structural proteins during the assembly of the head of bacteriophage T4. Nature *227*, 680–685.

237. Tang, G., Yan, J., Gu, Y., Qiao, M., Fan, R., Mao, Y., and Tang, X. (2012). Construction of short tandem target mimic (STTM) to block the functions of plant and animal microRNAs. Methods *58*, 118–125.

238. Pan, X., Welti, R., and Wang, X. (2010). Simultaneous quantification of major phytohormones and related compounds in crude plant extracts by liquid chromatography – electrospray tandem mass spectrometry. Phytochemistry *69*, 1773–1781.

239. van Wandelen, C., and Cohen, S. (1997). Using quaternary high-performance liquid chromatography eluent systems for separating 6-aminoquinolyl-N-hydroxysuccinimidyl carbamate-derivatized amino acid mixtures. J. Chromatogr. *763*, 11–22.

240. Gao, H., Wang, Z., Li, S., Hou, M., Zhou, Y., Zhao, Y., Li, G., Zhao, H., and Ma, H. (2018). Genome-wide survey of potato MADS-box genes reveals that StMADS1 and StMADS13 are putative downstream targets of tuberigen StSP6A. BMC Genomics *19*, 1–20.

241. Ditta, G., Pinyopich, A., Robles, P., Pelaz, S., and Yanofsky, M.F. (2004). The SEP4 Gene of Arabidopsis thaliana Functions in Floral Organ and Meristem Identity. Curr. Biol. *14*, 1935–1940.

242. Yoshida, H., and Nagato, Y. (2011). Flower development in rice. J. Exp. Bot. *62*, 4719–4730.

243. Lee, S., Kim, J., Han, J., Han, M., and Ã, G.A. (2004). Functional analyses of the Flowering time gene OsMADS50 , the putative SUPPRESSOR OF OVEREXPRESSION OF CO 1 / AGAMOUS-LIKE 20 (SOC1 / AGL20) ortholog in rice. Plant J. *38*, 754–764.

244. Sun, C., Fang, J., Zhao, T., Xu, B., Zhang, F., Liu, L., Tang, J., Zhang, G., Deng, X., Chen, F., *et al.* (2012). The Histone Methyltransferase SDG724 Mediates H3K36me2 / 3 Deposition at MADS50 and RFT1 and Promotes Flowering in Rice. Plant Cell *24*, 3235–3247.

245. Liu, X., Yang, Y., Hu, Y., Zhou, L., Li, Y., and Hou, X. (2018). Temporal-Speci fi c Interaction of NF-YC and CURLY LEAF during the Floral Transition Regulates Flowering. Plant Physiol. *177*, 105–114.

246. Lomax, A., Woods, D.P., Dong, Y., Bouch, F., Rong, Y., Mayer, K.S., Zhong, X., and Amasino, R.M. (2018). An ortholog of CURLY LEAF / ENHANCER OF ZESTE like-1 is required for proper flowering in *Brachypodium distachyon*. Plant J. *93*, 871–882.

247. Wu, H., Deng, S., Xu, H., Mao, H., Liu, J., Niu, Q., Wang, H., and Chua, N. (2018). A noncoding RNA transcribed from the AGAMOUS (AG) second intron binds to CURLY LEAF and represses AG expression in leaves. New Phytol. *219*, 1480–1491.

248. Zwack, P.J., Clercq, I. De, Howton, T.C., Hallmark, H.T., Hurny, A., Keshishian, E.A., Parish, A.M., Benkova, E., Mukhtar, M.S., Breusegem, F. Van, *et al.* (2016). Cytokinin Response Factor 6 Represses Cytokinin-Associated Genes during. Plant Physiol. *172*, 1249–1258.

249. Xu, X., Pan, S., Cheng, S., Zhang, B., Mu, D., Ni, P., Zhang, G., Yang, S., Li, R., Wang, J., *et al.* (2011). Genome sequence and analysis of the tuber crop potato. Nature *475*, 189–195.

250. Tempel, S., and Tahi, F. (2012). A fast ab-initio method for predicting miRNA precursors in genomes. Nucleic Acids Res. *40*, 1–9.

251. Zuker, M. (2003). Mfold web server for nucleic acid folding and hybridization prediction. Nucleic Acids Res. *31*, 3406–3415.

252. Dai, X., and Zhao, P.X. (2011). PsRNATarget: A plant small RNA target analysis server. Nucleic Acids Res. *39*, 155–159.

253. Soderlund, C., Bomhoff, M., and Nelson, W.M. (2011). SyMAP v3.4: A turnkey synteny system with application to plant genomes. Nucleic Acids Res. *39, e68*.

254. Darling, A.C.E., Mau, B., Blattner, F.R., and Perna, N.T. (2004). Mauve : Multiple Alignment of Conserved Genomic Sequence With Rearrangements. Methods *14,* 1394–1403.

255. Wolf, S., Marani, A, and Rudich, J. (1990). Effects of Temperature and Photoperiod on Assimilate Partitioning in Potato Plants. Ann. Bot. *66*, 513–520.

256. Jin, J., Zhang, H., Kong, L., Gao, G., and Luo, J. (2014). PlantTFDB 3 . 0 : a portal for the functional and evolutionary study of plant transcription factors. Nucleic Acids Res. *42*, 1182–1187.

257. Jin, J., Tian, F., Yang, D.C., Meng, Y.Q., Kong, L., Luo, J., and Gao, G. (2017). PlantTFDB 4.0: Toward a central hub for transcription factors and regulatory interactions in plants. Nucleic Acids Res. *45*, D1040–D1045.

258. Jin, J., He, K., Tang, X., Li, Z., Lv, L., Zhao, Y., Luo, J., and Gao, G. (2015). An Arabidopsis Transcriptional Regulatory Map Reveals Distinct Functional and Evolutionary Features of Novel Transcription Factors. Mol. Biol. Evol. *32*, 1767–1773.

259. Yan, J., Gu, Y., Jia, X., Kang, W., Pan, S., Tang, X., Chen, X., and Tang, G. (2012). Effective Small RNA Destruction by the Expression of a Short Tandem Target Mimic in Arabidopsis. Plant Cell *24*, 415–427.

260. Franco-Zorrilla, J.M., Valli, A., Todesco, M., Mateos, I., Puga, M.I., Rubio-Somoza, I., Leyva, A., Weigel, D., García, J.A., and Paz-Ares, J. (2007). Target mimicry provides a new mechanism for regulation of microRNA activity. Nat. Genet. *39*, 1033–1037.

261. Stockhaus, J., Eckes, P., Rocha-sosa, M., Schell, J., and Willmitzer, L. (1987). Analysis of cis-active sequences involved in the leaf-specific expression of a potato gene in transgenic plants. Proc. Natl. Acad. Sci. *84*, 7943–7947.

262. Müller-Röber, B., Ellenberg, J., Provart, N., Willmitzer, L., Busch, H., Becker, D., Dietrich, P., Hoth, S., and Hedrich, R. (1995). Cloning and electrophysiological analysis of KST1, an inward rectifying K+ channel expressed in potato guard cells. EMBO J. *14*, 2409–2416.

263. Kelly, G., Egbaria, A., Khamaisi, B., Lugassi, N., Attia, Z., Moshelion, M., and Granot, D. (2019). Guard-Cell Hexokinase Increases Water-Use Efficiency Under Normal and Drought Conditions. Front. Plant Sci. *10*, 1–12.

264. Yoshiba, Y., Nanjo, T., Miura, S., Yamaguchi-shinozaki, K., and Shinozaki, K. (1999). Stress-Responsive and Developmental Regulation Gene Expression in Arabidopsis thaliana. Biochem. Biophys. Res. Commun. *261*, 766–772.

265. Plantenga, F.D.M., Bergonzi, S., Abelenda, J.A., Bachem, C.W.B., Visser, R.G.F., Heuvelink, E., and Marcelis, L.F.M. (2018). The tuberization signal StSP6A represses flower bud development in potato. J. Exp. Bot., 1–12.

266. Plantenga, F.D.M., Heuvelink, E., Rienstra, J.A., and Visser, R.G.F. (2018). Coincidence of potato CONSTANS (StCOL1) expression and light cannot explain night-break repression of tuberization. Physiol. Plant., 1–14.

267. Morris, W.L., Hancock, R.D., Ducreux, L.J.M., Morris, J.A., Usman, M., Verrall, S.R., Sharma, S.K., Bryan, G., Mcnicol, J.W., Hedley, P.E., *et al.* (2014). Day length dependent restructuring of the leaf transcriptome and metabolome in potato genotypes with contrasting tuberization phenotypes. Plant, Cell Environ. *37*, 1351–1363.

268. Ewing, E.E., and Struik, P.C. (1992). Tuber formation in potato: induction, initiation, and growth.

269. Hannapel, D.J., Sharma, P., Lin, T., and Banerjee, A.K. (2017). The Multiple Signals That Control Tuber Formation. Plant Physiol. *174*, 845–856.

270. Abelenda, J.A., Navarro, C., and Prat, S. (2011). From the model to the crop: Genes controlling tuber formation in potato. Curr. Opin. Biotechnol. *22*, 287–292.

271. Hannapel, D., and Banerjee, A. (2017). Multiple Mobile mRNA Signals Regulate Tuber Development in Potato. Plants *6*, 8.

272. Natarajan, B., Bhogale, S., Banerjee, A.K., Micrornas, T.Á., and Á, Á. (2017). The essential role of microRNAs in potato tuber development : a mini review. Indian J. Plant Physiol. *22*, 401–410.

273. Natarajan, B., Kondhare, K.R., Hannapel, D.J., and Banerjee, A.K. (2019). Plant Science Mobile RNAs and proteins : Prospects in storage organ development of tuber and root crops. Plant Sci. *284*, 73–81.

274. Becker, A., and Ehlers, K. (2016). Arabidopsis flower development — of protein complexes , targets , and transport. Protoplasma *253*, 219–230.

275. Bou-Torrent, J., Martinez-Garcia, J.F., Garcia-Martines, J.L., and Prat, S. (2011). Gibberellin A1 Metabolism Contributes to the Control of Photoperiod- Mediated Tuberization in Potato Gibberellin A 1 Metabolism Contributes to the Control of Photoperiod-Mediated Tuberization in Potato. PLoS One *6*, 1–10.

276. Kolachevskaya, O.O., Lomin, S.N., Arkhipov, D. V, and Romanov, G.A. (2019). Auxins in potato : molecular aspects and emerging roles in tuber formation and stress resistance. Plant Cell Rep. *38*, 681–698.

277. Roumeliotis, E., Visser, R.G.F., and Bachem, C.W.B. (2012). A crosstalk of auxin and GA during tuber development. Plant Signal. Behav. *7*, 1360–1363.

278. Roumeliotis, E., Kloosterman, B., Oortwijn, M., Kohlen, W., Bouwmeester, H.J., Visser, R.G.F., and Bachem, C.W.B. (2012). The effects of auxin and strigolactones on tuber initiation. J. Exp. Bot. *63*, 4539–4547.

279. Hartmann, A., Senning, M., Hedden, P., Sonnewald, U., and Sonnewald, S. (2011). Reactivation of Meristem Activity and Sprout Growth in Potato Tubers Require Both Cytokinin and Gibberellin. Plant Physiol. *155*, 776–796.

280. Tao, G.Q., Letham, D.S., Yong, J.W., Zhang, K., John, P.C., Schwartz, O., Wong, S.C., and Farquhar, G.D. (2010). Promotion of shoot development and tuberisation in potato by expression of a chimaeric cytokinin synthesis gene at normal and elevated CO2 levels. Funct. Plant Biol. *37*, 43–54.

281. Eviatar-ribak, T., Shalit-kaneh, A., Chappell-maor, L., Amsellem, Z., and Eshed, Y. (2013). A Cytokinin-Activating Enzyme Promotes Tuber Formation in Tomato. Curr. Biol. *23*, 1057–1064.

282. Wit, M. De, Galv, V.C., and Fankhauser, C. (2016). Light-Mediated Hormonal Regulation of Plant Growth and Development. Annu. Rev. Plant Biol. *67*, 513–537.

283. Wilson, R.N., Heckman, J.W., and Somerville, C.R. (1992). Gibberellin Is Required for Flowering in Arabidopsis thaliana under Short Days1. Plant Physiol. *100*, 403–408.

284. Eriksson, M.E., Hoffman, D., Kaduk, M., Moritz, T., and Moritz, T. (2014). Transgenic hybrid aspen trees with increased gibberellin (GA) concentrations suggest that GA acts in parallel with FLOWERING LOCUS T2 to control shoot elongation. New Phytol. *205*, 1288–1295.

285. Zheng, Y., Luo, L., Liu, Y., Yang, Y., Wang, C., Kong, X., and Yang, Y. (2018). Plant Diversity Effect of vernalization on tuberization and fl owering in the Tibetan turnip is associated with changes in the expression of FLC homologues. Plant Divers. *40*, 50–56.

286. Lee, R., Baldwin, S., Kenel, F., Mccallum, J., and Macknight, R. (2013). bulb formation and flowering. Nat. Commun. *4*, 1–9.

287. Wang, Y., Liu, L., Song, S., Li, Y., Shen, L., and Yu, H. (2018). DOFT and DOFTIP1 affect reproductive development in the orchid Dendrobium Chao Praya Smile. J. Exp.

Bot. *68*, 5759–5772.

288. Xu, L., Wang, J., Lei, M., Li, L., Fu, Y., and Wang, Z. (2016). Transcriptome Analysis of Storage Roots and Fibrous Roots of the Traditional Medicinal Herb Callerya speciosa (Champ .) ScHot. PLoS One, 1–20.

289. Borges, F., and Martienssen, R.A. (2015). The expanding world of small RNAs in plants. Nat. Rev. Mol. Cell Biol. *16*, 727–741.

290. Khraiwesh, B., Zhu, J.-K., and Zhu, J. (2012). Role of miRNAs and siRNAs in biotic and abiotic stress responses of plants. Biochim. Biophys. Acta *1819*, 137–148.

291. Tang, J., and Chu, C. (2017). MicroRNAs in crop improvement: Fine-tuners for complex traits. Nat. Plants *3, 1-11*.

292. Shriram, V., Kumar, V., Devarumath, R.M., Khare, T.S., and Wani, S.H. (2016). MicroRNAs As Potential Targets for Abiotic Stress Tolerance in Plants. Front. Plant Sci. *7*, 1–18.

293. Xin, M., Wang, Y., Yao, Y., Xie, C., Peng, H., Ni, Z., and Sun, Q. (2010). Diverse set of microRNAs are responsive to powdery mildew infection and heat stress in wheat (Triticum aestivum L .). BMC Plant Biol. *10*, 1–11.

294. Wu, G., Park, M.Y., Conway, S.R., Wang, J., Weigel, D., and Scott, R. (2009). The sequental actions of miR156 and miR172 regulates developmetnal timing in Arabidopsis. Cell *138*, 750–759.

295. Wang, H., and Wang, H. (2015). The miR156/SPL module, a regulatory hub and versatile toolbox, gears up crops for enhanced agronomic traits. Mol. Plant *8*, 677–688.

296. Kim, J.J., Lee, J.H., Kim, W., Jung, H.S., Huijser, P., and Ahn, J.H. (2012). The microRNA156-SQUAMOSA PROMOTER BINDING PROTEIN-LIKE3 Module Regulates Ambient Temperature-Responsive Flowering via FLOWERING LOCUS T in Arabidopsis. Plant Physiol. *159*, 461–478.

297. Wu, L., Liu, D., Wu, J., Zhang, R., Qin, Z., Liu, D., Li, A., Fu, D., Zhai, W., and Mao, L. (2013). Regulation of FLOWERING LOCUS T by a MicroRNA in *Brachypodium distachyon*. *25*, 4363-4377.

298. Lakhotia, N., Joshi, G., Bhardwaj, A.R., Katiyar-Agarwal, S., Agarwal, M., Jagannath, A., Goel, S., and Kumar, A. (2014). Identification and characterization of miRNAome in root, stem, leaf and tuber developmental stages of potato (*Solanum tuberosum* L.) by high-throughput sequencing. BMC Plant Biol. *14*, 1–16.

299. Gu, M., Liu, W., Meng, Q., Zhang, W., Chen, A., Sun, S., and Xu, G. (2014). Identification of microRNAs in six solanaceous plants and their potential link with phosphate and mycorrhizal signaling. J. Integr. Plant Biol. *56*, 1164–1178.

300. Kondhare, K.R., Malankar, N.N., Devani, R.S., and Banerjee, A.K. (2018). Genome-wide transcriptome analysis reveals small RNA profiles involved in early stages of stolon-to-tuber transitions in potato under photoperiodic conditions. BMC Plant Biol. *18*, 1–19.

301. Ha, M., and Kim, V.N. (2014). Regulation of microRNA biogenesis. Nat. Publ. Gr. *15*, 509–524.

302. Ré, D.A., Lang, P.L.M., Yones, C., Arce, A.L., Stegmayer, G., Milone, D., and

Manavella, P.A. (2019). Alternative usage of miRNA-biogenesis co-factors in plants at low temperatures. Development *146*, 1-7.

303. Trapero-Mozos, A., Laurence, M., Craita, J.M.D., Wayne, E.B., Cosima, M., Morris, J.A., Paterson, C., Hedley, P.E., Hancock, R.D., and Taylor, M. (2018). A reversible light‐and genotype‐dependent acquired thermotolerance response protects the potato plant from damage due to excessive temperature. Planta *247*, 1377-1392.

304. Cui, L.G., Shan, J.X., Shi, M., Gao, J.P., and Lin, H.X. (2014). The miR156-SPL9-DFR pathway coordinates the relationship between development and abiotic stress tolerance in plants. Plant J. *80*, 1108–1117.

305. Djami-Tchatchou, A.T., Sanan-Mishra, N., Ntushelo, K., and Dubery, I.A. (2017). Functional Roles of microRNAs in Agronomically Important Plants—Potential as Targets for Crop Improvement and Protection. Front. Plant Sci. *8*, 1-24.

306. Zhang, R., Marshall, D., Bryan, G.J., and Hornyik, C. (2013). Identification and Characterization of miRNA Transcriptome in Potato by High-Throughput Sequencing. PLoS One *8*, 1-24.

307. Xie, F., Frazier, T.P., and Zhang, B. (2011). Identification, characterization and expression analysis of MicroRNAs and their targets in the potato (*Solanum tuberosum*). Gene *473*, 8–22.

308. Zhang, N., Yang, J., Wang, Z., Wen, Y., Wang, J., He, W., Liu, B., Si, H., and Wang, D. (2014). Identification of novel and conserved microRNAs related to drought stress in potato by deep sequencing. PLoS One *9, e95489*.

309. Kissoudis, C., Wiel, C. Van De, Visser, R.G.F., and Linden, G. Van Der (2016). Future-proof crops : challenges and strategies for climate resilience improvement. Curr. Opin. Plant Biol. *30*, 47–56.

310. Morris, W.L., Ducreux, L.J.M., Morris, J., Campbell, R., Usman, M., Hedley, P.E., Prat, S., and Taylor, M.A. (2019). Identification of TIMING OF CAB EXPRESSION 1 as a temperature-sensitive negative regulator of tuberization in potato. J. Exp. Bot. *70*, 5703–5714.

311. Shin, D., Moon, S., Han, S., Kim, B., Park, S.R., Lee, S., Yoon, H., Lee, H.E., Kwon, H., Baek, D., *et al.* (2011). Expression of StMYB1R-1 , a Novel Potato Single MYB-Like Domain Transcription Factor, Increases Drought Tolerance. Plant Physiol. *155*, 421–432.

312. Moon, S.-J., Han, S.-Y., Kim, D.-Y., Yoon, I.S., Shin, D., Byun, M.-O., Kwon, H.-B., and Kim, B.-G. (2015). Ectopic expression of a hot pepper bZIP‐like transcription factor in potato enhances drought tolerance without decreasing tuber yield. Plant Mol. Biol. *89*, 421–431.

313. Szalonek, M., Sierpien, B., Rymaszewski, W., and Gieczewska, K. (2015). Potato Annexin STANN1 Promotes Drought Tolerance and Mitigates Light Stress in. PLoS One, 1–38.

314. Rizhsky, L., Liang, H., and Mittler, R. (2002). The Combined Effect of Drought Stress and Heat Shock on Gene Expression in Tobacco. Plant Physiol. *130*, 1143–1151.

315. Rizhsky, L., Liang, H., Shuman, J., Shulaev, V., Davletova, S., and Mittler, R. (2004). When defense pathways collide. The response of Arabidopsis to a combination of drought and heat stress. Plant Physiol. *134*, 1683–1696.

316. Prasch, C.M., Ott, K.V., Bauer, H., Ache, P., Hedrich, R., and Sonnewald, U. (2015). ß-amylase1 mutant Arabidopsis plants show improved drought tolerance due to reduced starch breakdown in guard cells. J. Exp. Bot. *66*, 6059–6067.

317. Moore, B., Zhou, L., Rolland, F., and Hall, Q. (2003). Role of the Arabidopsis Glucose Sensor HXK1 in Nutrient , Light , and Hormonal Signaling. Science *300*, 332–337.

318. Liu, F., Shahnazari, A., Andersen, M.N., Jacobsen, S., and Jensen, C.R. (2006). Physiological responses of potato (Solanum tuberosum L .) to partial root-zone drying : ABA signalling , leaf gas exchange , and water use efficiency. J. Exp. Bot. *57*, 3727–3735.

319. Sharma, A., Shahzad, B., Kumar, V., and Kohli, S.K. (2019). Phytohormones Regulate Accumulation of Osmolytes Under Abiotic Stress. Biomolecules *9*, 1–36.

320. Alexieva, V., Sergiev, I., Mapelli, S., and Karanov, E. (2001). The effect of drought and ultraviolet radiation on growth and stress markers in pea and wheat. Plant, Cell Environ. *24*, 1337–1344.

321. Yamada, M., Morishita, H., Urano, K., Shiozaki, N., Yamaguchi-shinozaki, K., Shinozaki, K., Yoshiba, Y., and Division, B.R. (2005). Effects of free proline accumulation in petunias under drought stress. J. Exp. Bot. *56*, 1975–1981.

322. Hu, C.A., Delauney, A.J., and Verma, D.P.S. (1992). A bifunctional enzyme (Al-pyrroline-5-carboxylate synthetase) catalyzes the first two steps in proline biosynthesis in plants. Proc. Natl. Acad. Sci. *89*, 9354–9358.

323. Yoshiba, Y., Kiyosue, T., Katagiri, T., Ueda, H., Mizoguchi, T., Yamaguchishinozaki, K., Wada, K., Harada, Y., and Shinozaki, K. (1995). Correlation between the induction of a gene for D1-Pyrroline-5-Carboxylate Synthaseand the accumulation of proline in Arabidopsis thaliana under osmotic stress. Plant J. *7*, 751–760.

324. Kim, Y., Heinzel, N., Giese, J., Koeber, J., Melzer, M., Rutten, T., Wirén, N. von, Sonnewald, U., and Hajirezaei, M.-R. (2013). A dual role of tobacco hexokinase 1 in primary metabolism and sugar sensing. Plant, Cell Environ. *36*, 1311–1327.

325. Lehretz, G.G., Sonnewald, S., Hornyik, C., Corral, J.M., and Sonnewald, U. (2019). Post-transcriptional Regulation of FLOWERING LOCUS T Modulates Heat-Dependent Source-Sink Development in Potato. Curr. Biol. *29*, 1614–1624.

326. Chen, Q., Li, M., Zhang, Z., Tie, W., Chen, X., Jin, L., Zhai, N., Zheng, Q., Zhang, J., Wang, R., *et al.* (2017). Integrated mRNA and microRNA analysis identifies genes and small miRNA molecules associated with transcriptional and post-transcriptional-level responses to both drought stress and re-watering treatment in tobacco. BMC Genomics *18*, 1–16.

327. Wang, M., Moigne, M. Le, Bertheloot, J., Crespel, L., Ogé, L., Demotes-mainard, S., Hamama, L., Davière, J., Sakr, S., and Brewer, P.B. (2019). BRANCHED1 : A Key Hub of Shoot Branching. Front. Plant Sci. *10*, 1–12.

328. Martı, M., Marcel, F., Schmitz, G., Theres, K., and Bendahmane, A. (2011). Role of tomato BRANCHED1 -like genes in the control of shoot branching. Plant J. *67*, 701–714.

329. Nicolas, M., Rodríguez-Buey, M.L., Franco-Zorrilla, J.M., and Cubas, P. (2015). A Recently Evolved Alternative Splice Site in the BRANCHED1a Gene Controls Potato Plant Architecture. Curr. Biol. *25*, 1799–1809.

330. González-Grandío, E., Pajoro, A., Franco-Zorrilla, J.M., Tarancón, C., and Immink, R.G.H. (2016). Abscisic acid signaling is controlled by a BRANCHED1 / HD-ZIP I cascade in Arabidopsis axillary buds. Proc. Natl. Acad. Sci. *53*, 245–254.

331. Niwa, M., Daimon, Y., Kurotani, K., Higo, A., Breton, G., Mitsuda, N., Kay, S.A., Ohme-takagi, M., Endo, M., and Araki, T. (2013). BRANCHED1 Interacts with FLOWERING LOCUS T to Repress the Floral Transition of the Axillary Meristems in Arabidopsis. Plant Cell *25*, 1228–1242.

332. Braun, D.M. (2012). SWEET ! The Pathway Is Complete. Science *335*, 173–175.

333. Sonnewald, U. (2011). SWEETs-The missing sugar efflux carriers. Front. Plant Sci. *2*, 1–2.

334. Viola, R., Pelloux, J., Van Der Ploeg, A., Gillespie, T., Marquis, N., Roberts, A.G., and Hancock, R.D. (2007). Symplastic connection is required for bud outgrowth following dormancy in potato (*Solanum tuberosum* L.) tubers. Plant, Cell Environ. *30*, 973–983.

335. Spena, A., Aalen, R.B., and Schulze, S.C. (1989). Cell-Autonomous Behavior of the rolC Gene of Agrobacterium rhizogenes during Leaf Development : A Visual Assay for Transposon Excision in Transgenic Plants. Plant Cell *1*.

336. Deeken, R., Geiger, D., Fromm, J., Koroleva, O., Ache, P., Langenfeld-Heyser, R., Sauer, N., May, S.T., and Hedrich, R. (2002). Loss of the AKT2 / 3 potassium channel affects sugar loading into the phloem of Arabidopsis. Planta *216*, 334–344.

337. Gajdanowicz, P., Michard, E., Sandmann, M., Rocha, M., Gustavo, L., and Corrêa, G. (2010). Potassium (K+) gradients serve as a mobile energy source in plant vascular tissues. Proc. Natl. Acad. Sci. *108*, 864–869.

338. Chen, L.-Q., Lin, I.W., Qu, X.-Q., Sosso, D., E.McFarlane, H., Londoño, A., Samuels, A.L., and Frommer, W.B. (2015). A Cascade of Sequentially Expressed Sucrose Transporters in the Seed Coat and Endosperm Provides Nutrition for the Arabidopsis Embryo. Plant Cell *27*, 607–619.

339. Oparka, K.J., Duckett, C.M., Prior, O.A.M.I., and Fisher, D.B. (1994). Real-time imaging of phloem unloading in the root tip of Arabidopsis. Plant J. *6*, 759–766.

340. Knoblauch, M., Vendrell, M., Leau, E. De, Paterlini, A., Knox, K., Ross-elliot, T., Reinders, A., Brockman, S.A., Ward, J., and Oparka, K. (2015). Multispectral Phloem-Mobile Probes : Properties and Applications 1. Plant Physiol. *167*, 1211–1220.

341. Basu, P.S., and Minhas, J.S. (1991). Heat Tolerance and Assimilate Transport in Different Potato Genotypes 1. J. Exp. Bot. *42*, 861–866.

342. Wishart, J., George, T.S., Brown, L.K., Ramsay, G., Bradshaw, J.E., White, P.J., and Gregory, P.J. (2013). Measuring variation in potato roots in both field and glasshouse: the search for useful yield predictors and a simple screen for root traits. Plant Soil *368*, 231–249.

343. Wishart, J., George, T.S., Brown, L.K., White, P.J., Ramsay, G., Jones, H., and Gregory, P.J. (2014). Field phenotyping of potato to assess root and shoot characteristics associated with drought tolerance. Plant Soil *378*, 351–363.

344. Spitters, C.J.., and Schapendonk, A.H.C.M. (1990). Evaluation of breeding strategies for drought tolerance in potato by means of crop growth simulation. Plant Soil *203*, 193–203.

345. Haverkort, A.J., Waart, M. van de, and Bodlaender, K.B.A. (1990). The effect of early drought stress on numbers of tubers and stolons of potato in controlled and field conditions. Potato Res. *33*, 89–96.

346. Shock, C.C., Zalewski, J.C., Stieber, T.D., and Burnett, D.S. (1992). Impact of early-season water deficits on Russet Burbank plant development, tuber yield and quality. Am. Potato J. *69*, 793–803.

7 Supplementary data

7.1 Supplementary figures

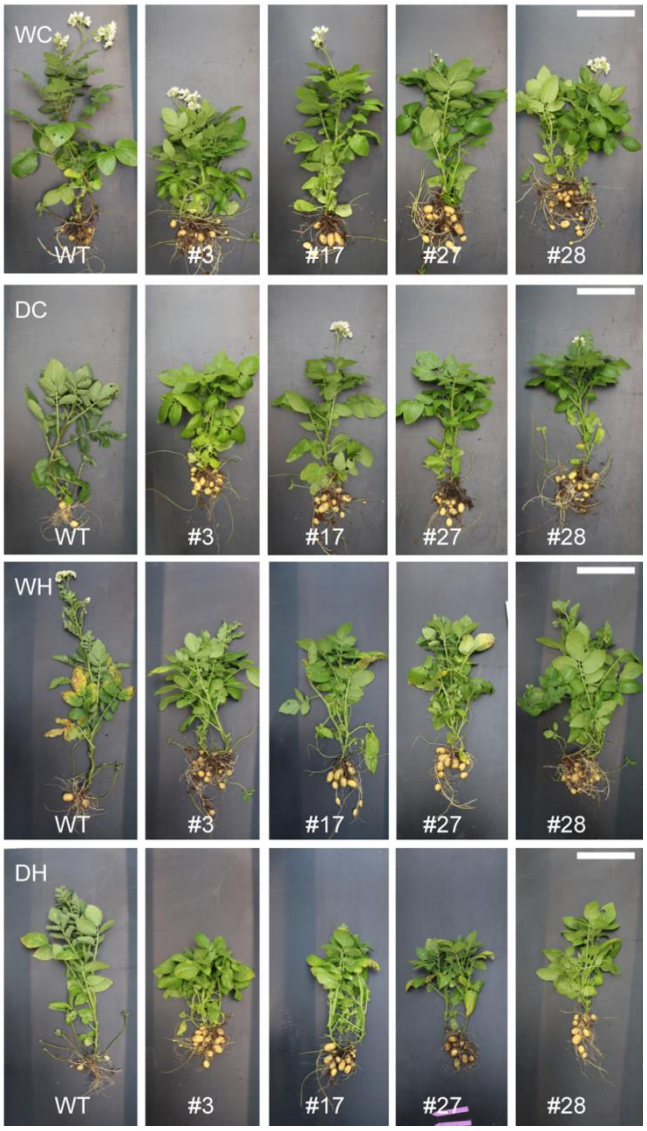

Figure S1. Phenotype of HXK+SP6A potato plants. Shoot and tuber phenotype under four different growth conditions 7 weeks after planting; scale bar 20cm.

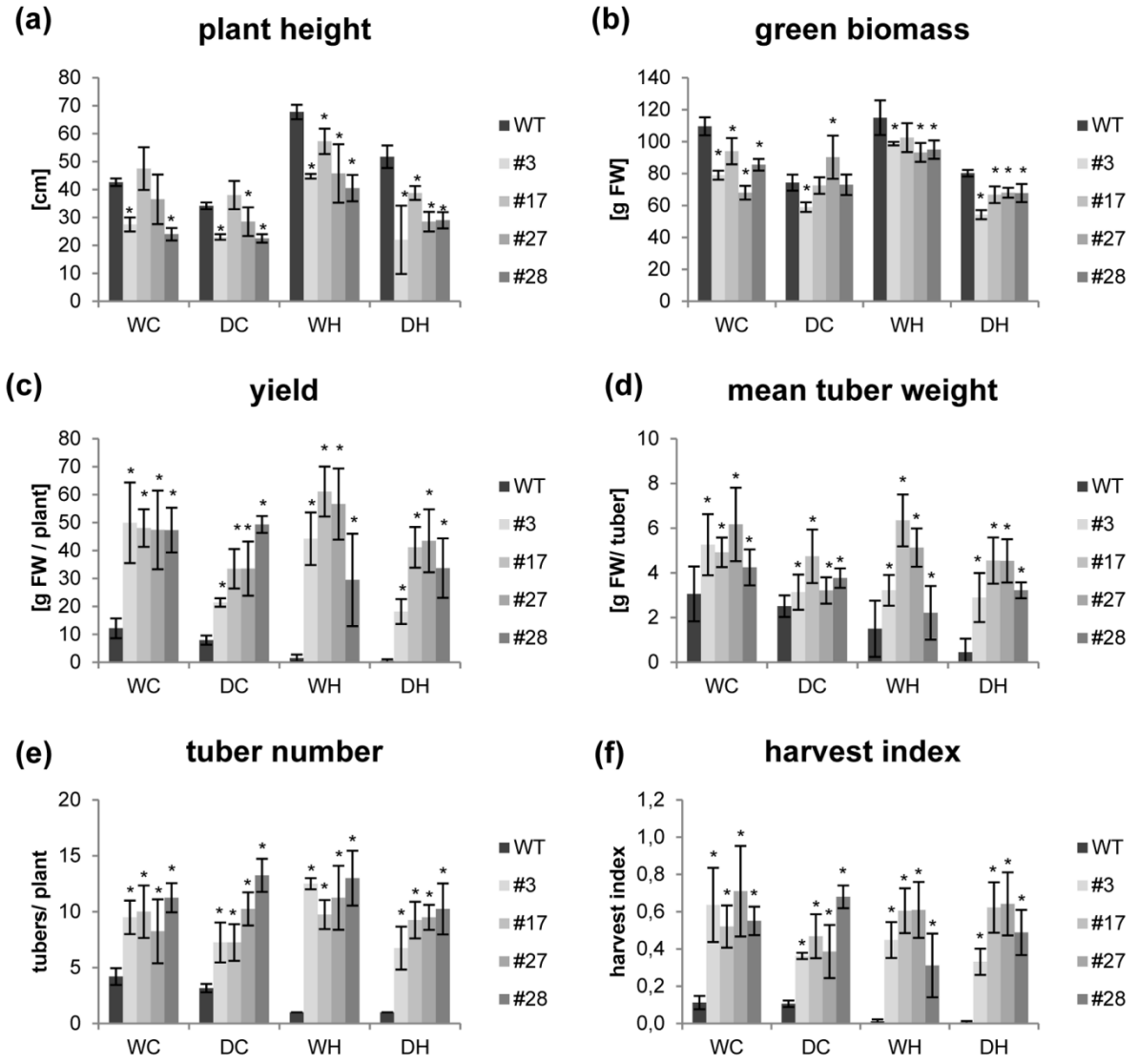

Figure S2. Yield data for HXK+SP6A potato plants. (a) Plant height **(b)** Green biomass **(c)** Yield **(d)** Stolon number **(e)** Tuber number **(f)** Harvest index; data form experiment 2, plants were harvested at the age of 7 weeks; values are the mean of 4 plants ± SD, Significance compared to WT was determined by two-tailed t-test (*; p-value < 0.05). Data from experiment 2.

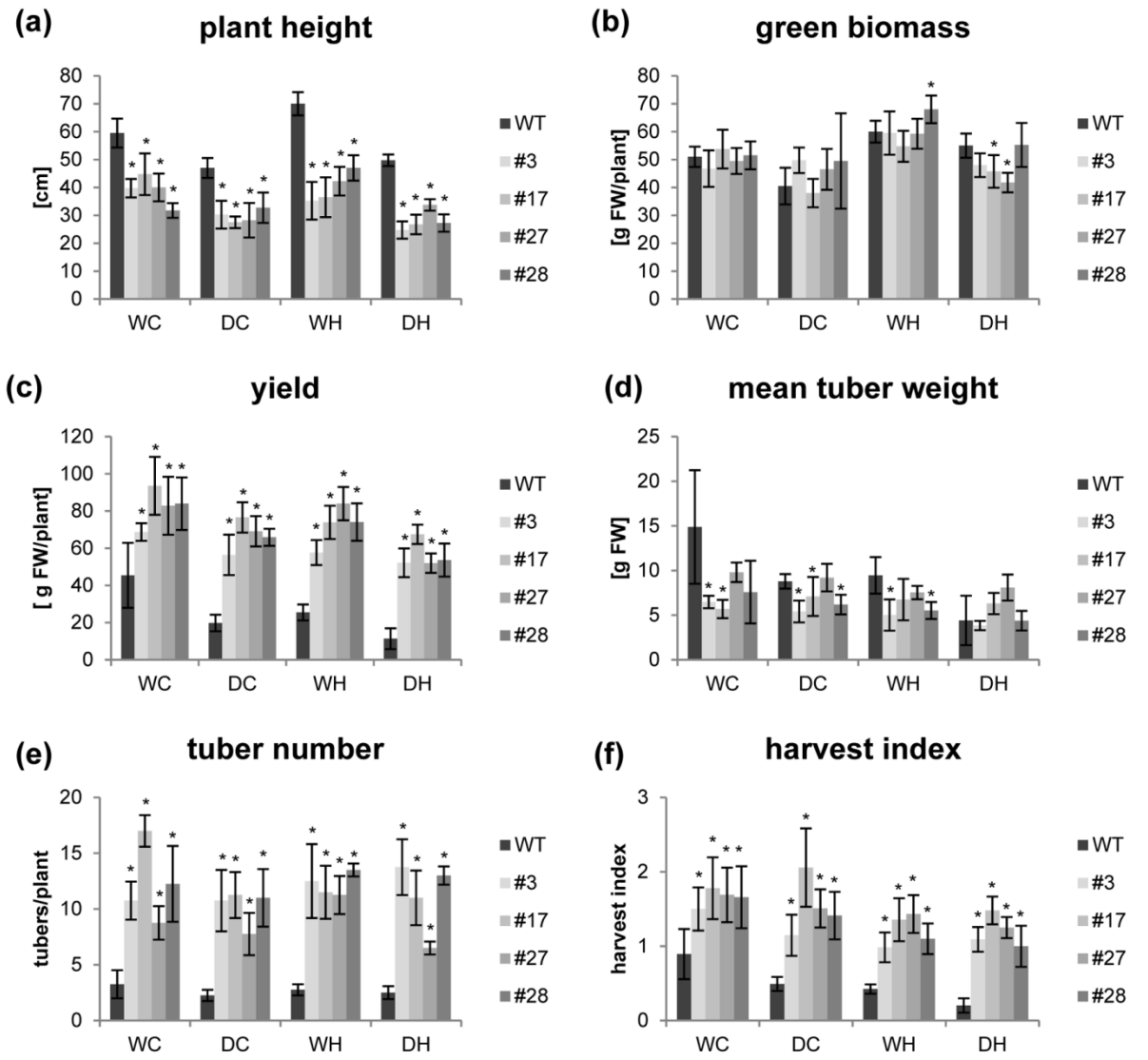

Figure S2. Yield data for HXK+SP6A potato plants. (a) Plant height **(b)** Green biomass **(c)** Yield **(d)** Stolon number **(e)** Tuber number **(f)** Harvest index; data form experiment 2, plants were harvested at the age of 7 weeks; values are the mean of 4 plants ± SD, Significance compared to WT was determined by two-tailed t-test (*; p-value < 0.05). Data from experiment 3.

7.2 Supplementary tables

Table S1. Differentially expressed transcripts in dormant buds of SP6A^{cop}-HA overexpressing tubers. (a) 677 transcripts showed significant ($p<0.05$) different expression in at least one transgenic line as compared to WT **(b)** 437 transcripts were regulated in the same manner in all three transgenic lines **(c)** 245 transcripts were regulated in the same manner in all three transgenic lines and filtered for a $\log_2$ fold change ≥ 0.5 or ≤ -0.5.

(from Lehretz et al., 2019)

Table S2. BLAST search for putative small RNAs cutting the *SP6A* transcript. For each one of the four identified cut sites 10 nucleotides up and downstream of the identified cut site were combined to a 20nt fragment, which was used for a blastn search. Additionally, these 20 nt were shifted 1 or 2 nt up and downstream, respectively, and also used for a BLASTn search. Each blast hit was aligned with the SP6A transcript

(from Lehretz et al., 2019)

Table S3. BLAST results for *SES* homologs in other *Solanaceae. The presence of the SES locus was verified by BLAST search in*

(from Lehretz et al., 2019)

Table S4. Transcription factor prediction for *SES* promoter

(from Lehretz et al., 2019)

8 List of figures

Figure 1. Regulation of tuberization in potato.

Figure 2. Drought and heat stress responses in potato.

Figure 3. Sequence alignment of SP6A and *SP6A^{cop}*-HA construct.

Figure 4. Characterization of transgenic potato plants overexpressing *SP6A^{cop}*-HA.

Figure 5. *SP6A^{cop}-HA* overexpression in potato plants induces early tuberization and alters biomass partitioning.

Figure 6. Phenotype of *SP6A^{cop}* overexpressing tubers.

Figure 7. Phenotype of SP6A^{cop}-HA plants grown from tubers.

Figure 8. Expression pattern of transcripts within the functional group "RNA regulation of transcription" differentially expressed in dormant buds of SP6A^{cop}-HA tubers.

Figure 9. Expression of *SP6A* and *SP6A^{cop}* in dormant buds of tubers of *SP6A^{cop}–HA* overexpressing potato plants.

Figure 10. Expression of *Sotub03g018760* in leaves of WT potato plants.

Figure 11. *In silico* identification of a small regulatory RNA suppressing expression of *SP6A* (*SES*).

Figure 12. The genomic locus of the small RNA (*SES*) coding region is different between potato and tomato.

Figure 13. Identification of a small regulatory RNA suppressing expression of SP6A (SES) via *in silico* analysis and transient assays.

Figure 14. Characterization of *SES/SP6A* interaction in transient assays.

Figure 15. Development of WT potato plants.

Figure 16. Expression of *SES* and its target *SP6A* during development.

Figure 17. Expression of *SES* and its target *SP6A* under elevated temperatures.

Figure 18. Expression of *SP6A* and *SES* under discontinuous heat treatment.

Figure 19. Promoter structure of *SES*.

Figure 20.Schematic depiction of the STTM construct.

Figure 21. Characterization of *Short Tandem Target Mimicry* (*STTM)* overexpressing potato plants.

Figure 22. Overexpression of a Short Tandem Target Mimicry (STTM) construct sequestering *SES* can overcome heat-mediated repression of tuberization.

Figure 23. HXK+SP6A potato plants.

Figure 24. Guard cells of HXK+SP6A potato plants.

Figure 25. Shoot phenotype of HXK+SP6A potato plants at the age of 5 weeks.

Figure 26. Photosynthesis of HXK+SP6A potato plants under different stress treatments at the age of 5-6 weeks

Figure 27. Yield data for HXK+SP6A potato plants.

Figure 28. Influence of *SP6A* expression on tuber yield.

Figure 29. Expression of genes regulating *SP6A* under drought and heat stress.

Figure 30. Dry weight/ fresh weight ratio and starch content in HXK+SP6A tubers.

Figure 31. Drought response in leaves of HXK+SP6A potato plants.

Figure 32. Phenotype of HXK+SP6A potato plants .

Figure 33. Stem phenotype of HXK+SP6A potato plants.

Figure 34. Sugar contents in stem cross sections taken of HXK+SP6A potato plants.

Figure 35. Visualization of esculin transport in longitudinal sections of stems of HXK+SP6A potato plants.

Figure 36. Root phenotype of HXK+SP6A potato plants at the age of 2 weeks.

Figure 37. SUSY and cwInv activities in tubers of HXK+SP6A potato plants at the age of 6 weeks.

Figure 38. Simplified model of regulation of *SP6A* under ambient and elevated temperatures.

Figure 39. Schematic model of SWEET11-SP6A mediated rerouting of assimilate transport.

9 List of publications and conference contributions

Publications

Lehretz, G.G., Sonnewald S., Hornyik, C., Corral, J.M., Sonnewald, U. (2019) Post-transcriptional Regulation of FLOWERING LOCUS T modulates heat dependent source sink development in potato, **Current Biology**, 29, 1614-1624,

Talks

"miRNA-mediated regulation of *FLOWERING LOCUS T* is required for coordinated source-sink development in potato", talk, **XIV Solanaceae and 3rd Cucurbitaceae Joint Conference,** Palau de Congresos, Valencia, SPAIN

"Posttranscriptional regulation of *FLOWERING LOCUS T* modulates heat-dependent source-sink development in potato", talk, **32nd Conference Molecular Biology of Plants**, February 2019, Haus Maria in der Aue, Dabringhausen, GERMANY

Posters

Lehretz, G.G., Sonnewald S., Hornyik, C., Corral, J.M., Sonnewald, U. "miRNA mediated regulation of *FLOWERING LOCUS T* is required for heat-modulated source-sink development in potato", poster, **31st Conference Molecular Biology of Plants**, February 2018, Haus Maria in der Aue, Dabringhausen, GERMANY

Sonnewald, S., Hastilestari, B.R., Lehretz, G.G., Reid, S., Sonnewald, U. Changes in source-sink balance in potato plants under elevated temperatures. **Botanikertagung,** September 2017, Kiel, GERMANY

10 Acknowledgements